UNIVERSITÀ DEGLI STUDI DI MILANO

Facoltà di Medicina e Chirurgia

Dipartimento di Scienze Biomediche per la Salute

Dottorato di Ricerca in Medicina Sperimentale e Biotecnologie Mediche

XXIX Ciclo

THE ROLE OF STEM CELL NICHE AND TUMOR-ASSOCIATED MACROPHAGES IN HUMAN CHOLANGIOCARCINOMA

Tesi di Dottorato di:

Margherita CORRENTI

Matr. n. **R10686**

Relatore: Prof.ssa **Stefania RECALCATI**

Correlatori: Dott. **Pietro INVERNIZZI**

Dott.ssa **Chiara RAGGI**

Coordinatore: Prof. **Massimo LOCATI**

Anno Accademico 2015 – 2016

TABLE OF CONTENTS

ABSTRACT

Background and Aims: Cholangiocarcinoma (CCA) is a highly malignant and extremely heterogeneous adenocarcinoma arising from epithelial cells of bile ducts. CCA is currently associated with poor clinical outcome and, together with hepatocellular carcinoma (HCC), is the major primitive liver cancer in adults. Severity of CCA, lack of good diagnostic markers and frustrating benefit of current therapeutic strategies has rendered this disease a major challenge. Therapeutically challenging subset, termed cancer stem cells (CSCs) has been proposed as a driving force of tumor initiation, dissemination and drug-resistance, including in liver cancer. CSCs could be responsible for CCA wide multi-layered heterogeneity and clinical severity. Although it has already been shown that HCC progression is driven by CSCs, little is known about the presence of CSCs in human CCA. Similar to normal stem cells, CSCs are believed to reside in a specialized microenvironment ("CSC-niche") within tumor-context that supports self-renewal and drug-resistance. Among various immune-subgroups within CSC-niche, tumor-associated macrophages (TAMs) represent a poor defined but very intriguing immune-subset, whose presence has prognostic significance in CCA and other malignancies. Thus, we hypothesized that CSCs may actively shape their tumor-supportive immune niche, specifically CCA-associated macrophages.

Methods: CCA cells were cultured in 3D-condition to generate spheres (SPH). CCA-SPH analysis of *in vivo* tumorigenic-engraftment in immune-deficient mice and molecular characterization was performed as well as evaluation of drug responsiveness. *In vitro* and *in vivo* effect of CCA-SPH on macrophage-precursors was tested after culturing healthy donor CD14+ with CCA-SPH conditioned medium (CM). Evaluation of monocyte recruitment as well as macrophage markers' expression and presence of macrophage functional properties. CCA cells grown in adherence conditions as monolayer (MON) and matched CM used as control. Validation in human specimens.

Results: CCA-SPHs engrafted 100% of transplanted mice, revealed a significant 20.3-fold increase in tumor-initiating fraction (p=0.0011) and a sustained tumorigenic potential through diverse xenograft-generations. Moreover, CCA-SPHs were highly enriched for CSC, liver cancer and embryonic stem cell markers both at gene and protein levels. CCA-SPH showed also a higher resistance to common chemotherapeutic drugs compared to MON. Analysis of CD14+ chemotaxis revealed that SPH-CM acted as a strong monocyte attractor. Next, fluorescence-activated cell sorting (FACS)-analysis showed that in presence of CCA-SPH-CM, CD14+ expressed key macrophage (MØ) markers (CD68, CD115, HLA-DR, CD206) indicating that CCA-SPH-CM was a strong MØ-activator. Gene expression profile of CCA-SPH activated MØ (SPH MØ) revealed unique molecular TAM-like features confirmed by high invasion capacity. Also, freshly isolated MØs from CCA-resections recapitulated similar molecular phenotype of *in vitro* educated-MØs. Consistently with invasive features, largest CD163+ set was found in tumor-front of human CCA specimens (n=23) and correlated with high level of serum CA19.9 (n=17). Among mediators released by CCA-SPHs, only IL13, IL34 and Osteoactivin (OA) were detected and further confirmed in CCA patient sera (n=12). Surprisingly, significant association of IL13, IL34 and OA with SPH stem-like genes was provided by CCA database (n=104). *In vitro* combination of IL13, IL34, OA was responsible for MØ-differentiation and invasion as well as for *in vivo* tumor-promoting effect.

Conclusion: CCA-CSCs molded a specific subset of stem-like associated-MØs, thus providing a rationale for a synergistic therapeutic strategy for CCA-disease.

GRAPHICAL ABSTRACT

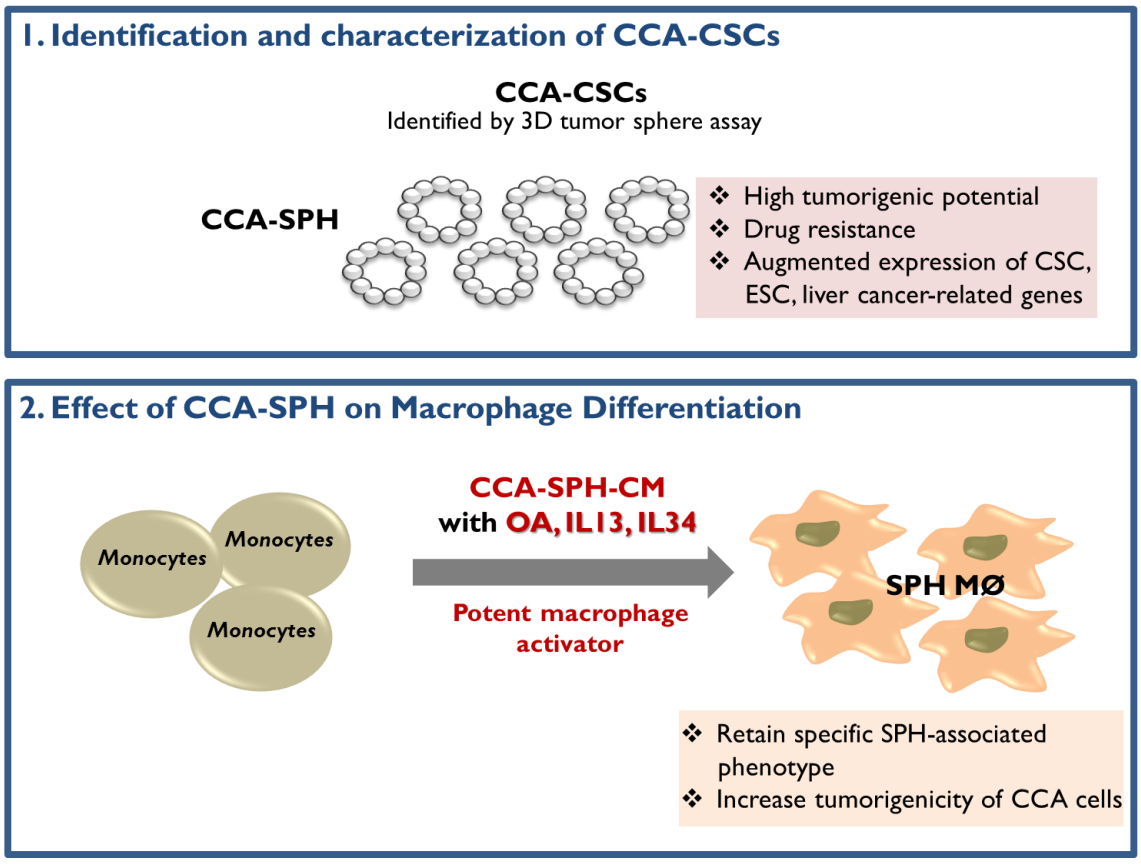

1. INTRODUCTION

1.1 Cholangiocarcinoma

Primary liver cancer (PLC) is one of the most common cancers worldwide and second leading cause of cancer-related mortality [1, 2]. Primary liver tumors are grossly classified in hepatocellular carcinoma (HCC) and cholangiocarcinoma (CCA) [1, 3-5]. HCC accounts for approximately 90% of all PLC [1, 3], while CCA, a rare tumor but with an increasing global incidence, is the second most common form and accounts for about 5% of all PLC [3-5].

CCA is a highly heterogeneous disease arising from neoplastic transformation of intra- and extra-hepatic biliary epithelial cells (cholangiocytes) and is characterized by a very poor prognosis [6, 7]. There are several established risk factors for CCA, whose frequency mostly differs depending on geographic area. For example, infection with liver flukes (*Opisthorchis viverrini* (Ov) and *Clonorchis sinensis*) is a common risk factor for CCA development in Southeast Asia [5, 8]. Instead, primary sclerosing cholangitis (PSC) is the most common predisposing condition for CCA in the west countries [5]. Hepatitis B virus (HBV) or hepatitis C virus (HCV) infection and cirrhosis have been also proposed as potential etiologies of CCA. Hence, CCA frequently arises under conditions of biliary tract's chronic inflammation, as demonstrated by all these risk factors, supporting the idea that inflammation is intimately linked to CCA initiation and progression. Indeed, chronic inflammation may support the malignant transformation through the release of growth-promoting factors and cytokines as well as by local intrahepatic accumulation of bile acids [5].

The high mortality rate of CCA may depend on its non-specific silent clinical features which make it difficult to diagnose [9]. Currently, CCA-diagnosis is based on a combination of modalities, however no specific markers have been identified [10, 11]. To date in fact, carbohydrate antigen 19-9 (CA 19-9) and carcinoembryonic antigen (CEA) are the only clinically used biochemical markers for CCA albeit their low sensitivity and specificity [11].

Another fundamental aspect contributing to the very poor CCA survival rate is its unresponsiveness to conventional therapies [6, 7]. Currently, the standard-of-care treatment for CCA is limited to surgical resection, with 5-year survival of 20% to 40% [1, 5, 10, 12-17]. Unfortunately, CCAs are generally asymptomatic in early stages and are usually diagnosed at an advanced unresectable stage and although chemotherapy improves the patients' quality of life, it still remains only a palliative treatment [5, 8, 16]. The majority of patients with unresectable CCA undergoes a rapid decline in clinical condition and died within 12 months of the onset of symptoms. Moreover, liver failure and sepsis caused by obstruction of the bile ducts contributed to increase the rate of mortality [4, 8, 11]. To improve the outlook for individuals with CCA, both clinical and bench science are therefore imperative.

1.2 Heterogeneity of CCA

Since CCA is highly heterogeneous and comprises a wide spectrum of malignancies, several classifications have been proposed, considering different aspects of these tumors. According to the anatomical location, CCA can be classified as intrahepatic (iCCA), located in large and small bile ducts within hepatic parenchyma, and extrahepatic (eCCA). The latter in its turn divided into perihilar (pCCA), originating from bifurcation of common bile duct, and distal (dCCA) CCA, involving the extrahepatic biliary tree. The second-order bile ducts serve as the point of separation between iCCA and pCCA, whereas the cystic duct between pCCA and dCCA [3, 5, 17, 18].

During the past two decades, the iCCA incidence, as well as its mortality rate, has been increasing worldwide, leading to the development of a growing scientific interest for this dismal malignancy. By contrast, eCCA rate is stable or even decreasing [5, 8, 18, 19]. Both iCCA and eCCA, besides showing opposite epidemiological behavior, are associated with different risk factors and histological features, diverse clinical outcomes and dissimilar background in terms of expression profiling, pattern of genetic mutations, and epigenetic

changes [5, 17, 18, 20, 21]. For example, PSC is a risk factor mainly for pCCA, whereas HBV and HCV infections are stronger associated with iCCA than pCCA [5]. Moreover, while V-Ki-ras2 Kirsten rat sarcoma viral oncogene homolog (*KRAS*) and tumor protein p53 (*TP53*) mutations are relatively common in all subtypes of CCA, mutations in isocitrate dehydrogenase (*IDH*) and v-raf murine sarcoma viral oncogene homolog B (*BRAF*) are considerably more prevalent in iCCA [17, 19, 22]. Next generation sequencing (NGS) of 150 CCAs has revealed that the majority of CCAs shows a driver gene mutation, although anatomically distinct tumors (iCCA versus pCCA and dCCA) seem to have different genetic profiles [5, 23]. The presence of such a large number of genetic abnormalities could lead to the occurrence of different subpopulations within the tumor, each of these possessing different combinations of genetically derived predispositions for growth, survival and dominance in the tumor microenvironment [24].

1.3 CCA Multiple Cells of Origin

The cellular origin of HCC and CCA has been a subject of intense debate in the last decades. For a long time, most HCC and CCA have been commonly accepted to derive from hepatocytes and cholangiocytes, respectively, as a consequence of genetic and/or epigenetic alterations. Anyway, detailed analysis of a wide range of PLC tumor types have reported that a rare form of mixed hepatocellular-cholangiocarcinoma (CHC) has intermediate characteristics between HCC and iCCA, suggesting that they both could share the same stem/progenitor cell origin [25-30]. Hepatic progenitor cells (HPCs) act as a reserve cell compartment activated when hepatocytes and/or cholangiocytes are damaged or inhibited in their replication [18, 31, 32]. HPCs situated in the canal of Hering are bipotential, thus, they can differentiate into hepatocytes or cholangiocytes. During differentiation in malignant cells, bipotential HPCs undergoes maturation arrest and give rise to a spectrum of tumor phenotypes with varying hepatocellular and cholangiocellular differentiation characteristics, such as colangiolocellular carcinoma (CLC) and

CHC [21, 31, 33]. More recently a new subtype of CCA-like HCC (CLHCC) has been discovered and characterized as HCC expressing CCA-like traits [34]. CLHCC co-expressed embryonic stem cell (ESC) traits and hepatoblast-like genomic signatures, suggesting its derivation from bipotential HPCs. These evidences gave insights into the heterogeneous progression of liver cancers, which imply a common cellular origin from different developmental stages [21, 34, 35]. The hypothesis of progenitor cell origin has been recently supported by new advancement of genome wide analysis. Indeed, it has been suggested that iCCA and HCC are closely related at molecular level [18, 20, 26, 31], since both tumor types share common copy number variations [6, 36].

Such phenotypic variability and presence of progenitor cell features in CCA can be explained in two ways: either the cell of origin is a progenitor cell or, alternatively, tumors dedifferentiate acquiring progenitor cell features during carcinogenesis (dedifferentiation theory (reviewed in [37-39]) (Figure 1). Interestingly, new finding provided direct evidence that any cell in the hepatic lineage can be the cell of origin of primary liver cancer [40]. At this regard, it has been recently suggested the development of iCCA by lineage conversion of malignant hepatocytes, through a simultaneous activation of Notch and protein kinase B (AKT) signaling, contributing to the acquisition of stem/progenitor cell features [41, 42] (Figure 1). Although a marked diversity/plasticity of the underlying cells of origin is emerging, current evidence suggests that most CCAs are derived from undifferentiated cells with stem-like capabilities.

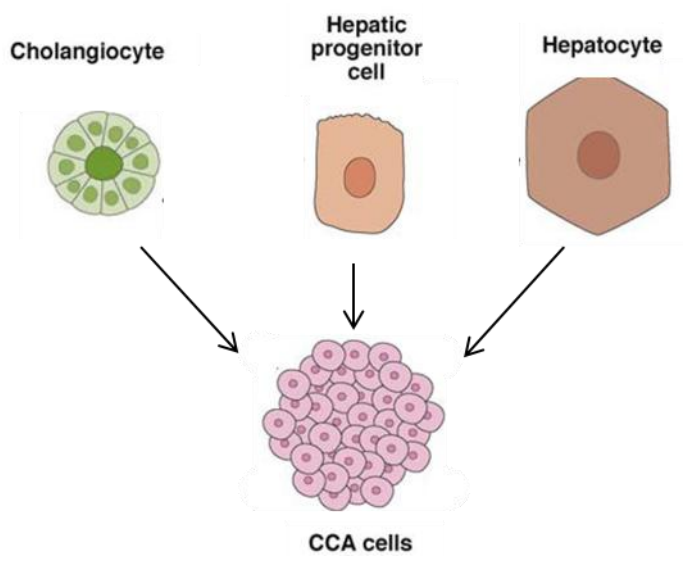

Figure 1. Different cells of origin of CCA. CCA is classically considered to arise from malignant transformation of cholangiocytes. Despite this, recent evidences suggest that CCA has multiple cellular origins, including differentiating mature hepatocyte and bipotential hepatic progenitor cells (Modified by [8]) .

1.4 Understanding the Concept of Cancer Stem Cell

Extensive heterogeneity in cellular morphologies, genetic fingerprints and responses to therapeutic interventions is a cardinal hallmark of cancer. As previously mentioned, heterogeneity is also a hallmark of CCA and occurs at different layers. Such tumor complexity may reflect the presence of distinct cell subtypes with different potentials to self-renew and differentiate [43-45]. Unlike the stochastic model, which states that every cell within a tumor can equally be the responsible for tumor initiation and progression, the hierchical or cancer stem cell (CSC) model may explain tumor heterogeneity and provide the potential to better understand the stem-like biology that underlies long-term cancer propagation [46-49]. Hierchical model designates malignant tumor-propagating cells as CSC. According to this model, CSCs represent a fraction of cells resident in the tumor endowed with stem-like properties such as the ability for self-renewal and differentiation as well as the resistance to drugs [50, 51]. Due to the self-renewal capacity, CSCs represent the unit of selection in a tumor, while any of the other cells lead to clonal exhaustion [49]. More importantly, CSC are thought to be the unique cellular subset responsible for tumor initiation, recurrence and metastasis showing reduced sensitivity to chemotherapy compared to bulk tumor cells [50, 52-54]. So, the concept of cancer-stemness has recently added a

new level of complexity in understanding CCA heterogeneity as well as CCA drug resistance and the existence of CSCs represents an entirely distinct dimension of intra-tumoral heterogeneity [24].

This idea that tumor initiation and progression are driven by stem-like cells was first proposed >150 years ago [55] and has long been debated. While their existence has been confirmed across numerous different tumor entities, including acute myeloid leukemia, pancreatic cancer, breast cancer, lung cancer, hepatocellular carcinoma, head and neck cancer, colon cancer, prostate cancer, melanoma, and glioblastoma, the origin of putative CSCs has long been debated and is not fully understood [56]. It has been proposed that CSCs originate from resident stem cells. The inherent self-renewal capacity and long life span of these cells may allow them to accumulate oncogenic and epigenetic alterations, resulting in neoplastic transformation (Figure 2). Alternatively, CSCs may originate from more differentiated transit-amplifying/progenitor cells [48], or even from differentiated non-CSCs that have been reverted back to a stem-like state by acquiring long-term self-renewal capacity after alterations in key regulators of differentiation or stem cell fate [57, 58] (Figure 2). Thus, tumor hierarchical organization does not imply that it originated from normal stem cells, and the CSC model does not address the cell-of-origin, that represents the normal cell that acquires the first cancer-promoting mutation(s) and is not necessarily related to CSC-concept [59, 60].

Although, it has already been shown that HCC progression is driven by CSCs [29, 61-64], very few studies have indicated the presence of CSCs in CCA (reviewed in [65]). Hence, it's important to shed light on pathobiological and clinical aspects of putative stem-like features in CCA, in order to develop novel targeted strategies.

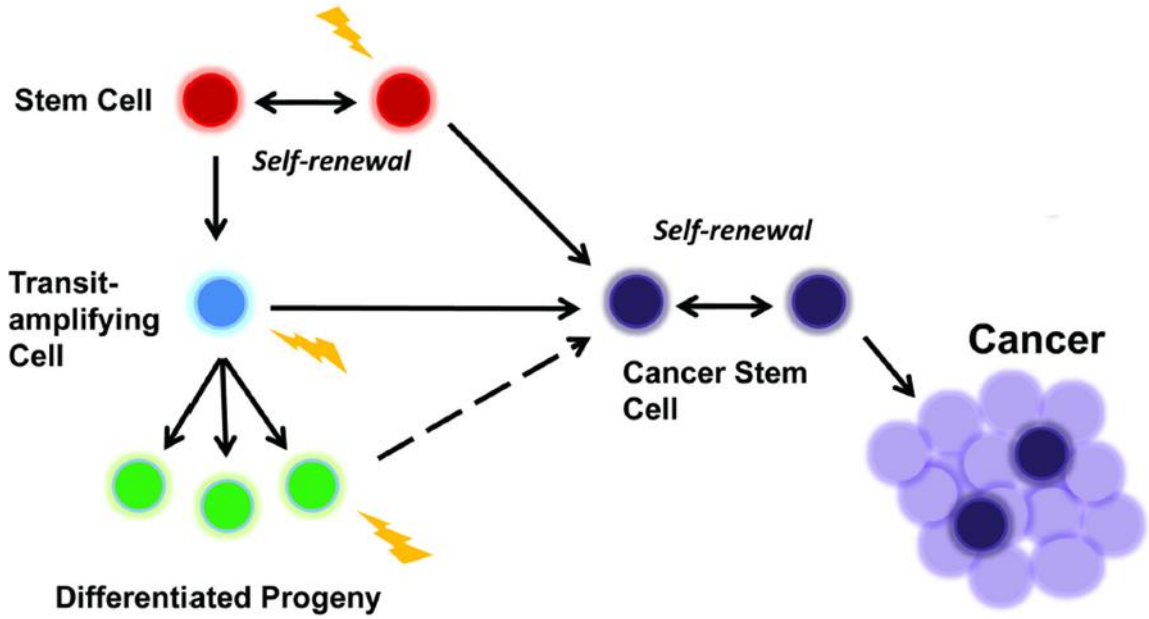

Figure 2. CSC model. According to CSC model, CSC are thought to be the unique cellular subset responsible for tumor initiation, recurrence and metastasis and are endowed with stem-like properties such as the ability for self-renewal and differentiate in more mature cancer cells. CSC model does not address the cell-of-origin, that represents the normal cell acquiring the first cancer-promoting mutation(s) (yellow bolts), which could be normal stem cell as well as transit-amplifying/progenitor cell or differentiated non-CSCs (Modified by [60]).

1.4.1 Identification of Liver CSC

During the last decade there has been a great quantity of studies aimed to identify liver CSCs and several attempts have been made to enrich CSCs in hepatic tumors. Common strategies for PLC-CSC enrichment, varied from the widely used classical antigenic approaches based on the identification of surface stem-like markers (e.g., CD133 [54, 66, 67], CD44 [68], OV6 [69], CD90 [70, 71], epithelial cell adhesion molecule [EpCAM] [29, 64], CD13 [72], CD24 [73], CD47 [74]) to functional methodologies including Side Population (SP) analysis [61, 75], Aldefluor assay [76] and sphere formation coupled with serial sphere passaging [63, 77]. In all diverse published studies, enriched PLC stem-like subsets were tested in immune-deficient mice for the *in vivo* tumorigenic potential [29, 54, 61, 63, 64, 66-77]. More interestingly, only those putative PLC stem-like subpopulations capable to initiate tumor development at low cell numbers, were further tested for 'self-renewal'

capacity in serial tumor transplantations and at molecular level for presence of hepatic stemness-related pathways (e.g., developmental signaling and transcription factors, epigenetic regulation including specific miRNAs) [61, 63, 78-108].

The antigenic approach is one of the first methods to isolate CSCs and relies on cell-surface markers. Among several cell-surface antigens, CD133 is one of the most common markers of stem/progenitor cells in adult tissue (brain, prostate, liver and kidney) and is expressed in diverse tumor stem-like subsets, including HCC and CCA [45, 109-111]. As alternative, CD44, a glycoprotein and receptor for hyaluronic acid, is expressed only on CSC [65, 110, 111]. CD24 is a cell adhesion molecule associated with tumor motility, invasiveness and poor response to chemo- and radio-therapy and is a useful marker for early CCA carcinogenesis [110, 111]. CD90, a cell surface molecule, has been identified in a variety of cells including stem and progenitor cells with a function of stemness maintenance [112]. It has been used to isolate liver tumor cells with stem-like properties [71, 113]. EpCAM is a hemophilic, Ca^{2+}-independent cell-cell adhesion molecule that is expressed in many human epithelial tissues and although has been increasingly recognized as an important CSC marker for a variety of tumors, its expression in CCA is not well investigated [65, 114]. However the antigenic approach has several shortcomings, such as lack of clearly defined surface markers specific for individual tumor type, and specifically for CCA [77]. So, stem cell markers may not be specific for liver CSCs, and they are generally not universally expressed in all liver CSCs [115]. So far, none of stem-like markers is exclusively expressed by normal or cancer stem cells (e.g., CD133 is expressed in both liver CSCs and hepatocytes [115]). In addition, the surface marker expression can vary depending on specific context. Thus, marker expression can be drastically altered after plating stem cells in culture [77].

In addition to the classical antigenic approach, there are several assays based on functional properties rather than the expression of surface markers. Among

functional features, resistance to classic chemotherapeutic agent represents a key CSC property [116, 117]. CSC drug resistance is generally mediated by different molecular mechanisms including the well-known ATP-binding cassette (ABC) transporters that prevent drug accumulation by its exclusion across the plasma membrane [61, 118]. Based on this property, SP analysis allows to select a stem-like subset by the exclusion of Hoechst-33342 dye via ABC sub-family G member 2 (ABCG2) transporter. SP assay was originally developed to isolate a fraction of hematopoietic stem cells [119] and it's widely used for CSC purification from many solid tumors, including liver cancer [120-122]. However, Hoechst 33342 is cytotoxic and unprotected non-SP cells could suffer toxicity, with a consequent inability to grown once placed in culture. Thus, the differing tumor-initiation abilities of SP and non-SP fractions are most likely due to an artifact of Hoechst 33342 toxicity rather than to intrinsic stem-cell properties [123]. An additional functional strategy for identifying stem-like tumor cells involves the measurement of aldehyde dehydrogenase activity; aldehyde dehydrogenase is involved in intracellular retinoic acid production and is responsible for stem cell development, differentiation and self-protection [124-126].

Another functional approach is tumor-sphere assay, based on long-term self-renewal capability [63, 127, 128]. To enrich cancer stem/progenitor cell population, cells are cultured in an anchorage-independent manner in selective serum-free medium rich in growth factors. This *in vitro* technique was developed in 1992 to grow undifferentiated multipotent neural cells as neurosphere [129]. Similar culture systems have been developed for mammary stem cells, and it has been shown that mammospheres can be serially passaged to demonstrate self-renewal activity *in vitro* [130, 131]. Sphere assay is particularly useful to enrich the potential CSC subpopulation when specific CSC markers have not been identified, as the case for CCA [123]. In this assay, CSC can be serially passaged for many cycles by generating tumor spheres resembling the primary spheres. Moreover, tumor cells may be passaged directly on plastic or embedded in Matrigel, a substitute for

the basement membrane that replicate the stem cell natural environment, to evaluate the cell ability to differentiate [123, 130]. Moreover, tumor sphere-forming cells possess higher tumorigenicity compared to bulk tumor cells [123]. Researchers have reported the application of sphere culture to isolate, enrich, maintain or expand potential CSC population from various types of cancers, including HCC [61, 63, 123]. To our knowledge, there are no reports on CSC isolation by sphere assay in human CCA. The *in vitro* sphere forming assay appears to be the best useful surrogate for the *in vivo* tumorigenic assay in immunodeficient mice and doesn't possess so many shortcomings than those shown by antigenic and SP approaches [132]. Anyway, it's important to emphasize that stem cells and progenitors cannot be distinguished in these assays.

1.4.2 Regulatory Pathways Involved in CCA-Associated Stemness

Interestingly, many of the identified CSC regulatory pathways are also known to be involved in stem-cell maintenance as well as embryonic self-renewal and pluripotency [133, 134]. Indeed, several studies have shown that the majority of aggressive human cancers are characterized by the activation of embryonic stem-associated genes that might serve to sustain the stem-like state of cancer cells [135-138]. We will briefly review the key molecular networks that are recognized to induce or support stem-like features in the context of liver tumor.

Wingless-type MMTV integration site family member (Wnt)/β-catenin pathway. Increasing evidence has shown that the Wnt/β-catenin canonical signaling pathway plays a major role in maintaining stemness in both embryonic and cancer stem cells [139, 140]. The binding of extracellular Wnt to Frizzled cell surface receptors results in increased cytoplasmic β-catenin levels, with the following transcription of Wnt target genes, which play important roles in liver carcinogenesis [53, 141]. Notably, β-catenin is expressed in 58% of CCA, mutated in 8% of cases and is considered an early determinant in CCA-progression [65].

Notch signaling pathway. The Notch canonical signaling is a highly conserved pathway controlling cell differentiation, proliferation and apoptosis, and plays an important role in the maintenance of stem cells, including HPCs [65, 142, 143]. Moreover, Notch signaling plays an important role in bile duct morphogenesis (reviewed in [144]), and dysfunction in this pathway may result in reduced detoxification of the liver that ultimately leads to liver damage and iCCA development. Interestingly, the expression of Notch receptors 1 and 3 correlates with CCA progression and poor survival [65], whereas overexpression of Notch receptors 1 and 4 in HCC exert tumorigenic effect [145]. Since Notch signaling can contribute to either CCA or HCC, it has been suggested that this pathway could be deregulated in bipotential HPCs [142].

Hedgehog signaling pathway. The Hedgehog (Hh) pathway is associated to embryonic development, cell differentiation, regeneration and stem cell biology. The aberrant activation of the Hh pathway has been reported in different malignancies [146], and its correlation with prognosis is well described [147]. Activation of this pathway promotes CCA proliferation and survival in addition to HCC carcinogenesis and HPC proliferation [65, 140]. Notably, the aberrantly activated Hh pathway induces the upregulation of several molecules, such as Nanog homeobox (NANOG), octamer-binding transcription factor 4 (OCT-4), vascular endothelial growth factor (VEGF), PDGF receptor A (PDGFR-A) and Snail [142].

Hippo signaling pathway. *T*he Hippo-signaling cascade is an evolutionarily conserved pathway involved in organ development [148-150]. Hippo pathway has been implicated in multiple events during tumor onset. Strong evidence also points to a significant role of Hippo signaling in regulating stem cells, including HPCs [151-153]. Yes-associated protein 1 (YAP1) is a primary effector of the Hippo cascade and is frequently expressed in HCC and CHC mixed tumor types, which retain stemness-related features [152]. Furthermore, it has been proposed that bile

duct's constitutive activation of YAP, in association with AKT, is essential of inducing CCA in a murine biliary injury model [154].

Phosphatidyl inositol 3-kinase (PI3K)/AKT signaling. AKT plays a critical role in many human cancers, including HCC and CCA [3, 155]. AKT signaling can be triggered downstream of tyrosine kinase receptors activation, PI3K constitutive activation or loss of phosphatase and tensin homolog (*PTEN*)[3]. *PTEN* deletion results in a proliferation of CD133+ cell population [65, 156]. Notably, the co-activation of *AKT* and neuroblastoma rat sarcoma viral oncogene homolog (*N-RAS*) oncogenes leaded to development of CHC-like liver tumors, through the expansion of HPCs or malignant conversion of hepatocyte into progenitor-like cells [41].

Mitogen-activated protein kinase (MAPK)/extracellular signal-regulated kinases (ERK) signaling pathway. The MAPK cascade regulates many important cell function, such as proliferation, invasion and survival and is critical for HPCs proliferation [65]. Gain-of-function mutations of *KRAS* are some of the most frequent mutations observed in iCCA, defining a class of patients characterized by poor outcome. This poor outcome class was enriched for CCA stem cell-like and tumor recurrence predicting signatures. Moreover, these mutations are also detected in patients with PSC, so this could an early event that contributes to the malignant transformation of cholangiocytes [36].

Transforming growth factor-β (TGF-β) signaling. The TGF-β pathway plays a key role in self-renewal and maintenance of undifferentiated stem cell state. Its disruption impairs stem cell differentiation and causes deregulated proliferation of HPCs, resulting in CCA development [156]. TGF-β acts as a tumor suppressor early in tumor initiation, whereas at late stages it promotes tumor growth, metastasis and epithelial-mesenchymal transition (EMT). It has been

demonstrated that TGF-β1/Snail activation induces EMT in CCA both *in vitro* and *in vivo,* and this is associated with a higher CCA aggressiveness [157].

Janus kinase/signal transducers and activators of transcription (JAK/STAT) signaling. Several evidences highlight also the central role of interleukin (IL)-6/STAT3 signaling in CCA. Binding of IL-6 to the gp130 receptor leads JAK kinases (JAK1, JAK2 and TYK2) and subsequent STAT3 activation, inducing the transcription of target genes essential for cell growth, differentiation and proliferation (reviewed in [18, 158]). STAT3 signaling is also involved in maintenance of CSC population [159-161] and in EMT-triggering in diverse tumors [162, 163].

1.5 The CSC Niche and Macrophage Component

Similar to normal stem cells, CSCs require input from the surrounding microenvironment to achieve an optimal balance between self-renewal and differentiation as well as to protect themselves from immune surveillance, apoptosis and chemotherapeutic drugs; this inputs might affect tumor initiation, progression and outcome [21, 56, 164-166]. More specifically, there is a propensity to refer to CSC-associated microenvironment as 'CSC-niche'. Niches are anatomically distinct microenvironments within the overall tumor microenvironment (TME) [49, 167]. The CSC-niche is enriched in growth factors, cytokines, prostaglandins and extracellular matrix (ECM) components. Key cellular players include cancer-associated fibroblasts, mesenchymal stem cells, immune cells and endothelial cells (Figure 3). Cells within the CSC-niche produce factors that stimulate CSC self-renewal, induce angiogenesis, and recruit immune and other stromal cells that, in turn, secrete additional factors to promote tumor invasion and metastasis [49]. The idea that the tumor stroma is not only a supportive 'soil' but, more importantly, an active participant in tumorigenesis, challenges the old paradigm of tumor functional organization [21, 53, 167]. While each cell or environmental component has a particular function on its own, together they create a dynamic niche replete with secreted factors that

synergize and cooperate to develop a complex communication network known as cross talk, with the CSC at center stage [56] (Figure 3). Therefore TME and tumor cells, including CSC, create a complex cellular system with reciprocal signaling and alterations [168]. An area of great interest is the role of inflammatory cells within the CSC niche. Indeed, the TME is characterized by chronic inflammation, which, instead of inhibiting tumor growth, favors tumor formation by stimulating cell proliferation, activating CSCs, and promoting metastasis [56]. Among various immune-subgroups within CSC-niche (e.g., T cells, neutrophils, granulocytes) [169-172], tumor-associated macrophages (TAMs) represent a poor defined but very intriguing immune-subset and seem to lead tumor inflammatory response [56].

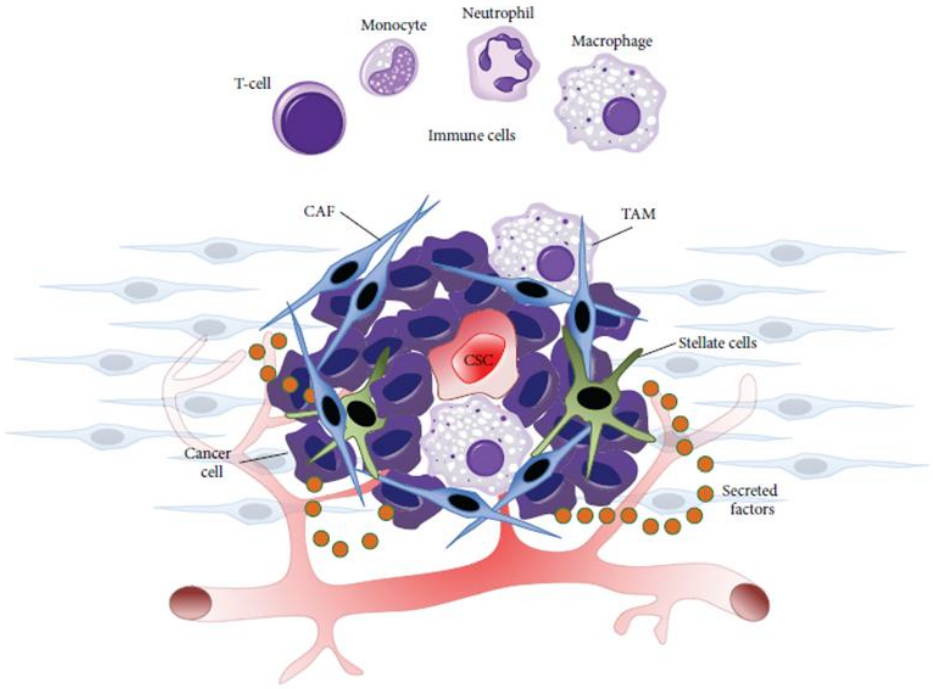

Figure 3. CSC-niche. CSCs are located within a specialized microenvironment, the so called 'CSC-niche'. Key cellular players of CSC-niche include other cancer cells, stellate cells, cancer-associated fibroblasts (CAFs), and immune cells (T-cells, monocytes, neutrophils, and tumor-associated macrophages (TAMs)). Cells communicate with one another and directly with the CSC via secreted factors, forming a complex and dynamic cellular network [56].

1.5.1 Functional Roles of TAMs

Notably, the TME supports tumor initiation and evolves together with tumor cells during progression. Among the immune cells present at the tumor site, macrophages are particularly abundant in solid tumors [173]. Accumulating evidence has validated the critical role of TAMs in immune escape, cancer progression and metastasis [174-177]. Diversity in TAM functions has led to the notion that macrophages are extremely plastic and can assume multiple phenotypes depending on their location in the tumor context [178, 179].

Historical consideration of macrophage function was directed to the idea of two main macrophage phenotypes: *M1*, also called 'classically activated macrophages', and *M2*, also called 'alternatively activated macrophages'. The M1-polarized macrophages manifest high levels of pro-inflammatory cytokines (IL-1, tumor necrosis factor alpha [TNF-α], IL-6 and IL-23), high production of nitric oxide (NO) and reactive oxygen species (ROS) intermediates that promote Th1 responses and contribute to tumoricidal activity and antitumor immunity. On the other hands, M2 macrophages express anti-inflammatory cytokines (IL-10, TGF-β and IL-4), suppress T cell proliferation and activity and are the main players facilitating parasite containment, tissue remodeling/repair and immune tolerance, which may be linked to tumor progression [180-187]. TAMs classically have characteristics and functions similar to M2 macrophages [182]. For example, TAMs are inefficient to present antigens and trigger adaptive immune response [188]. However, in line with the microenvironmental heterogeneity, it has been shown that M1 and M2 classes are not discrete and represent a broad phenotypic spectrum. It is now believed that different subpopulations of TAMs are found in different tumor microenvironments, representing the different functional roles that macrophages assume in tumorigenesis [21, 189, 190]. Thus, merely classifying tumor macrophages as M1 or M2 does not accurately reflect the differentiated or biological state of TAMs. Rather, the classification of TAMs should be related to the function of the macrophage subpopulation within the tumor (e.g., metastasis-promoting macrophage, angiogenic macrophage, and

immunosuppressive macrophage) as has been proposed by others [56, 190-193]. Within tumor invasion areas, TAMs promote cancer cell motility, whereas they promote metastasis in perivascular areas and stimulate angiogenesis in perinecrotic areas [194-196]. Moreover, it has been speculated that dynamic changes in TME may occur during the transition from early neoplastic events to advanced tumor stages, which result in progressive conversion of TAMs from an M1 to an M2 phenotype [182, 197]. This seems to correlate with diverse functional roles exerted by TAMs during different tumor stages. In pre-tumoral stages, TAMs mediate DNA damage, oncogenic transformation, survival of transformed cells and cancer- related inflammation through the release of reactive nitrogen intermediates/reactive oxygen intermediates, tumor necrosis factor, IL-6 and IL-1β [198]. After the establishment of the tumor, a new wave of factors (e.g., human macrophage colony-stimulating factor [M-CSF] and C-C motif ligand 2 [CCL2]) may be released to recruit more monocytes/macrophages to the tumor site [199] (Figure 4). In more advanced neoplasia, the production of several factors (e.g., epidermal growth factor [EGF], fibroblast growth factor [FGF], VEGF, PDGF and TGF-β) by TAMs may be responsible for promoting the proliferation and survival of tumor and stromal cells as well as the process of angiogenesis [199] (Figure 4).

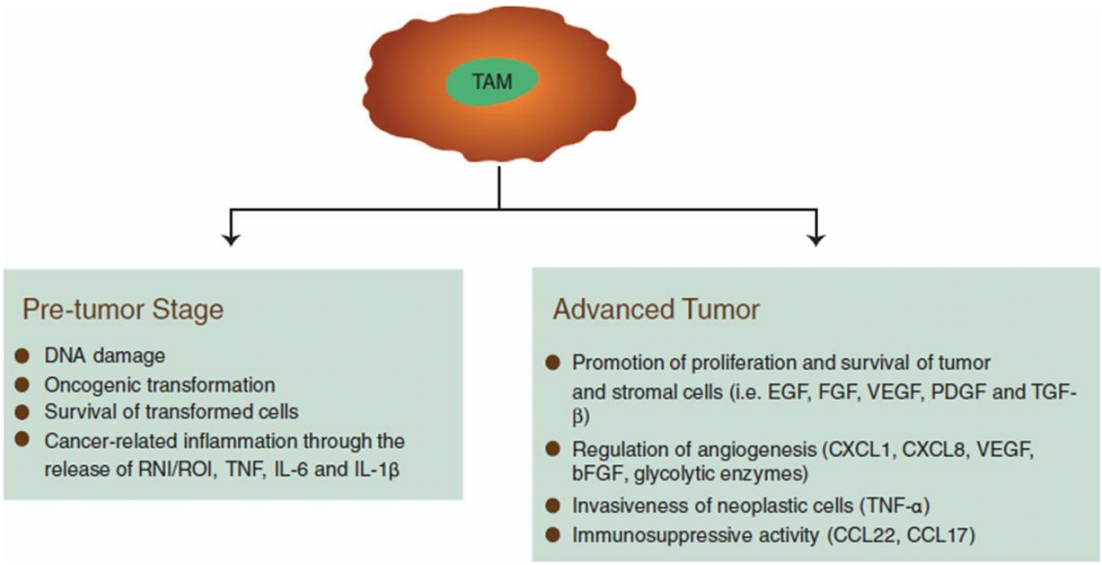

Figure 4. Functional roles of TAMs. The figure shows a summary of different TAM roles in tumor initiation and progression [235].

TAM with overlapping characteristics between M1 and M2 have also been reported in some tumor models [198]. Of relevance, tissue macrophages were shown to regulate homeostasis in the normal hematopoietic stem cell (HSC) niche, thus raising the question of how macrophage plasticity affects CSC functions [200].

1.5.2 TAMs in CCA

Although many studies have shown the contribution of TAMs in tumor development and patients' poor prognosis, the significance of TAM infiltration in human CCA is still unclear. Interestingly, an association between the ratio of $CD68^+/CD163^+$ macrophages, regulatory T (Treg) cells and number of vessels has been recently described in iCCA. Specifically, degree of microvascularization and Treg cells was more intimately correlated with the number of $CD163^+$ M2 macrophages rather than $CD68^+$ macrophages. Strikingly, patients with elevated levels of $CD163^+$ macrophages had a shorter disease-free survival compared to patients with $CD68^+$ [201]. Additionally, an association between newly infiltrated tumor macrophages and poor prognosis has also been reported in CCA patients, highlighting the critical role of tissue macrophages in degrading the ECM and facilitating tumor metastasis [202]. Other recent studies also supported the correlation between macrophage density and poor prognosis as well as tumor recurrence in patients with CCA [203, 204]. Moreover, the exposure of human macrophages to tumor cell-conditioned medium derived from different iCCA cell lines resulted in STAT3 activation and macrophage polarization toward the M2-phenotype with an increased expression of M2-type factors, such as IL-10, VEGF-A, TGF-β, matrix metalloproteinase (MMP)-2 and TNF-α, which in turn was associated with an increased migration and invasion potential [201, 205, 206]. These results suggest that macrophage differentiation into the M2-phenotype together with the contribution to angiogenesis and immunosuppression are dependent on STAT3-signaling pathway in iCCA. Macrophages switch towards a M2-phenotype (CD68+ CD163+) seems to occur at early stage of CCA and

contribute to CCA metastasis, likely via activation of EMT processes [207]. EMT induction in CCA is likely due to various cytokines secreted by activated M2 macrophages, such as IL-4, IL-6, IL-10, TGF-β and TNF-α, that can modify the expression of EMT-related genes. Indeed, addition of macrophage-conditioned medium to CCA cells reduced the expression of E-cadherin and cytokeratin (CK)19, whereas induced the expression of mesenchymal markers S100 calcium-binding protein A4 (S100A4) and MMP-9 [208, 209].

Moreover, bile duct tumors generally proliferate surrounded by a rich vascular network, which provides an adequate support of oxygen and metabolites to malignant cholangiocytes in order to enhance tumor growth. The angiogenic potential is favored by overexpression of VEGF-C, that is expressed by surrounding mesenchymal as well as malignant cells (reviewed in [15]). This suggests the existence of an autocrine/paracrine mechanism in the production of VEGF by malignant cholangiocytes, and further indicates that TAMs play an important role in regulating angiogenesis through VEGF, with important consequent implication in pro-fibrotic processes and cholangiogenesis [210].

1.6 CSC–TAM Interplay in Diverse Tumor Models

Accumulating evidence supports the hypothesis that macrophages interact with, and support, normal stem cell as well as CSC functions, thus contributing to tissue repair and remodeling as cancer progression, respectively [211]. Moreover, recent data indicate that CSCs respond differently to antitumor agents *in vitro* and *in vivo*, reinforcing the hypothesis that the bidirectional interplay between polarized macrophages and CSC seems to be a key event affecting tumor-promoting conditions in TME as well as CSC drug responsiveness. In support of this notion, tumor cell products, including ECM components, IL-10, M-CSF and chemokines (CCL2, CCL18, CCL17 and chemokine C-X-C motif ligand 4 [CXCL4]), polarize macrophages toward an M2-like, cancer-promoting phenotype [212]. On the other hand, emerging evidence indicates a trophic role for M2 macrophages on CSCs in various tumors. For example, an increased

number of M2-like CD163+ TAMs correlates with poor prognosis and presence of CSC in oral squamous cell carcinoma [213]. Moreover, the TAM-specific secretion of TGF-β promotes CSC-like properties by inducing EMT in HCC [214]. Interestingly, factors released by cancer stem-like cells from chemoresistant tumors generated M2-like immunoregulatory myeloid cells from CD14+ monocytes, thus contributing to create a pro-tumor microenvironment [215].

Several recent studies have emphasized the bidirectional TAM–CSC crosstalk in different tumor models, rather than the unidirectional interaction between the two components.

Colon and lung cancer. CSC present in murine colon and lung cancer are shown to stimulate the release of milk fat globule-EGF factor 8 protein (MFG-E8) and IL-6 from TAM. MFG-E8, in concert with IL-6, in turn promotes CSC tumorigenicity and chemoresistance, likely through the activation of STAT3 and Hedgehog signaling pathways [216].

Breast cancer. It has been reported that TAMs promote CSC-like phenotypes in murine breast cancer cells through the binding EGF-EGFR, suggesting the presence of a positive feedback paracrine loop between TAMs and breast CSC The resulting CSC-like phenotype was characterized by increased sex determining region Y-box 2 (*SOX-2*), *OCT-4*, *NANOG*, *ABCG2*, and caspase 3 (*CASP3* or *SCA-1*) gene expression, in addition to increased drug-efflux capacity, resistance to chemotherapy, and increased tumorigenicity *in vivo* [217]. Moreover it seems that breast CSC-niche is supported and maintained by juxtacrine signaling from macrophages through the physical interaction between CD90+ CSC and TAMs, mediated by binding of plasma membrane-associated Ephrin ligands to the corresponding EphA4 receptor present on CD90+ CSC [218].

Pancreatic adenocarcinoma. It has been shown that TAMs can directly induce stem-like properties including chemoresistance in pancreatic ductal adenocarcinoma through the activation of STAT3 signaling [219]. Furthermore, an

additional immunosuppressive effect versus cytotoxic T lymphocytes has been described only in those macrophages exposed to the CSC compartment [219].

Glioma. In glioma tissue, CSCs play a pivotal role in recruiting macrophages through the production of several chemo-attractants such as CCL2, CCL5 and VEGF. In addition CSCs polarize macrophages towards an M2 phenotype, which in turn may induce T-cell immunosuppression [220]. Moreover, CD133+/CD15+ CSCs preferentially express periostin (POSTN), a protein involved in tumor EMT, ECM degradation, tumor invasion and metastasis. In turn, POSTN is able to recruit peripheral blood monocyte-derived macrophages (C-C motif chemokine receptor 2 [CCR2]+/chemokine C-X3-C motif receptor 1[CX3CR1]-) but not resident CX3CR1+ macrophages through the binding with TAM-expressed integrin aγβ3, leading to the promotion of malignant growth [221].

HCC. HCC TAMs promote the expansion of CD44+ stem-like hepatocellular carcinoma cells *in vitro*, likely through IL-6-dependent activation of STAT3 signaling pathway. This statement is validated by CSC enhanced sphere-forming ability, expression of stem-like genes and tumorigenic potential in NOD-SCID/IL2Rγ^{null} (NSG) mice *in vivo* [222]. These results demonstrated the importance of targeting the immune component of TME as a strategy to shrink the CSC subset in human HCC.

Hence CSCs are able to polarized macrophages towards a tumor-supportive phenotype and TAMs may serve as a component of the "immunological niche" by which CSC activities are maintained and amplified within TME [223]. Nevertheless, the investigation of macrophages-CSC interaction in CCA is still unexplored.

2. AIMS AND EXPERIMENTAL DESIGN

2.1 Hypothesis and Aims

Due to its desmoplastic nature, CCA is associated with massive presence of stromal cells [5, 21]. Among various immune-subgroups (e.g., T cells, neutrophils, granulocytes) [169-172], CCA-associated macrophages represent a poor defined but very intriguing immune-subset. Indeed, high TAM density significantly correlated with poor prognosis, unfavorable survival and metastasis tendency in CCA patients, suggesting a major role of macrophages in CCA progression (reviewed in [5]).

Recently, CSCs have been proposed as a driving force of tumor initiation, dissemination and drug-resistance, thus representing a primary therapeutic target. Although it has been shown that HCC progression is driven by CSCs [61, 63], identification of CCA stem-subset is still largely unexplored and limited to classical antigenic approaches (reviewed in [5]). Similar to normal stem cells, CSCs are believed to reside in specialized microenvironment ("CSC-niche") within tumor-context [45, 49, 224] that supports self-renewal and drug-resistance [216, 218, 221, 222, 225].

Tumor-stroma co-evolves together with cancer cells and plays a critical part in both malignancy initiation as well as key steps of growth and metastasis [226]. Since macrophages show a remarkable degree of plasticity during tumor development [180, 182], we assumed that, depending on CSC tumorigenic-state, CSCs might actively release soluble mediators that engaged circulating-monocytes to tumor-initiating niche [24, 225] and prompted macrophage differentiation towards an exclusive subset of TAMs, the *'CSC-associated TAMs'*. Although bulk tumor cells support TAMs recruitment and activation, specific effects of CSCs on TAMs phenotype are still unexplored in human CCA.

Hence, the goal of this project is to shed light on the critical interaction between CCA stem-like compartment and macrophage component. Specifically the current study sought to:

1. *Identify and characterize a functional CSC-subset in human CCA*
2. *Verify the existence of a peculiar CSC-associated TAM-compartment as result of bioactive CCA stem-like cells.*

2.2 Experimental Design

1. Identification and characterization of a functional CSC-subset in human CCA

To identify a stem-like compartment in four human CCA cell lines, 3D tumor sphere forming assay was used. The term CSC refers to some properties shared with normal stem cells, including self-renewal. Based on this concept, non-adherent 3D sphere assays has been increasingly used as a tool to identify, enrich and expand cells endowed with long-term self-renewal capability in both normal and tumor tissue [61, 63, 129]. To our knowledge, 3D sphere assays has never been used to isolate the stem-like subset in human CCA. Obtained spheres (SPH) were subjected to a global characterization in terms of tumorigenic potential in immune-deficient NSG mice (subcutaneous tumorigenic engraftment with low cell number, limiting dilution and serial transplantation assay), resistance to a panel of common chemotherapeutic drugs (cisplatin, 5-fluorouracil, oxaliplatin, gemcitabine), molecular activation of key liver cancer-, CSC-, ESC-related signaling pathways (use of pathway-focused PCR arrays). Results were compared with those obtained with the same CCA cells grown in standard adherence condition as monolayer (MON), so not potentially enriched in stem-like cells. Expression of key significant CSC surface markers were confirmed using transcriptome data from CCA patients.

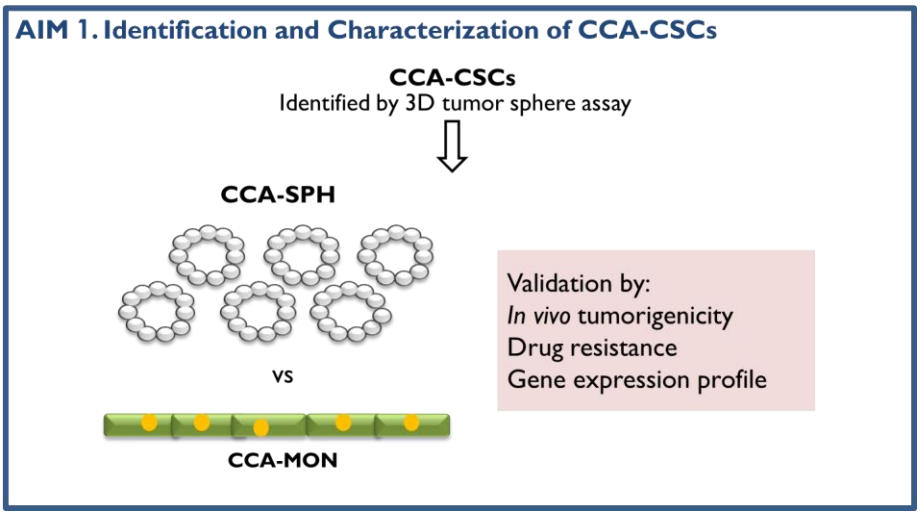

2. Confirmation of the existence of a peculiar CSC-associated TAM-compartment as result of bioactive CCA stem-like cells

CD14+ obtained from healthy donors were placed in presence of 30% of tumor-conditioned medium (CM) for 6h to verify SPH-dependent monocyte recruitment. Analysis of monocyte migration towards tumor-CM was performed. Moreover, the same CD14+ cells were cultured with 30% of tumor-CM for 6 days to allow monocyte differentiation towards macrophages. Specifically, tumor-CM was derived from CCA-SPH as well as CCA-MON (as control) in order to highlight the effect of conditioned medium presumably enriched in factors released by tumor stem-like compartment. End-point analysis concerning the impact on macrophage differentiation/activation comprised evaluation of macrophage markers' expression (including surface proteins and gene expression) and presence of macrophage functional properties (invasion, adhesion). A global investigation of CCA patient-associated TAM distribution and phenotype was performed, also in order to validate results of *in vitro* obtained SPH-specific TAM subpopulation.

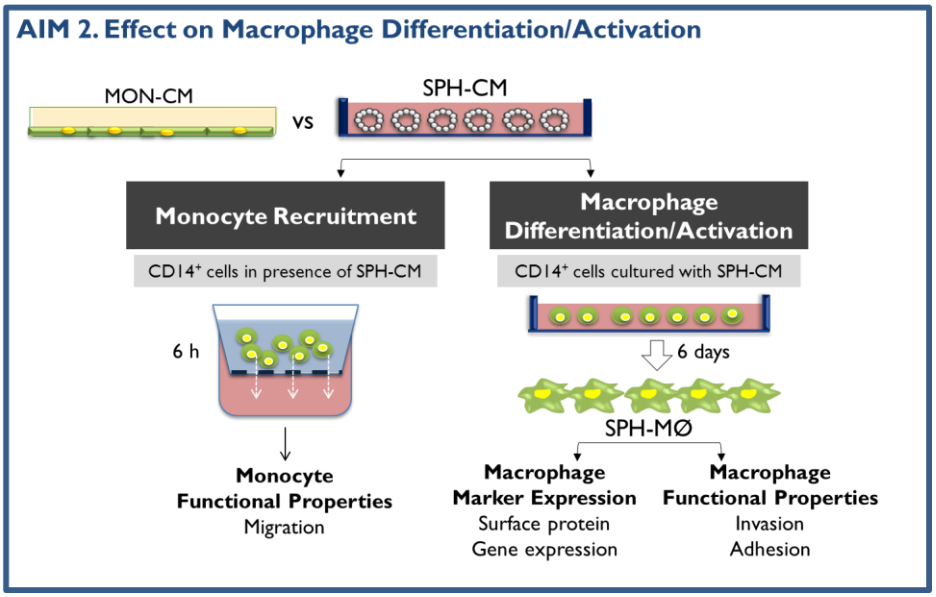
AIM 2. Effect on Macrophage Differentiation/Activation
MON-CM
vs
SPH-CM
Monocyte Recruitment
Macrophage Differentiation/Activation
CD14+ cells in presence of SPH-CM
CD14+ cells cultured with SPH-CM
6 h
6 days
SPH-MØ
Monocyte Functional Properties
Migration
Macrophage Marker Expression
Surface protein
Gene expression
Macrophage Functional Properties
Invasion
Adhesion

3. METHODS

3.1 Patient Samples

All patients gave written, informed consent. Study was approved by local institutional review boards. CCA samples and peritumoral non-cancerous liver were obtained from patients submitted to surgical resections (Department of Hepatobiliary Surgery, Istituto Clinico Humanitas). Distinctions between iCCA and pCCA were based on clinical records including surgical reports.

3.2 Mice

The Humanitas Animal Care and Research Advisory Committee approved housing and experimental animal procedures. NSG mice (Jackson Laboratory) were used in all experiments. The mice were used at 6 weeks of age, in accordance with the guidelines and with the approval of the local Experimental Animal Committee [225].

3.3 Sphere Assay

To calculate sphere-forming efficiency, CCA cells were single-cell sorted into 96-well plates coated with an Ultra-Low Attachment Surface (Corning) using a FACS Aria (BD Biosciences). The cells were grown in anchoring-independent conditions with selective serum-free DMEM/F12 medium supplemented with 1X B27 supplement minus vitamin A (Life Technologies), human recombinant EGF (hrEGF) (R&D System) (20 ng/mL), and basic FGF (bFGF) (R&D System) (20 ng/mL). After 10 days, the spheres formed were counted, and the sphere-forming efficiency (SFE) was calculated by dividing the number of spheres formed by the original number of single cells seeded and expressed as a percentage. An Olympus IX81 confocal microscope in a closed humidified chamber at 37°C in a CO_2-enriched atmosphere with a 20x objective was used to obtain pictures of sphere morphology [63, 216].

Additionally, large-scale sphere cultures were established plating 1.8 x 10^3 cells/cm^2 into poly (2-hydroxyethyl methacrylate) (poly-HEMA [Sigma Aldrich]) coated dishes. To prevent cell aggregation, 1% methylcellulose (R&D System) was added to the culture medium.

3.4 Monocyte Isolation and Macrophage Differentiation

Human monocytes were obtained from healthy blood donor buffy coats by gradient centrifugation using a Ficoll gradient (GE Healthcare) and further purified from peripheral blood mononuclear cells (PBMC) by magnetic-activated cell sorting (MACS) using CD14 microbeads (Miltenyi Biotech). After MACS purification, two fractions were obtained: the CD14+ fraction and the eluate (composed of all PBMC CD14- cells). The purity of CD14+ cells was >90%.

Macrophages and tumor-conditioned macrophages were obtained by culturing 1 x 10^6/mL monocytes for 6 days in RPMI 1640 with 10% FBS supplemented with 100 ng/mL of recombinant human M-CSF (Peprotech) or in presence of 30% CCA sphere- or monolayer-CM.

M1 and M2 polarized macrophages were obtained by culturing 1 x 10^6/mL monocytes for 6 days in RPMI 1640 with 10% fetal bovine serum (FBS) supplemented with 100 ng/mL of recombinant M-CSF. M1 cells were polarized by stimulating M-CSF macrophages for 24 h with lipopolysaccharides (LPS) (100 ng/mL) (Peprotech) and interferon gamma (IFN-γ) (20 ng/mL) (Peprotech). M2 cells were polarized by stimulating human M-CSF macrophages for 24 h with IL-4 20 ng/mL (Peprotech).

3.5 Cell Cultures

HUCCT1, CCLP1 and SG231 cells, from intrahepatic bile ducts, were a kind gift from Dr. A.J. Demetris (University of Pittsburgh, Pittsburgh,PA) and were cultured as described [227-229]. The primary CCA4 cell line (mucinous iCCA, female 50 years old) was a kind gift from Dr. D. Alvaro (University La Sapienza, Rome, Italy) [77]. Human immortalized non-malignant cholangiocyte cell line H69 from Dr. G. J.

Gores, Mayo Clinic, Rochester, MN and primary human intrahepatic cholangiocyte cell line HiBEC from ScienCell. Experiments were performed using cells between passages 2 and 8. All cell lines were incubated at 37°C in a humidified chamber supplemented with 5% CO_2 [227].

3.6 Preparation of Conditioned Medium

To collect tumor-CM, 1.8 x 10^3 CCA cells/cm^2 were grown as spheres for 7 days, while 5.5 x 10^3 CCA cells/cm^2 were grown as monolayer for 5 days. Then, the medium was discarded, the plates were rinsed two times with saline solution, and the cells were incubated with fresh medium for 24 h. CM was harvested and clarified by centrifugation, and the supernatants were filtered at 0.20 µm and used fresh or stored at -80°C [181].

3.7 Enzyme-Linked Immunosorbent Assay (ELISA)

The concentration of 37 molecules (cytokines, chemokines, interleukins and other factors described in the Results section) in the sphere- or monolayer-CM was measured using commercially available ELISA kits according to the manufacturer's instructions (R&D Systems). RPMI 1640 with 10% FBS, DMEM with 10% FBS, or serum-free DMEM/F12 was used as a negative control. A seven-point standard curve was used to calculate the concentration of the molecules. ELISA expression values were log2 transformed and log Fold-change values were created by subtracting control from treated log2 intensities, for each molecule and each cell line analyzed. When both treated and control Elisa expressions were null, then "NA" was used. Molecules with "NA" in all conditions and cell lines were excluded from further analysis. A matrix with four columns (cell lines) and 23 rows (proteins with at least one log Fold-change available) was loaded in TMeV (http://www.tm4.org/) [230] and hierarchical clustering with "Euclidean distance" as similarity metrics and "average" as linkage method was applied to cluster proteins and cells according to their expression profiles upon treatment.

3.8 Lymphocyte Reaction Assay

Human peripheral blood lymphocytes (PBL) were obtained from healthy blood donor buffy coats by gradient centrifugation using a Ficoll gradient (GE Healthcare) and further purified from PBMC by MACS using CD4+ T cell isolation kit (Miltenyi Biotech). CD4+ were collected and labeled with carboxyfluorescein succinimidyl ester (CFSE) 2 µM (eBioscience) for 10 min at 37°C. Cells were washed extensively and 2 x 10^5 cells/well were cultured in round-bottomed 96-well plates in RPMI-1640 with 10% FBS with 30% of sphere- and monolayer-CM for 5 days. As a negative control we used CD4+ not stimulated. At day 5, cells were collected and stained against CD4 using the described conjugated antibody.

3.9 Flow Cytometry

A total of 1 x 10^5 purified monocytes, *in vitro*-differentiated macrophages, CD4+ or patient-derived PBMCs were washed and resuspended in fluorescence-activated cell sorting (FACS) buffer (phosphate buffered saline [PBS] plus 2% FBS). The anti-human antibodies used included anti-CD14-PerCP/Cy5.5, anti-CD45-PB, anti-CD4-PE and anti-CD3-APC (Biolegend); anti-CD206-PE, anti-CD56-APC, anti-CD68-PE, and anti-HLA-DR-PerCP/Cy5.5 (BD Biosciences); and anti-CD115-PE (R&D System). Dead cells were excluded using the LIVE/DEAD Fixable Aqua or Violet Dead Cell Stain Kit (Life Technologies). The cells were stained for 20 min at 4°C and detected using an LSRFortessa (BD Biosciences). A fluorescence minus one (FMO) sample, containing all antibodies except the one of interest, was used as a negative control. Data analysis was performed with the FlowJo software (FlowJo, LLC).

3.10 Tube Formation Assay

The tube formation assay was carried out as described [231], with slightly modifications. In brief, 96-well plates were coated with 70 µl of pre-thawed growth factor-reduced Matrigel (BD Biosciences). The plate was then kept at 37 °C for 1 h to allow the matrix solution to gel. 1.5 x 10^4 HUVEC cells were

resuspended in the respective conditioned media, added to each well and incubated at 37°C for 24 h. Images were acquired under an inverted microscope. Pro-angiogenic activity was quantified by measuring the number of tube structures formed between discrete endothelial cells in each well. Each experiment was performed in triplicate.

3.11 Cell Migration and Invasion Assay

CD14+ cells (1.5 x 10^6/well) were seeded into the upper chamber of 6-well transwell supports with a membrane with an 8 µm pore size (Corning) in serum-free RPMI 1640 (migration assay). Tumor-conditioned macrophages (9 x 10^4/well) were placed into the upper chamber of a 24-well BioCoat™ Matrigel® Invasion Chamber with a membrane with a 0.4 µm pore size (BD Biosciences) in RPMI 1640 supplemented with 10% FBS (invasion assay). The cells were allowed to migrate or invade toward the lower compartment of the system, which contained either 30% tumor-CM or RPMI 1640 alone. After 6 h (migration assay) or 18 h (invasion assay) of incubation at 37°C, the cells that had not penetrated the filter were removed with cotton swabs, and cells that had migrated to the lower surface of the filter were fixed with methanol, stained with Diff Quick solutions, and photographed with an Olympus BX51 microscope with a 20x objective. The values for migration/invasion were expressed as the average number of migrated/invaded cells per microscopic field (20x) over five fields. Each experiment was performed in triplicate [232].

3.12 Gene Expression

The total RNA was extracted with the RNeasy kit (Qiagen) according to the manufacturer's instructions. The RNA concentration and quality were measured using an optical Nanodrop ND1000 spectrophotometer (Thermo Scientific).

Total RNA (500 ng) from the CCA spheres or monolayer was reverse transcribed into cDNA using an RT² First Strand Kit (SabBioscience, Qiagen) according to the manufacturer's instructions. RT2 Profiler™ human cancer stem cell (PAHS-1776Z),

human embryonic stem cell (PAHS-081Y) and human liver cancer cell (PAHS-133Z) 384-well PCR arrays (SabBioscience, Qiagen) were performed for quantitative PCR using the ABI ViiA™ 7 System (Applied Biosystems) with the following cycling conditions: 10 min at 95°C, 40 cycles of 15 s at 95°C followed by 1 min at 60°C and a final infinite 4°C hold. Data were centered and normalized, and hierarchical clustering of genes/samples using centered correlation metrics with complete linkage was performed. The grouping of the genes from top to bottom is given for each heatmap.

Total RNA (500 ng) from tumor-conditioned macrophages was transcribed with a High-Capacity cDNA Reverse Transcription Kit (Applied Biosystems). PCR was performed on the cDNA with gene-specific primer pairs (see table below). The qPCR human primers for CD163 were purchased from Qiagen. Changes in the mRNA expression level of target genes were detected using FAST SYBR-Green PCR Master Mix and the 7900HT Fast Real Time PCR System (Applied Biosystems). The cycling conditions consisted of 20 s at 95°C, 40 cycles of 1 s at 95°C followed by 20 s at 60°C, and a final infinite 4°C hold. The mRNA levels of glyceraldehyde 3-phosphate dehydrogenase (GAPDH) were used for normalization. The fold difference ($2^{-\Delta\Delta Ct}$) was calculated using the ΔCt of monolayer-conditioned macrophages as a control. All reactions were performed in triplicate.

Table 1. List of Primers

Gene	Primer Forward	Primer Reverse
CD80	GGGAAAGTGTACGCCCTGTA	GCTACTTCTGTGCCCACCAT
CXCL9	TTTTCCTCTTGGGCATCATC	TCAATTTTCTCGCAGGAAGG
CXCL10	AGCCAATTTTGTCCACGTGT	TGATGGCCTTCGATTCTGGA
ALOX15	CTTGCTCTGACCACACCAGA	GCTGGGGCCAAACTATATGA
CCL18	GTGGAATCTGCCAGGAGGTA	CCCAGCTCACTCTGACCACT
CCL17	CACCCCAGACTCCTGACTGT	CCCTCACTGTGGCTCTTCTT
CCL5	TATTCCTCGGACACCACACC	ACACACTTGGCGGTTCTTTC
OA	TCCGACGAAACCTTCCTCAA	TCCCCGAAGCTCCACTTCTA
OPN	TTGCAGTGATTTGCTTTTGC	GTCATGGCTTTCGTTGGACT
AD10	CTGGCCAACCTATTTGTGGAA	GACCTTGACTTGGACTGCACTG
AD17	GAAGGCCAGGAGGCGATTA	CGGGCACTCACTGCTATTACC
FN	ATCAACCTTGCTCCTGACAG	GTCTCAGTAGCATCTGTCAC
MMP2	TTGACGGTAAGGACGGACTC	ACTTGCAGTACTCCCCATCG
EDA	CGGGATCCAACATTGATCGCCCTAAAGG	TCCCCCGGGTGTGGACTGGGTTCCAATC
GAPDH	GATCATCAGCAATGCCTCCT	TGTGGTCATGAGTCCTCCCA
CD13	CAGTGACACGACGATTCTCC	CCTGTTTCCTCGTTGTCCTT
LGR5	CTTCCAACCTCAGCGTCTTC	TTTCCCGCAAGACGTAACTC
VEGFR1	ATTTGTGATTTTGGCCTTGC	CAGGCTCATGAACTTGAAAGC
VEGFR2	GTGACCAACATGGAGTCGTG	CCAGAGATTCCATGCCACTT
VEGFR3	CATCCAGCTGTTGCCCAGG	GAGCCACTCGACGCTGATGAA
IL4R	GCGTCTCCGACTACATGAGC	GGTTGCTCCAGGTCAGCAGC
IL13Ra1	AGGATGACAAACTCTGGAG	CTCAAGGTCACAGTGAAGG
IL13Ra2	ATACCTTTGGGACTTATTCC	TGAACATTTGGCCATGACTG
CD44	TTATCAGGAGACCAAGACAC	ATCAGCCATTCTGGAATTTG
ITGA5	AAGCTTGGATTCTTCAAACG	TCCTTTTCAGTAGAATGAGGG
ITGB3	CTCCGGCCAGATGATTC	TCCTTCATGGAGTAAGACAG
SDC4	CAGGGTCTGGGAGCCAAGT	GCACAGTGCTGGACATTGACA
SDC1	TACTAATTTGCCCCCTGAAG	GATATCTTGCAAAGCACCTG

3.13 Adhesion Assay

Tumor-conditioned macrophages (15 x 10^4/dish) were seeded onto 60 mm dishes coated with fibronectin (FN) (Millipore) in RPMI 1640 supplemented with 10% FBS and allowed to adhere to the surface. After 10 min, non-adherent cells were discarded, and cells that had adhered to the surface were fixed with

methanol, stained with Diff Quick solutions, and photographed with an Olympus BX51 microscope with a 10x objective. The values for adhesion were expressed as the average number of adherent cells per microscopic field (10x) over five fields. Each experiment was performed in triplicate [232].

3.14 Drug Treatment and MTT Assay

The cell viability was measured with the 3-(4,5-dimethylthiazolo-2-yl)-2,5-diphenyltetrazolium bromide (MTT) (Sigma-Aldrich) assay. CCA cell lines were cultured as spheres or monolayers in 96-well plates and then exposed to the following drugs or relative vehicles: cisplatin (0-112 μM) (Sigma-Aldrich) for 24 h, oxaliplatin (0-500 μM) (Sigma-Aldrich) for 24 h, 5-Fluoruracil [5-FU (0-40 mM)] (Sigma-Aldrich) for 48 h and gemcitabine (0-1000 μM) (Axxora) for 72 h. The optimal drug concentrations were determined by calculating the 50% inhibitory concentration values (IC50) in CCA-monolayer cultures. Five replicates were performed for each condition. At the end of the treatments, 20 μL of 5 mg/mL MTT solution was added to each well, and the plates were incubated for 3 h at 37°C. Next, 100 μL of 100% dimethyl sulfoxide (DMSO) per well was added to solubilize the precipitate, and the absorbance of each well was measured with a VersaMax microplate reader (Molecular Devices Corporation) at a wavelength of 570 nm. The percent viability was calculated as follows: (sample OD570-blank control OD570)/(control OD570- blank control OD570) x100 .

3.15 Immunohistochemistry (IHC)

Frozen tissues form SPH and MON derived tumors were cut at 8 μm put on SuperFrost slides and stored at -80°C. For Sirius red staining, tissues were fixed in 4% neutral buffer formalin for 5 min. Tissues were placed in 0.1% of Sirius red solution for 1 hour and then washed under tap water for 20 min. Haematoxylin were used for counterstaining and then mounted with Eukitt (Sigma-Aldrich). For immunohistochemistry tissues were fixed with 4% paraformaldehyde for 15 minutes, endogenous peroxidase was blocked with H_2O_2 0.03% for 5 min, then

unspecific binding sites were blocked with Rodent Block M (Biocare Medical) for F4/80 and alpha smooth muscle actin (α-SMA) while PBS+2% bovine serum albumin (BSA) was used for CD31 for 30 minutes. Rat anti mouse F4/80 (MCA497g, clone Cl:A3-1, AbD Serotec) were diluted 1:400, goat anti mouse CD31 (AF3628, R&D System) were diluted 1:1000 and mouse anti mouse α-SMA (A 2547, clone 1A4, Sigma-Aldrich) were diluted 1:200 and then incubated for 1 hour at room temperature. As secondary antibody Rat on mouse HRP polymer (RT517 L, Biocare Medical) were used for F4/80, goat on rodent (GHP516 L, Biocare Medical) were used for CD31, mouse on mouse HRP (MM620H, Biocare Medical) were used for α-SMA. Reactions were developed with 3,3'-Diaminobenzidine (DAB) (Biocare Medical) and counterstained with haematoxylin. Slides were then dehydrated through an ascending scale of alcohols and xylene, and mounted with Eukitt.

Human CCA specimens were fixed in 10% formalin before being processed in paraffin. Hematoxylin and eosin-stained sections from each tissue block were evaluated to obtain the diagnosis and the pathological T stage. A representative block for each case was selected for immunohistochemical analysis with CD68 and CD163 markers. The primary antibodies included anti-CD163 (Rabbit Monoclonal clone EPR4521 dilution 1:250, Epitomics), anti-CD68 (Mouse Monoclonal clone PGM-1 dilution 1:60), anti-CD44 (555476, 1:50 dilution; BD Pharmingen), anti-EPCAM (clone VU-1D9; 1:1000 dilution; Merck Millipore). The chromogen diaminobenzidine (DAB) was used for CD163, CD44 and EPCAM whereas FAST RED was used for CD68. The tissue sections were counterstained with Mayer's hematoxylin. The negative control was performed by substituting the primary antibody with non-immune serum at the same concentration. The control sections were treated in parallel with the samples.

The ratio between CD163 intensity values evaluated in tumor front and intralesion were calculated and log transformed. One sided Student t-test was then applied to log ratios in order to compare G1 to G2-G3 and such test

yielded a *p-value* of 0.006, with average G2-G3 values bigger than average G1 values. Fisher Exact test was applied as well, to test any association between grade and CD163 log ratios and this gave a *p-value* of 0.05, with 1.1 used as cut-off.

3.16 *In Vivo* Study

In vivo experiments were performed in accordance with the guidelines and approval of the local Experimental Animal Committee. The following materials were used: 1,000 sphere- or monolayer-derived cells to measure the tumorigenic potential of CCA cells and 1,000 monolayer-derived cells and 300 macrophages for TAMs + CCA monolayer co-injection experiments. The cells were dissociated into single-cell suspensions and resuspended in 100 µL of DMEM and reduced Matrigel growth factor (BD Bioscience) (1:1), and the mixture was subcutaneously (s.c.) injected into the right flank of 6-week-old NSG mice. Tumor growth was monitored, and the diameter of the growing tumors was measured in millimeters every week using a caliper. The animals were sacrificed when the xenografts reached 2.0 cm in diameter [216, 225, 233]. The limiting dilution analysis was performed by sorting 1,000/100/10 alive cells from dissociated CCA monolayer and spheres. Web-based Extreme Limiting Dilution Analysis (ELDA) statistical software (http://bioinf.wehi.edu.au/software/limdil/index.html) was used [234].

3.17 TAM Isolation from Human CCA Resections

Human TAMs were isolated from fresh CCA samples as previously described with slight modifications [225]. Briefly, the tissues were minced into small (1 to 2 mm) pieces and digested with PBS containing 2 mg/ml collagenase D (Roche) at 37°C for 2 h. The resulting suspension was sequentially filtered through sterile 100- and 70-µm nylon cell strainers. The cells were then centrifuged at 1,400 RPM for 30 min with Ficoll (GE Healthcare). CD14+ macrophages were further isolated by MACS using CD14 Microbeads (Miltenyi Biotec) according to the manufacturer's instructions.

3.18 Statistical Analysis, CCA Patient Data Base

Graphpad Prism v5 was used for data analysis. The error bars represent 1+/- SEM. The *p value* was calculated with Student's *t* test. The statistical significance and *p-value* are shown when relevant.

The GSE26566 series matrix containing expression values from Illumina humanRef-8 v2.0 expression beadchip Array [transcript (gene) version] of 104 CCA samples was downloaded from GEO [6]. Differences in gene expression of specific genes of tumor tissue (T) versus surrounding liver (SL) and CCA epithelial compartment (EPI) versus stromal component (S) were evaluated.

Pearson correlation between gene pairs was calculated using R and the "cortest" function, yielding correlation coefficients and *p-values*.

4. RESULTS

4.1 Human CCA-Spheres Retain Stem-Like Tumor-Initiating Features

CCA-stem like cells were identified by using a functional tool of 3D culture system based on defined serum-free medium, as shown in many patient-derived tumors. First, established (SG231, HUCCT1, CCLP1) [227-229] and primary human intrahepatic CCA-derived (CCA4) cell lines [77] were tested for sphere-forming efficiency (SFE) as a representation of tumor stem-like subset. To this end, CCA FACS-sorted single cells were cultured in 3D non-adherent condition in a 96-well plate. Importantly, single-cell sorting prevents formation of cell-aggregation and avoids large fraction of non-stem cells to form clusters. Accordingly, only those cells that possessed stem-like properties were able to survive in the selective condition and to grow in non-adherent condition as 3D-SPH. As control, immortalized cholangiocytes (H69) and human intrahepatic biliary epithelial cells (HiBECs) were tested for sphere initiation capacity. As expected, only malignant cholangiocytes retained sphere-forming potential in contrast to normal counterparts (Figure 5A). However, CCA-SPH revealed a high grade of heterogeneity in terms of efficiency (HUCCT1 and CCLP1, approximately 20%; SG231 and CCA4, 10%), size and morphology (Figures 5A-6A).

Next, an extensive characterization, including evaluation of *in vivo* tumorigenicity in immune-deficient NSG mice, drug-responsiveness and gene expression analysis of CCA-SPH, was performed.

To assess CCA-SPH ability to generate tumors, spheres formed by HUCCT1, SG231, CCLP1 and CCA4 were dissociated and 1,000 cells s.c. injected into NSG mice (Figures 5B-D). Consistently with their *in vitro* SFE (Figure 5A), CCA-SPH were highly tumorigenic and engrafted 100% of transplanted mice in all examined cell lines albeit with differences in tumor size (Figures 5B-D). In contrast to CCA-MON, including H69-MON, CCA-SPH were responsible for early tumor initiation and formation (3 weeks for HUCCT1, CCLP1; 5 weeks for SG231; 6 weeks for CCA4)

during 13 weeks of observation. In addition, SPH-derived tumors (SPH-T) showed a large difference in terms of tumor weight and size compared to CCA-MON derived tumors (MON-T) (Figure 5D), indicating that SPH-T retained high tumorigenic potential when xenotransplanted in animal hosts and represented an important source of *de novo* tumor growth. The most common method to determine frequency of self-renewing cells within tumors is a limiting-dilution cell transplantation assay. Thus, due to slight differences in tumor potential between SPH and MON in CCLP1, we specifically performed limiting-dilution transplantation assay in NSG mice with this cell line. After s.c. injection of 1,000, 100 or 10 cells of both CCLP1-MON and SPH conditions, data analysis using ELDA software revealed a significant 20.3-fold increase in the absolute number of tumor-initiating fraction (TIF) within CCLP1-SPH (TIF=1/25) compared to MON (TIF=1/505) ($p=0.0011$, Figure 5E). Indeed, as few as 10 SPH cells produced tumors, whereas 1,000 MON cells gave rise to fewer tumors at 13 weeks (Figure 5E) confirming that SPH were remarkably enriched in self-renewing CCA-propagating cells. Additionally, since self-renewing stem-like cancer cells have an unlimited ability to promote tumor growth, capability for serial transplantation was also tested (Figure 5F). in this case cells were re-isolated from CCLP1-T established from both 1000 SPH and MON cells, propagated in short-term cultures and re-transplanted into secondary recipient mice in order to verify SPH-capability to generate the same tumors through successive tumor generations. Notably, SPH not only sustained tumorigenic potential in serial transplantations but also progressively improved in tumor frequency. Conversely, corresponding MON showed either dramatic increase in tumor latency and decrease in tumor incidence at later generations (Figure 5F). Together these data indicated that, in accordance with long-term self-renewal potential, SPHs significantly maintained tumorigenic potential through diverse xenograft-generations while MON reduced it.

Furthermore, because drug-resistance represents a key feature of cancer stem/initiating cells, 3D cultures were tested for susceptibility to chemotherapeutic agents. Indeed, in presence of common anti-CCA drugs such as cisplatin, 5-fluorouracil, oxaliplatin and gemcitabine, CCA-SPH revealed a better survival rate compared to parental CCA-MON, as measured by proliferation MTT assays and indicated by the IC50 (Figure 6B). Although a remarkable heterogeneity in terms of drug-sensitivity, SPH-resistance was a common phenomenon observed across all CCA lines.

Next, to corroborate our *in vivo* and *in vitro* findings, an extensive molecular characterization of CCA-SPH was achieved by PCR-arrays specific for CSC, liver cancer and ESC pathways. In accordance with the observed heterogeneity in SFE, tumor potential and drug-resistance, clustering analysis of differentially expressed genes for each pathway revealed cell line-specific SPH gene-enrichment as compared to respective MON (Figure 7A-C, Figure 8A). Indeed, CCLP1, HUCCT1 and CCA4 SPH presented augmented expression for CSC- (55-69%) and liver cancer-related (61-77%) genes, whereas SG231-SPH retained the highest fraction of ESC-related (37%) genes (Figure 8A). However, a core of 30 common deregulated genes in all CCA-SPH was identified. Specifically, expression of 23 CSC-genes, including key molecules for pluripotency and self-renewal (*SOX2,* POU class 5 homeobox 1 *[POU5F1],* Kruppel like factor 4 *[KLF4],* B cell-specific moloney murine leukemia virus integration site 1 *[BMI1], NOTCH1, MYC,* KIT ligand *[KITLG],* lin-28 homolog A *[LIN28A],* mastermind like transcriptional co-activator 1 *[MAML1], YAP1*), drug-resistance and survival (*ABCG2,* large tumor suppressor kinase 1 *[LATS1],* nuclear factor kappa B subunit 1 *[NFKB1],* nitric oxide synthase 2 *[NOS2])*, metastasis (TGF-β receptor 1 [*TGFBR1],* bone morphogenetic protein 7 *[BMP7],* FGF receptor 2 *[FGFR2]*) and stem-like surface markers (*CD24, CD44,* prominin 1 *[PROM1],* Thy-1 cell surface antigen *[THY1], EPCAM*), resulted enhanced. Moreover, this common gene-set revealed overexpression of 6 hepatic oncogenic drivers (cyclin dependent kinase inhibitor

1A [*CDKN1A],* B-cell lymphoma 2 like 1 *[BCL2L1],* β-catenin 1 *[CTNNB1],* insulin like growth factor 2 *[IGF2],* integrin subunit beta 1 *[ITGB1],* lymphoid enhancer binding factor 1 [*LEF1]*) and key ESC factors such as hepatocyte nuclear factor 4 (*HNF4)* (Figure 7B), in addition to the well-described liver CSC markers CD13 and LGR5 (not included in the arrays) (Figure 7C). Accordantly, further confirmation of stem-cell content was considered at protein level by FACS-analysis. Indeed, superior expression of CD13, CD44, THY1 and EPCAM were verified in CCA-SPHs from all cell lines (Figures 7D-8B), thus suggesting that 3D cultures were effectively enriched for tumorigenic cells endowed with stem-like molecular traits.
Particularly, presence of the most significant CSC surface markers, such as *CD44, PROM1, THY1* and *EPCAM* was validated using CCA transcriptome of 104 patient database [6] (Figure 8C).

Whereas gene expression profile was consistent with stem-like traits of SPH-condition, we also tested the strength of 3D culture system compared to antigenic approach. To this end, primary CCA4 was immune-sorted for standard stem-related marker THY1 and verified for *in vitro* sphere-ability. However, no significant differences in *in vitro* self-renewing capability were found between THY+ and parental cells as control (Figure 8D, left). Next, we combined expression of stem-like markers to sphere-forming capacity, thus THY+ cells were grown in 3D condition (THY+ SPH) and tested for tumorigenic potential. Notably, *in vivo* analysis revealed similar TIF subset between THY+ SPH (TIF=1/47.8) and parental SPH (TIF=1/35.7) (*p*=0.2028 Figure 8D, right) also confirmed by expression of liver cancer, CSC and ESC-like markers (Figure 8D, down). Rather, parental CCA4 cells seem to be even slightly more enriched in stem-like fraction compared to THY+ cells. These results indicated that 3D culture system potentially represents a reliable tool and valid alternative to the antigenic approach for CCA stem-like cell selection and enrichment.
Altogether, this broad functional and molecular characterization proposed the existence of a stem/progenitor-like compartment in human CCA identified by

3D culture system. Indeed, CCA-SPH exhibited typical stemness hallmarks, such as up-regulated stem-cell biomarkers, augmented drug-resistance and enhanced capability to initiate malignancy.

4.2 CCA Stem-Like Compartment Educates Macrophage Precursors Toward Acquisition of CSC-Associated TAM Phenotype

In addition to diverse cellular components and ECM, CSC-milieu is enriched with tumor cell products such as growth factors, cytokines, prostaglandins and diverse protein factors [235]. Thus, to mimic a bioactive CSC-niche, freshly isolated healthy donor circulating monocytes (CD14+) were exposed to CCA-SPH-CM and tested for 1) monocyte chemotactic recruitment based on migration properties and 2) macrophage (MØ) differentiation verified by analysis of marker expression and functional properties (Figure 9). First, by using a chemotaxis chamber, a higher number of CD14+ migrating towards SPH-CM gradient than MON-CM was recorded within 6h, suggesting that SPH-CM acted as a strong monocyte attractor (Figure 9A). Hence, greater amount of recruited mononuclear cells by CCA-SPH maybe find a potential explanation in creating a tumorigenic-niche supporting CSC-maintenance.

It is widely accepted that MØs constitute an extremely heterogeneous population, of which the extremes are schematically identified as M1 and M2. It is now generally recognized that TAMs are constituted by MØ differentiating from blood monocytes rather than tissue resident MØ and show a M2-like cancer-promoting phenotype [236-238]. Therefore, to determine the effect of CCA stem-like component on MØ-precursors, healthy donors CD14+ were cultured in presence of CCA SPH-CM, and after 6 days, investigated for MØ-differentiation and polarization. Consistently with observed changes in morphology (data not shown), by employing a panel of conventional markers typically used for M0 classical differentiation (CD115, M-CSF receptor), M1 (HLA-DR, human leukocyte antigen and MHC class II) and M2-TAM (CD206, macrophage mannose

receptor) polarization (Figure 10A), FACS-analysis revealed that in presence of CCA SPH-CM, *in vitro*-educated CD14+ expressed higher CD115 level in contrast to CD14+ exposed to MON-CM or M-CSF, which acted as control for M0 classical differentiation (Figure 9B, Table 2). As expected and regardless SPH or MON culture conditions, CCA-CM induced MØ-differentiation of human monocytes as indicated by the presence of CD14+ CD68+ cells in both MON and SPH–CM (Figure 10B-C). Notably, more than 94% of SPH-educated CD14+ expressed CD14, CD68 and CD115 markers (Figure 9B, Figure 10B-C). Moreover, differentiation towards neutrophil lineage and dendritic cells was excluded by CD66b and CD1a staining [181, 239], also confirmed in M0-MØs (Figure 10D-E). Furthermore, CCA-SPH activated-MØ (SPH MØ) expressed greater levels of CD206 and HLA-DR TAM-like markers in contrast to CCA-MON activated-MØ (MON MØ) (Figure 9B, Table 2). All these data indicated that both MON- and SPH-CM induced MØ-differentiation, but SPH-CM was responsible for MØ-acquisition of a specific CSC-dependent phenotype.

Likewise, in *in vitro*-educated MØs, expression of genes belonging to M1 (e.g., *CD80, CCL5, CXCL9, CXCL10*), M2 (arachidonate 15-lipoxygenase (*ALOX15), CCL18*, and *CCL17*) and TAM–like (*CD163*) categories, including genes involved in ECM-remodeling and adhesion such as osteoactivin (*OA*), fibronectin (*FN*), osteopontin (*OPN*), metalloproteinase ADAM (*AD10, AD17*), and *MMP-2*, were determined (Figure 9C). Notably, SPH MØs retained unique molecular features with concomitant expression of TAM-like (e.g., *CD163*), M1-like (e.g., *CCL5, CXCL9, CXCL10*), M2-like (e.g., *CCL17, CCL18*) and matrix remodeling-related (e.g., *OA, AD17* and *MMP2*) genes (Figure 9C).

Consistent with our gene expression data, SPH MØs possessed greater adhesion ability on FN-support (Figure 9D) and better invasion capacity as shown by *in vitro* Matrigel-coated transwell assays (Figure 9E) [232] compared to MON MØs. Both these features are likely associated with dynamic properties of TAM-like cells within tumor-initiating niche because of their incessant and deregulated activity

regarding ECM-reorganization and turnover. Owing to their potential ability to remodel tumor-stroma, SPH MØs may invade and at the same time adhere to the ECM-component, thus providing sustenance to tumor-environment. This result showed concordance with the evidence that mononuclear phagocytes support stem-cell functions, thus contributing to tissue repair and remodeling [211].

4.2.1 CCA humanized-mice recapitulate in vitro educated-MØ traits

To translate our *in vitro* data in a human-like setting, we analyzed the *in vivo* immunological response of human mononuclear cells to CCA stem-like component at tumor site. Thus, a co-transplantation of human PBMC (hPBMC) and patient derived CCA4-SPH into NSG mice was performed (Figure 11A-B, Figure 12A). As already extensively demonstrated, NSG mice bearing a targeted mutation in IL2rγ gene (responsible for a severe defective murine immune component) support considerably high levels of human hematopoietic and lymphoid cell engraftment providing an exciting substitute for human immunobiology studies [225]. Therefore, CCA4-SPH-T bearing mice (when tumor size reached 50 mm^3, 51 days after s.c. injection) were engrafted with three successive doses of hPBMC ($15x10^6$/dose) intravenously (i.v) in the retro-orbital sinus. Efficiency of human engraftment was tested 6 days after first hPBMC dose and presence of human circulating mononuclear cells (mCD45-hCD45+hCD14+) was confirmed in mouse peripheral blood by FACS-analysis. In agreement with published data [225], frequency of mCD45-hCD45+hCD14+ circulating cells were almost 0,7% indicating an effective human cell-engraftment (Figure 12B-C).

At the end of experiment, both CCA4-SPH-T and CCA4-MON-T were removed and FACS-analyzed for human mononuclear cells presence. Well-matched with *in vitro* data, CCA4-SPH-T retained higher number of human CD45+CD68+ (83.55%) in comparison with CCA4-MON-T (70%) (Figure 11A). Again, infiltrated human CD45+CD14+ in CCA4-SPH-T displayed enhanced expression of M1-like (e.g., *CD80, CXCL9*), M2-like (e.g., *CCL18, CCL17*) and matrix remodeling-related

genes (e.g., *OPN, AD10, AD17, MMP2*, full-length FN and oncofetal FN (*ED-B*)) (Figure 11B).

Collectively, our *in vitro* and *in vivo* observations indicated that SPH recruit higher amount of mononuclear cells at tumor site and CCA-SPH MØs retain a unique phenotype compared to MON MØs.

4.2.2 Mixed phenotype of infiltrating-MØs in CCA patients

Since a broad analysis of human CCA-TAMs has not been provided yet, we corroborated our *in vitro* data with a global investigation of CCA patient-associated MØs. Abundance, phenotypes and distribution of MØs residing in CCA intratumoral and peritumoral tissue were evaluated via IHC. Paraffin-embedded tissue samples from 23 CCA patients were tested for tumor-promoting MØs (CD163) presence. An immunohistochemical analysis of tumor sections showed that CD163+ cells were more highly expressed in tumor than peripheral tumor region (Figure 13A upper, Table 3). Remarkably, analysis of MØ-distribution within tumor lesion revealed that the largest proportion of CD163+ was located in the tumor front (Figure 13A, lower). On further evaluation of relationships between TAM-marker density and clinical pathological features of CCA patients, we found that CD163+ cells present in tumor front progressively increased along with tumor grade (G2/G3>>G1) and were significantly associated with CCA pathological grade (p=0.006,) (Figure 13B, Table 3) as well as CA19.9 serum marker levels (Figure 13C).

Likewise, FACS-profiling of mononuclear subsets from fresh resected CCA samples confirmed CD115, CD206 as well as HLA-DR higher expression of infiltrating CD68+ cells (Figure 13D, Figure 14A-D) in tumor tissue (T) compared to peritumoral counterpart (PT). In addition, isolated CD14+ cells from fresh CCA tissue revealed increased expression of M1-like (e.g., *CD80, CXCL9*) and M2-like (e.g., *CCL18*) markers as well as genes involved in ECM remodeling including *OA, FN* and *ED-B* (Figure 13E) respect to those present in PT regions.

Similarly, transcriptome of laser capture microdissected epithelium (EPI) and stroma (S) components from 23 CCA patients revealed a significant deregulation of CD115, HLA-DR, CXCL9, MMP2 and CD206 in CCA-S compared to CCA-EPI compartment (Figures 13F-14E). Further validation was provided by tumor (T) transcriptome versus surrounding liver tissue (SL) in an independent data set of CCA patients (n=104) (Figure 14F).

Furthermore, IHC analysis of CCA sections revealed a co-localization of both CD163 positive elements together with cells expressing CSC-related markers (CD44 or EPCAM), thus strongly supporting the potential relationship of infiltrating TAMs with CSC-niche (Figure 13G).
Therefore, our comprehensive characterization showed that phenotype of CCA patient MØs retained mixed M1-M2 features, further strengthening our *in vitro* results.

4.3 CCA-SPH Secretory Profiling Specifically Involved in MØ-Differentiation

Intriguingly, IHC data revealed that SPH-derived tumors retained a prominent and well-defined stromal compartment attested by α-SMA staining (indicative of murine fibroblast presence), massive collagen presence (Sirius Red) and abundance of tumor-associated CD31-positive vessels as well murine F4/80 tumor-macrophages (Figure 15A). This evidence suggested that SPH-cells acted differentially than MON-cells in creating their associated specific surrounding microenvironment.

Furthermore, we tested the diverse functionality of CCA cells on the surrounding niche, in particular we verified the effect of both SPH and MON on lymphocytes as well as endothelial cells. Thus, CellTrace CFSE labeled CD4+ peripheral blood lymphocytes (CD4+ T) were cultured in presence of both MON and SPH-CM. It was found that SPH-CM was not able to induce CD4+ T cell proliferation, unlike

MON-CM did (Figure 15B), suggesting a more immunosuppressive properties of SPH-associated microenvironment [193, 212].

Since angiogenesis is an important hallmark of tumor progression, we evaluated the biological activity of CCA-CM on the induction of *in vitro* capillary-like structures formation [231]. By using the well-known matrigel angiogenesis assay, the effects of SPH-CM and MON-CM on HUVEC cells in term of capillary tube-like formation were examined *in vitro*. In accordance with IHC data (Figure 15A), HUVEC cells treated with SPH-CM for 24h revealed the highest neovascular response in comparison to those subjected to MON-CM treatment (Figures 15C-16A).

Hence, based on this result, we investigated the presence of specific soluble mediators released by SPHs using ELISA profiling of conditioned media, trying to understand why SPH could differentially affect macrophage differentiation compared to MON. Among 37 tested molecules (chemokines, cytokines, interleukins and other molecules) specifically involved in MØ-differentiation, activation and recruitment, several factors were secreted at extremely low levels (<50 pg/mL), whereas 16 showed significant amount in both CCA MON- and SPH-CM (Figure 15D, Table 4). A 3-level analysis identified 1) common SPH and MON, 2) MON-specific, 3) SPH-specific released factors. First, we found that both SPH and MON produced high VEGF concentrations. Therefore, VEGF role in driving MØ-differentiation was *in vitro* investigated. For that reason, healthy donor CD14+ were cultured for 6 days in presence of VEGF added to fresh monocyte medium, not tumor conditioned (Figure 16B). Clearly, FACS-profile reveals enriched expression of CD68 and CD115 as classical MØ markers (Figure 16B) suggesting its contribution in CCA MØ-differentiation instead of classically described M-CSF. Notably, both SPH and MON MØs overexpressed corresponding VEGF receptors (VEGFR1-3) (Figure 16C).

Nevertheless, a cell line-specific MON secretory profile was identified, with altered supernatant levels of granulocyte-macrophage colony-stimulating factor

(GM-CSF), M-CSF, TNF-α, TGF-β (HUCCT1), GM-CSF, CCL22, CCL20, CXCL8 (SG231), CCL2, and CXCL18 (CCLP1 cells), CXCL11 (CCA4) (Table 4). However, release of soluble mediators was cell line-dependent and no common molecules among CCA-MONs were recognized.

Crucially, a specific secretory SPH-profile consisting of IL13, OA and IL34 was identified in all tested cell lines (Figures 15D-16D) and, more importantly, SPH MØs overexpressed receptors for IL13 (*IL13Ra1, IL13Ra2, IL4R*), OA (*CD44, ITGA5, ITGB3, SDC1, SDC4*) (Figure 15E) as well as for IL34 (CD115) already shown in Figure9B. Therefore, these data proposed the potential implication of IL13, OA and IL34 in the MØ-acquisition of CSC-specific phenotype.

Surprisingly, elevated levels of circulating IL13, OA and IL34 were significantly found in CCA patient group (n=12) compared to healthy control subjects (n=12), proposing a potential association with CCA-disease (Figure 15F, Table 5). However, due to limited availability of human CCA specimens, important question such correlation between serum level and abundance of TAMs as well clinical pathological features of CCA patients was not addressed. Nonetheless, correlative data were provided by a well-described transcriptome database of 104 CCA patients [6]. Amazingly, Pearson correlation coefficient test showed significant associations of specific CCA-SPH released molecules *(IL13, OA, IL34*) with SPH stem-like genes such as *BMI1, CTNNB1, CD44, KITGL, KLF4, LEF1, LIN28A, MAML1, POUF5, SOX2 and THY1* (Table 6) reinforcing the importance of CCA stem-secretory profiling in tumor context in CCA patients. Furthermore, intimate connection between CSCs and tumor-MØs in human CCA was also denoted by meaningful correlations between stem-like SPH genes and SPH MØ-specific molecular traits (Table 7).

4.4 IL13, OA, and IL34 are Required for Acquisition of CSC-like TAM Identity

To confirm the contribution of IL13, OA, IL34 in shaping molecular and functional aspects of SPH MØs, inhibition of these molecules by addition of neutralizing

antibodies to SPH-CM (previously *in vitro* tested, to define an effective and non-toxic concentration, Figures 17-18A) used in single or in combination, was tested *in vitro* and *in vivo*. Strikingly, MØ differentiated in presence of SPH-CM added with antibodies our showed a down-regulation of CD115, CD206 and HLA-DR proteins (Figure 17A, Table 8) as well as SPH MØ-associated genes (*CXCL9, CXCL10, CCL18, CCL5, CD163, OPN* and *AD17*) (Figure 17B) in addition to loss of functional properties such as CD14+ migration, MØ-invasion and adhesion (Figure 17C). These results suggested a shift towards a MON MØ-phenotype. Particularly, each single IL13, IL34, or OA seemed to be independently and likewise involved in CD115 expression (Figure 17A). Interestingly, only OA molecule is accountable for CD206 and HLA-DR expression (Figure 17A) as well as MØ-invasion and adhesion (not statistically significant) (Figure 17C), whereas combination of neutralizing antibodies has a major impact in diminishing the expression of M1, M2 and ECM remodeling genes (Figure 17B).

Well-matched with antibodies-dependent inhibition of SPH-CM effect, the addition of these three SPH-specific molecules to MON-CM reproduced same SPH-CM impact on MØ differentiation. Indeed, IL13, OA, and IL34 were able to restore SPH MØ-like profile with overexpression of CD115, HLA-DR and CD206 markers and presence of an equal amount of CD68 protein (Figure 17A, Figure 18B-C, Table 8). Remarkably, our data displayed the re-expression of specific gene-set (*CXCL9, CXCL10, CCL18, CCL5, CD163, OPN* and *AD17*) (Figures 17B-18D) as well as re-acquisition of functional properties such as monocyte recruitment, MØ-invasion and adhesion (Figure 17C, Figure 18E-F). Pertinently, all these results pointed to a peculiar contribution of these molecules in driving SPH MØ-differentiation. Thus, we concluded that although the underlying mechanism needs to be explored, combination of IL13, OA, IL34 directly triggers differentiation of monocytes into stem-like TAM-subtype.

Furthermore, to investigate the significance of diverse MØ-subsets in supporting tumorigenicity, three diverse *in vitro*-educated MØ-subsets such as 1) SPH MØ, 2) MON MØ, 3) MON (+IL13+OA+IL34) MØ, 4) SPH (+single or combination of antibodies against IL13, OA, IL34) MØ were co-injected with CCA-MON cells into NSG mice. As expected, MON MØs enhanced tumor growth compared to MON cells injected alone, as already described in diverse study for TAMs. Outstandingly, SPH MØs boosted tumorigenic potential compared to MON MØs, indicating that CSC-associated TAMs increased *in vivo* tumor-promoting effect of CCA-CSC. As confirmation, co-injected MON with (+IL13+OA+IL34) MØs reproduced similar SPH MØ tumorigenic effect (Figure 17D), proving direct functional relationship between CSC-associated TAMs and tumor outcome.

4.5 Figures

Figure 5

A

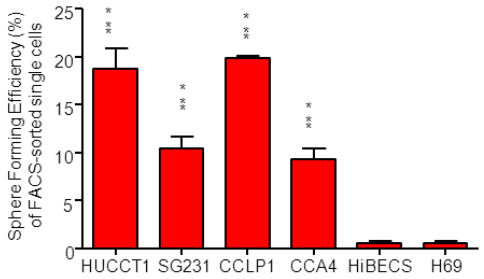

B

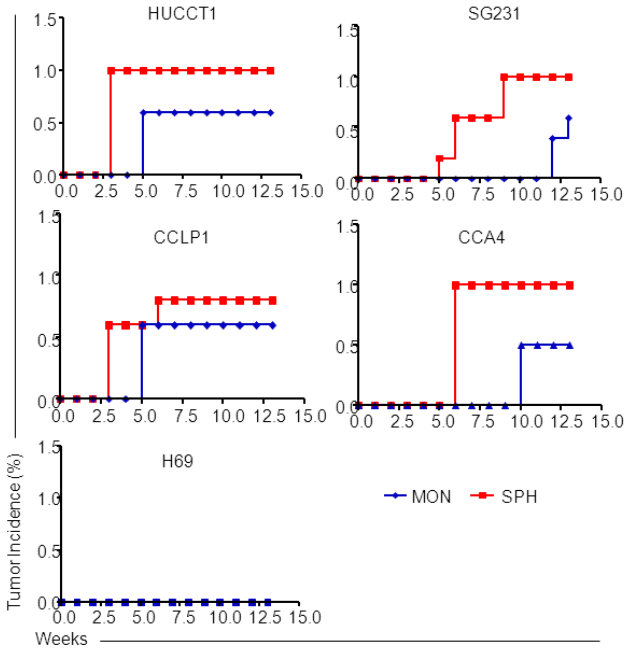

C

Generated Tumors (%)			
Cell Line	**MON**	**SPH**	***p value***
HUCCT1	60 (3/5)	100 (5/5)	*0.0003*
SG231	40 (2/5)	100 (5/5)	*0.0000*
CCLP1	60 (3/5)	100 (4/4)	*0.0003*
CCA4	50 (2/4)	100 (4/4)	*0.0000*

The data are mean ± SEM
(*p value* versus MON by Student t test)

D

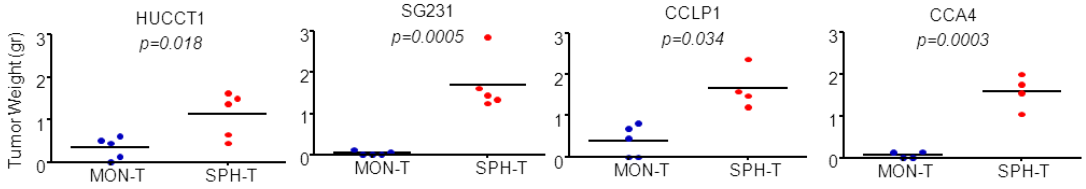

E

N° of injected cells	1000	100	10	Tumor Initiating Fraction (TIF) (95% CI)	*p value*
	N° of tumors formed/ total n° of transplants				
CCLP1 MON	3/5	3/6	1/6	1/505 (1/1295-1/197)	*0.0011*
CCLP1 SPH	4/4	5/6	5/6	1/25 (1/69-1/9)	

F

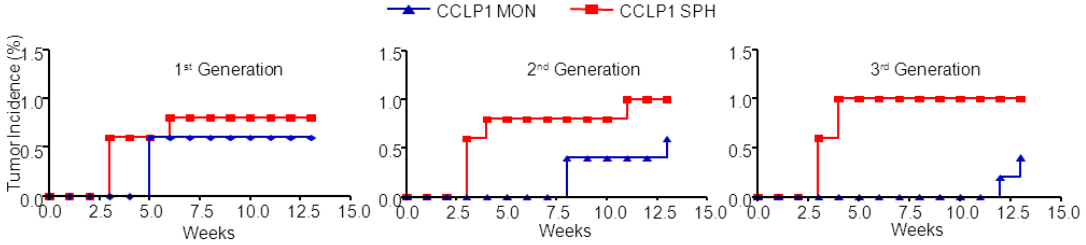

Figure 5. CCA self-renewal capacity in vitro and tumorigenic potential in vivo.

A) Sphere-forming efficiency (SFE) of CCAs (HUCCT1, SG231, CCLP1, CCA4) and normal cholangiocytes (HiBECs,H69) calculated by dividing the sphere number by number of single cells seeded and expressed as a percentage. Mean ± SEM (n=4, p value versus H69 and HiBECS by Student t test, *** p≤0.001).

Sphere tumorigenic capacity in NSG mice: B) Tumor growth kinetic (n=5) , C) frequency and D) weight of generated tumors at 13weeks after subcutaneous injection into NSG mice of 1,000 SPH/MON isolated cells as monitored by weekly palpation. Mean ± SEM (p value versus MON-T by Student t test).

E) Self-renewing CCLP1 cells calculated by ELDA program (see Methods section) (p value versus MON-tumor initiating fraction (TIF) by Student t test).

F) Serial transplantations of 1,000 CCLP1 SPH/MON cells into flanks of NSG mice (n = 4).

Figure 6

A

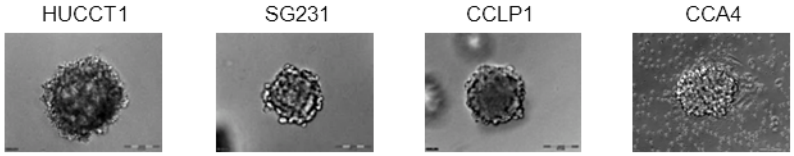

B

Half Maximal Inhibitory Concentration (IC50) %					
		Drugs			
		Oxaliplatin (μM)	5-Fluorouracil (mM)	Cisplatin (μM)	Gemcitabine (μM)
HUCCT1	MON	1318.3 ± 48	44.7 ± 16	37.2 ± 7	10.5 ± 2
	SPH	1698.2 ± 37	158.5 ± 19	1412.5 ± 72	251.2 ± 22
	p value	*0.0000*	*0.0000*	*0.0000*	*0.0000*
SG231	MON	44.7 ± 10	61.7 ± 14	79.4 ± 11	18.6 ± 4
	SPH	245.5 ± 17	416.9 ± 31	1174.9 ± 105	95499.3 ± 230
	p value	*0.0000*	*0.0000*	*0.0000*	*0.0000*
CCLP1	MON	91.2 ± 21	30.9 ± 12	13.3 ± 5	0.01 ± 0.005
	SPH	1659.6 ± 143	380.2 ± 67	309.0 ± 23	251188.6 ± 209
	p value	*0.0000*	*0.0001*	*0.0000*	*0.0000*
CCA4	MON	43.7 ±	0.7 ±	26.3 ±	147.9 ±
	SPH	1584.8 ±	229.1 ±	31.6 ±	181970.1 ±
	p value	*0.0000*	*0.0000*	*0.1676*	*0.0000*

The data are mean ± SEM (n=5, *p value* versus MON by Student t test)

Figure 6. CCA-derived spheres: morphology and drug-response

A) Representative images of CCA-derived spheres.

B) IC50s of CCA monolayers and spheres assayed for sensitivity to oxaliplatin, 5-fluorouracil, cisplatin and gemcitabine (n=5). Data are mean ± SEM (*p value* versus MON by Student t test).

Figure 7

A

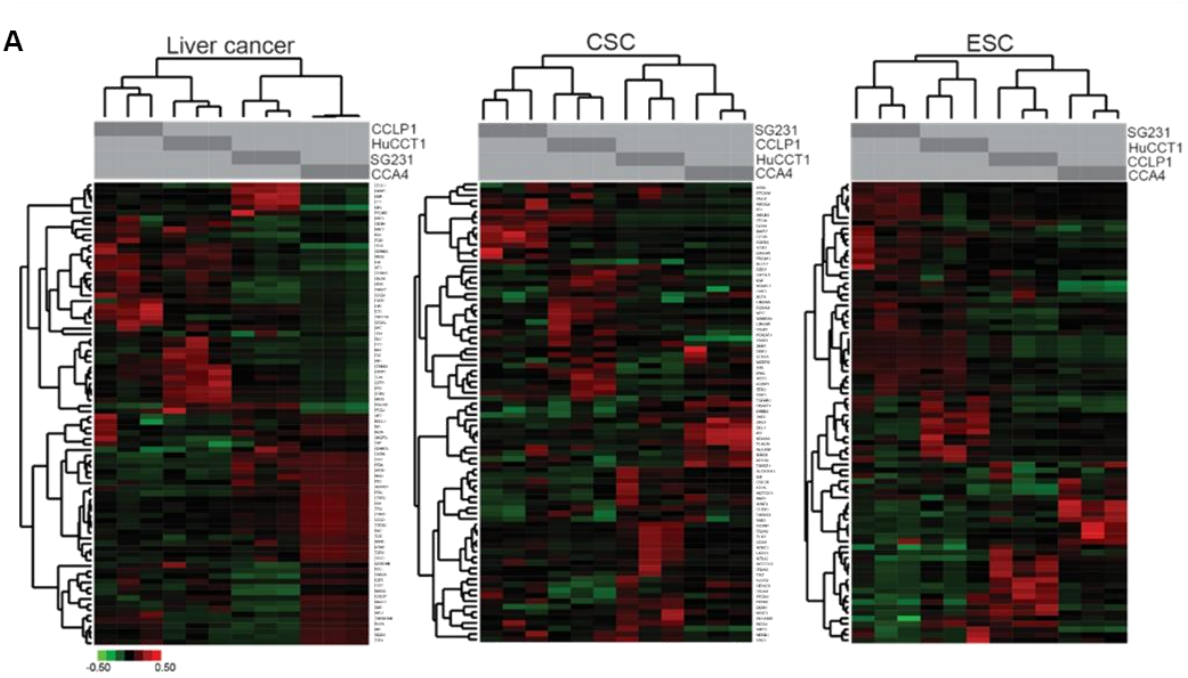

B

Common CCA-SPH Deregulated Genes		
Liver Cancer	**CSC**	**ESC**
BCL2L1, CDKN1A, CTNNB1, IGF2, ITGB1, LEF1	ABCG2, BMI1, BMP7, CD24, CD44, EPCAM, FGFR2, KITLG, KLF4, LATS1, LIN28A, MAML1, MYC, NFKB1, NOS2, NOTCH1, POU5F1, PROM1, SOX2, STAT3, TGFBR1, THY1,YAP1	HNF4A

C

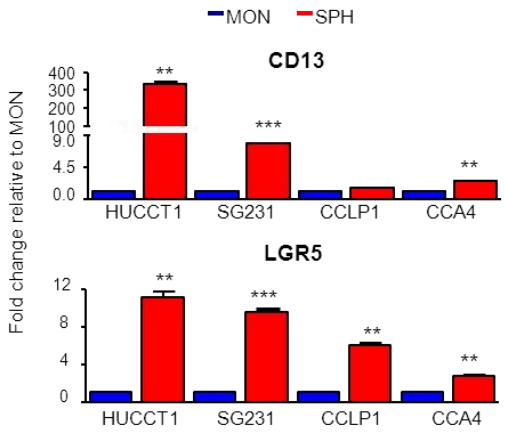

D

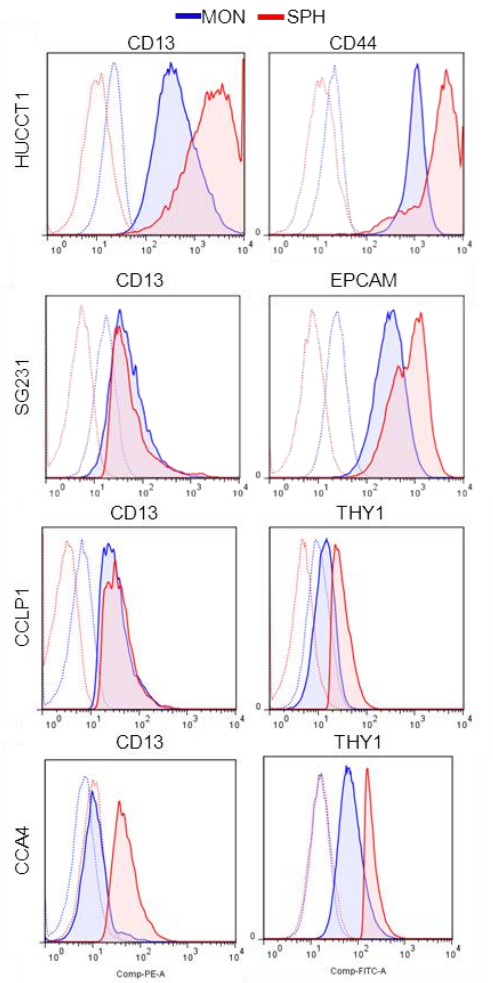

Figure 7. Molecular properties of CCA spheres.

A) Pathway-focused qRT-PCR arrays. Hierarchical clustering distinguished each CCA-SPH type based on significant gene expression compared to CCA-MON. Data first centered and normalized, then clustered using centered correlation metrics with complete linkage. Dendrograms depict similarity of individual genes and cases. Right side figure indicates clusters of coordinately expressed genes with higher expression levels in CCA-SPH than CCA-MON. Relative gene expression level depicted according to the scale bar.

B) List of commonly up-regulated genes in SPH of all CCA cell lines. Genes divided according to pathway of belonging.

C) Relative expression of CD13 and LGR5 transcript-encoding markers. GAPDH as internal control. All mRNA levels are presented as fold changes normalized to 1 (mean expression of monolayer). Mean ± SEM (n=3, *p value* versus MON by Student t test, * $p \leq 0.05$, ** $p \leq 0.01$, *** $p \leq 0.001$).

D) FACS-profile of CD44, CD13, THY, EPCAM.

Figure 8

A

Up-regulated genes in CCA-spheres			
Cell Lines	**Liver Cancer**	**CSC**	**ESC**
HUCCT1	61% (51/84)	69% (58/84)	27% (23/84)
SG231	42% (35/84)	48% (40/84)	37% (31/84)
CCLP1	75% (63/84)	55% (46/84)	24% (20/84)
CCA4	77% (65/84)	64% (54/84)	19% (16/84)

B

Cell Line	Marker	MON MFI ± SEM	SPH MFI ± SEM	*p value*
HUCCT1	**CD13**	624.7 ± 58	3359.8 ± 97	*0.0000*
	CD44	1070.9 ± 75	3852.9 ± 103	*0.0002*
SG231	**CD13**	60.6 ± 14	102.5 ± 17	*0.0459*
	EPCAM	334.5 ± 52	930.6 ± 34	*0.0005*
CCLP1	**CD13**	35.3 ± 6	51.2 ± 9	*p>0.05*
	THY1	2.5 ± 0.4	29.2 ± 8	*0.0287*
CCA4	**CD13**	7 ± 2	49.9 ± 7	*0.0095*
	THY1	66.6 ± 14	196.9 ± 26	*0.0047*

The data are mean ± SEM (n=3, *p value* versus MON by Student t test)

C

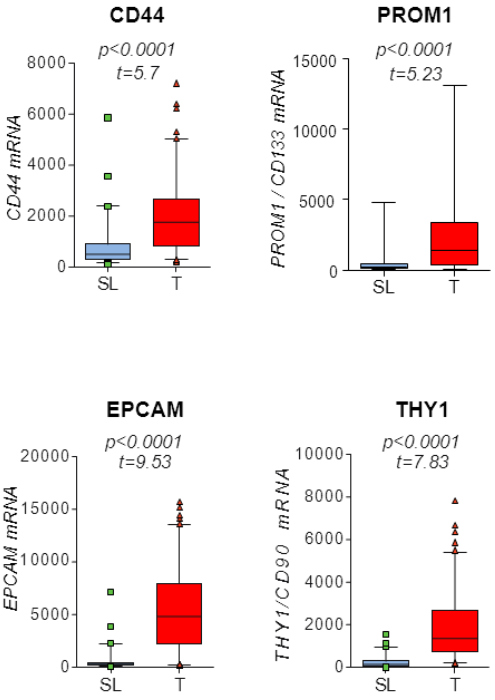

D

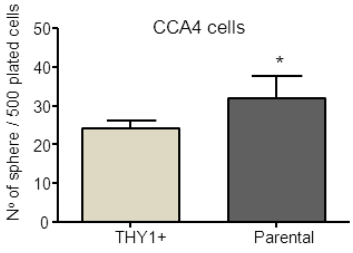

N° of injected cells	1000	100	10	Tumor Initiating Fraction (TIF) (95% CI)	*p value*
	N° of tumors formed/ total n° of transplants				
THY+ SPH	8/8	6/8	3/4	1/47.8 (1/108-1/21.3)	*0.2028*
Parental SPH	4/4	3/4	3/4	1/35.7 (1/110-1/11.8)	

The data are mean ± SEM (*p value* versus Parental SPH by Student t test)

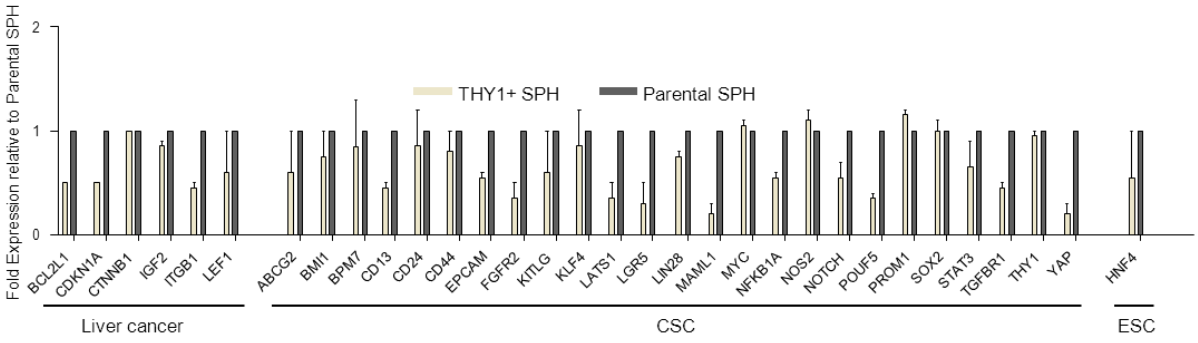

Figure 8. CCA-derived spheres: molecular features and comparison with THY enriched spheres

A) Up-regulated sphere-specific genes using pathway-focused arrays. Significant up-regulated genes compared to monolayers expressed as a percentage of the total number.

B) Mean Fluorescence Intensity (MFI) of CSC surface markers in spheres (SPH) and monolayers (MON) by FACS.

C) Validation of the key significant CSC surface markers (CD44, PROM1, THY and EPCAM) in tumor lesions (T) and surrounding liver (SL) using transcriptome data from 104 CCA patients. Pearson correlation between gene pairs was calculated using R and the "cortest" function, yielding correlation coefficients and *p-value* versus SL.

D) Upper left: capacity of spheroid formation by THY+ sorted and Parental CCA4 cells. Upper right: limiting-dilution cell transplantation assay. Tumor initiating fraction (TIF) of THY+ and Parental CCA4 derived spheres. A web-based calculation was performed by the ELDA program (see Methods section). *p value* versus Parental-tumor initiating frequency (TIF) by Student t test. Lower: comparison of gene expression of CCA4 THY+ SPH and Parental SPH. All mRNA levels are presented as fold changes normalized to 1 (mean expression of Parental-SPH). Data are mean ± SEM (*p value* versus Parental by Student t test, * $p \leq 0.05$, ** $p \leq 0.01$, *** $p \leq 0.001$).

Figure 9

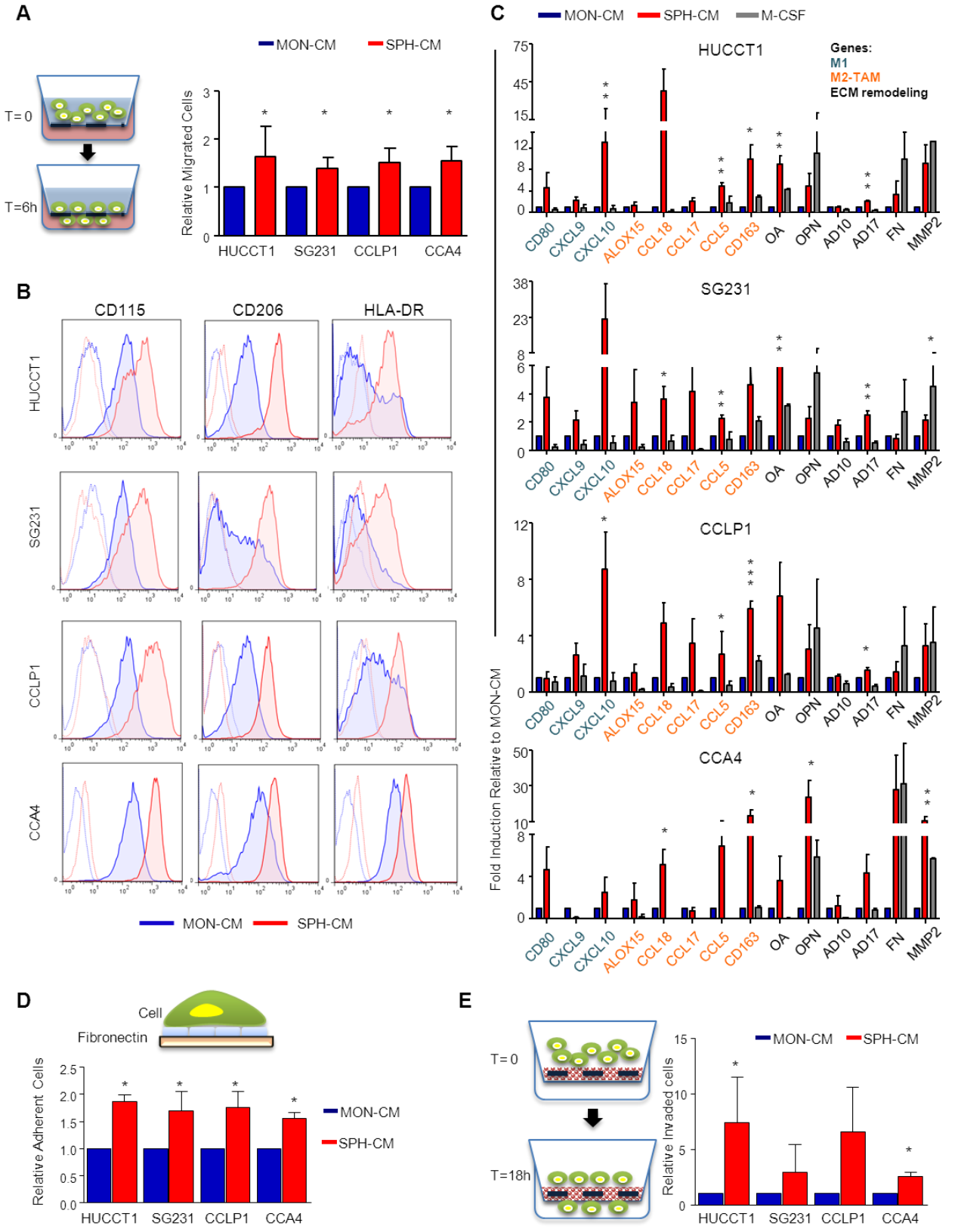
A
MON-CM
SPH-CM
T= 0
T=6h
Relative Migrated Cells
HUCCT1
SG231
CCLP1
CCA4
B
CD115
CD206
HLA-DR
HUCCT1
SG231
CCLP1
CCA4
MON-CM
SPH-CM
C
MON-CM
SPH-CM
M-CSF
Genes:
M1
M2-TAM
ECM remodeling
HUCCT1
SG231
CCLP1
CCA4
Fold Induction Relative to MON-CM
CD80
CXCL9
CXCL10
ALOX15
CCL18
CCL17
CCL5
CD163
OA
OPN
AD10
AD17
FN
MMP2
D
Cell
Fibronectin
Relative Adherent Cells
MON-CM
SPH-CM
HUCCT1
SG231
CCLP1
CCA4
E
T= 0
T=18h
MON-CM
SPH-CM
Relative Invaded cells
HUCCT1
SG231
CCLP1
CCA4

Figure 9. Effect of CCA stem-like cells on MØ-precursors.

A) Migrated CD14+ towards SPH-CM (6h). Relative migrated CD14+cells normalized to migrated CD14+ in presence of MON-CM. Mean ± SEM (n=3, *p value* versus MON) .

B) FACS-profile of CD115, HLA-DR and CD206 expression in MØs obtained by culture of CD14+ with SPH- and MON-CM. Histograms represent three independent experiments with MØ from three different healthy donors.

C) Relative expression of M1/M2 and matrix remodeling-related genes. As control MØ-differentiated with M-CSF. GAPDH as internal control. All mRNA levels presented as fold changes normalized to 1 (n=3).

D) Adhesion assay using FN-supports. Cells counted and normalized to MON MØs (n=3). E) SPH MØ invasion assay using Matrigel-coated transwells. Cells counted and normalized to migrated MON MØs (n=5). Mean ± SEM (*p value* versus MON MØ by Student t test, * $p \leq 0.05$, ** $p \leq 0.01$, *** $p \leq 0.001$).

Figure 10

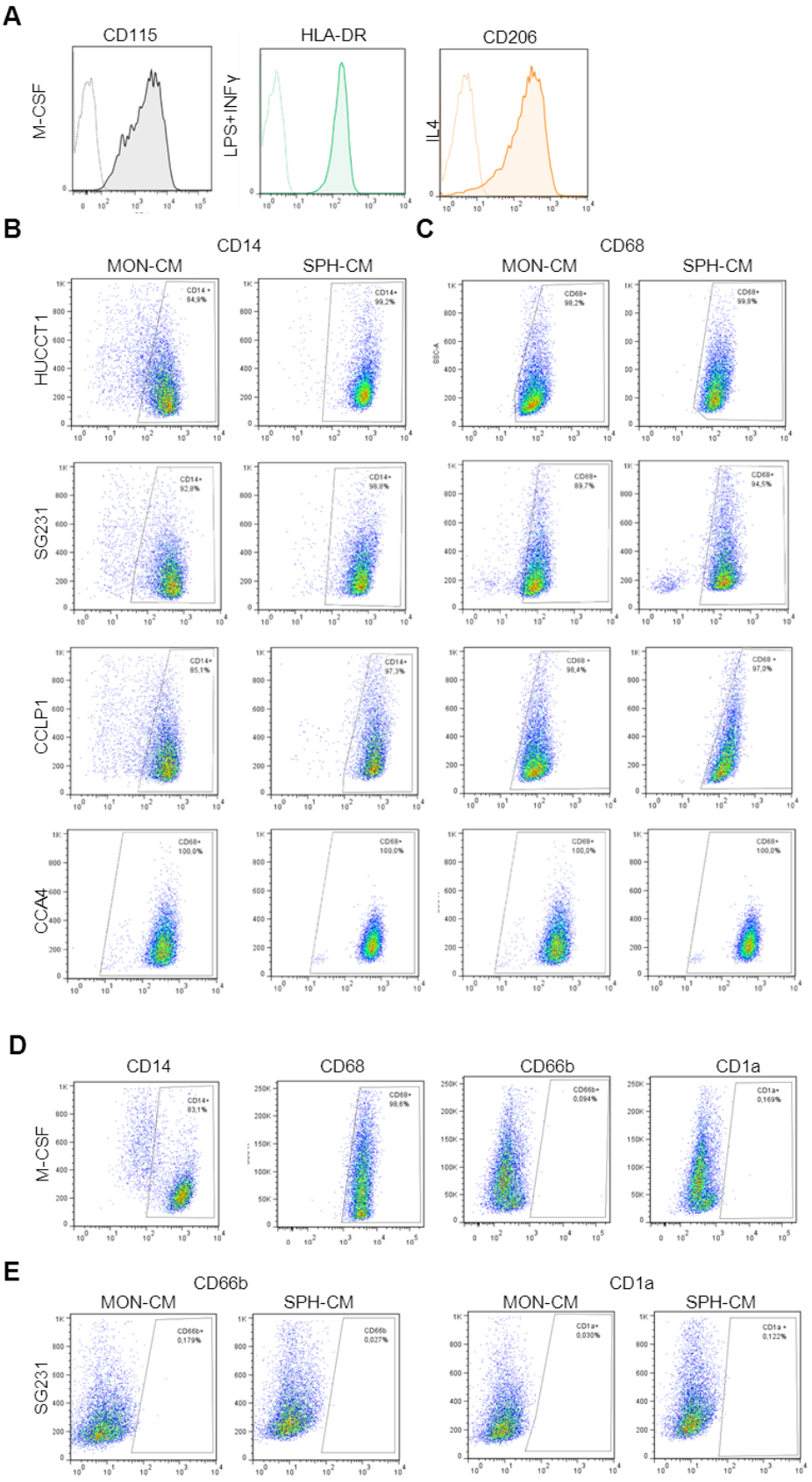
A
CD115
HLA-DR
CD206
M-CSF
LPS+ INFγ
IL4
B
CD14
MON-CM
SPH-CM
C
CD68
MON-CM
SPH-CM
HUCCT1
SG231
CCLP1
CCA4
D
CD14
CD68
CD66b
CD1a
M-CSF
E
CD66b
MON-CM
SPH-CM
CD1a
MON-CM
SPH-CM
SG231

Figure 10. Phenotypic analysis of monocytes cultured with SPH- and MON-CM for 6 days.

A) CD115, HLA-DR and CD206 staining of M0 classically differentiated macrophages in the presence of M-CSF and *in vitro*-activated M1 (LPS+INFγ) and M2 (IL4) macrophages.

B) CD14 and C) CD68 profile expression determined by FACS. The dot plots are representative of three independent experiments using macrophages from three different healthy donors.

D) CD14, CD68, CD66b, and CD1a expressing monocytes differentiated in the presence of M-CSF as a classical control for M0 macrophages. The dot plots are representative of three independent experiments using macrophages from three different healthy donors.

E) CD66b and CD1a staining determined by FACS was used to exclude differentiation toward granulocytes and dendritic cells. The dot plots are representative of three independent experiments using macrophages from three different healthy donors. Data are mean ± SEM (*p value* versus Parental by Student t test, * $p \leq 0.05$, ** $p \leq 0.01$, *** $p \leq 0.001$).

Figure 11

A

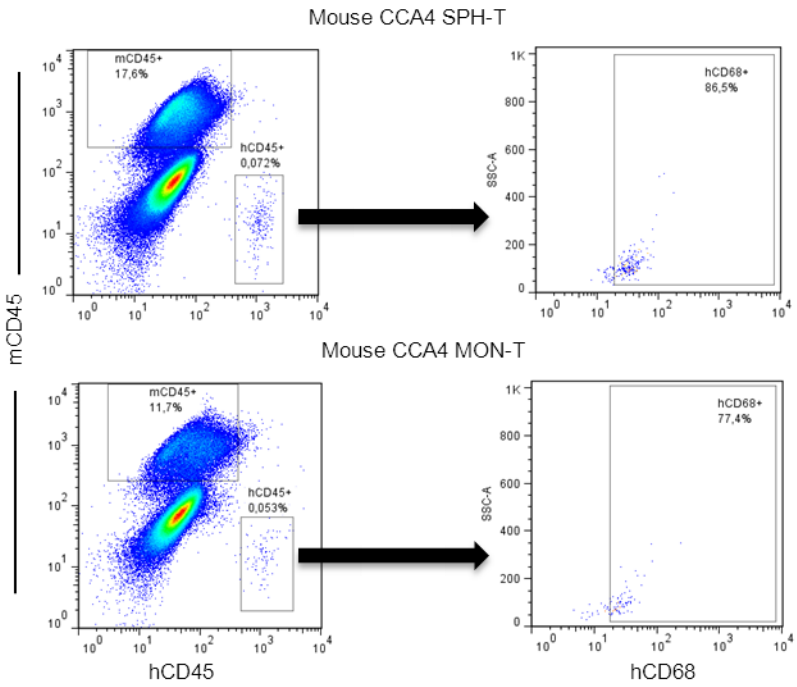

s.c. injected cells	% hCD45+ (Mean ± SEM)	*p value*	% hCD45+ hCD68+ (Mean ± SEM)	*p value*
CCA4 SPH	0.068 ± 0.006		83.55 ± 2.19	
		0.0405		*0.0072*
CCA4 MON	0.048 ± 0.008		70.00 ± 2.83	

The data are mean ± SEM (n=3, *p value* versus MON by Student t test)

B

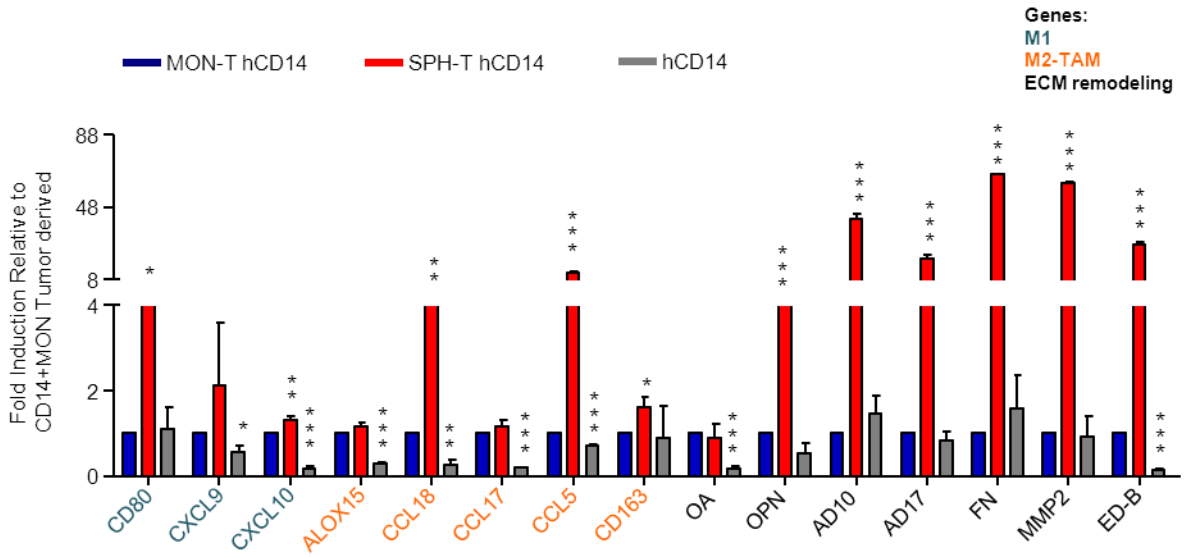

Figure 11. Evaluation of TAM-infiltration in mouse model.

A) FACS-profile of mouse CD45-, human CD45+ CD68+cells in isolated mononucleate subset from CCA4-SPH-T and CCA4-MON-T. Upper, Representative dot plots shown. Lower, Table with percent of human CD45 CD68 double positive cells determined by FACS. Data are mean ± SEM (n=3, *p value* versus MON-injected mice by Student t test).

B) Relative gene expression of humanCD14+ isolated from CCA4-T. As control, human CD14+. Human GAPDH as internal control. All mRNA levels presented as fold changes normalized to 1 (mean expression of CCA4 MON-T CD14+ cells). Mean ± SEM (n=3, *p value* versus MON-T CD14+ cells). Student t test, * $p \leq 0.05$, ** $p \leq 0.01$, *** $p \leq 0.001$.

Figure 12

A

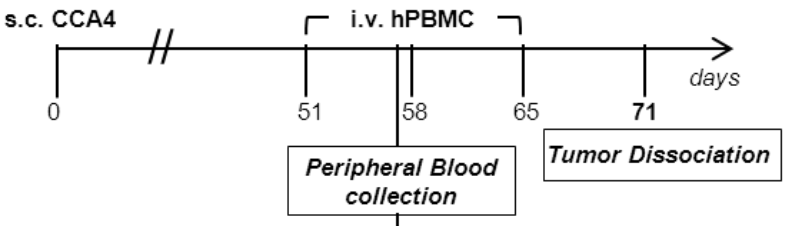

B

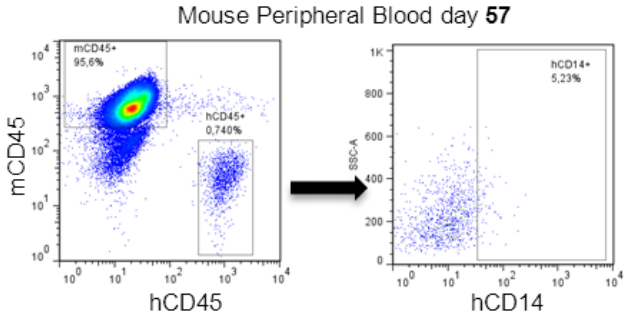

C

s.c. injected CCA4 cells	% hCD45+ (Mean ± SEM)	*p value*	% hCD45+ hCD14+ (Mean ± SEM)	*p value*
MON	0.626 ± 0.161		4.985 ± 0.346	
		0.452		*0.078*
SPH	0.747 ± 0.182		6.520 ± 0.707	

The data are mean ± SEM (n=3, *p value* versus MON by Student t test)

Figure 12. Phenotype of CCA-infiltrated macrophages in humanized mice

A) Upper: schematic illustration of experimental protocol for human CCA4-SPH derived cells and human PBMC co-injection. CCA4-SPH engrafted NSG mice were injected with three doses of human PBMC. At day 71, tumors were removed and associated-mononuclear component analyzed.

B) Presence of human CD45+ and human CD45+ CD14+ cells was assessed in mouse peripheral blood 6 days after first human PBMC engraftment in NSG mice (day 57) and expressed as percentage. The dot plots are representative of three independent experiments, using three different mice.

C) Presence of human CD45+ and human CD45+CD14+ cells determined by FACS. Data are mean ± SEM (n=3, *p value* versus MON-injected mice by Student t test).

Figure 13

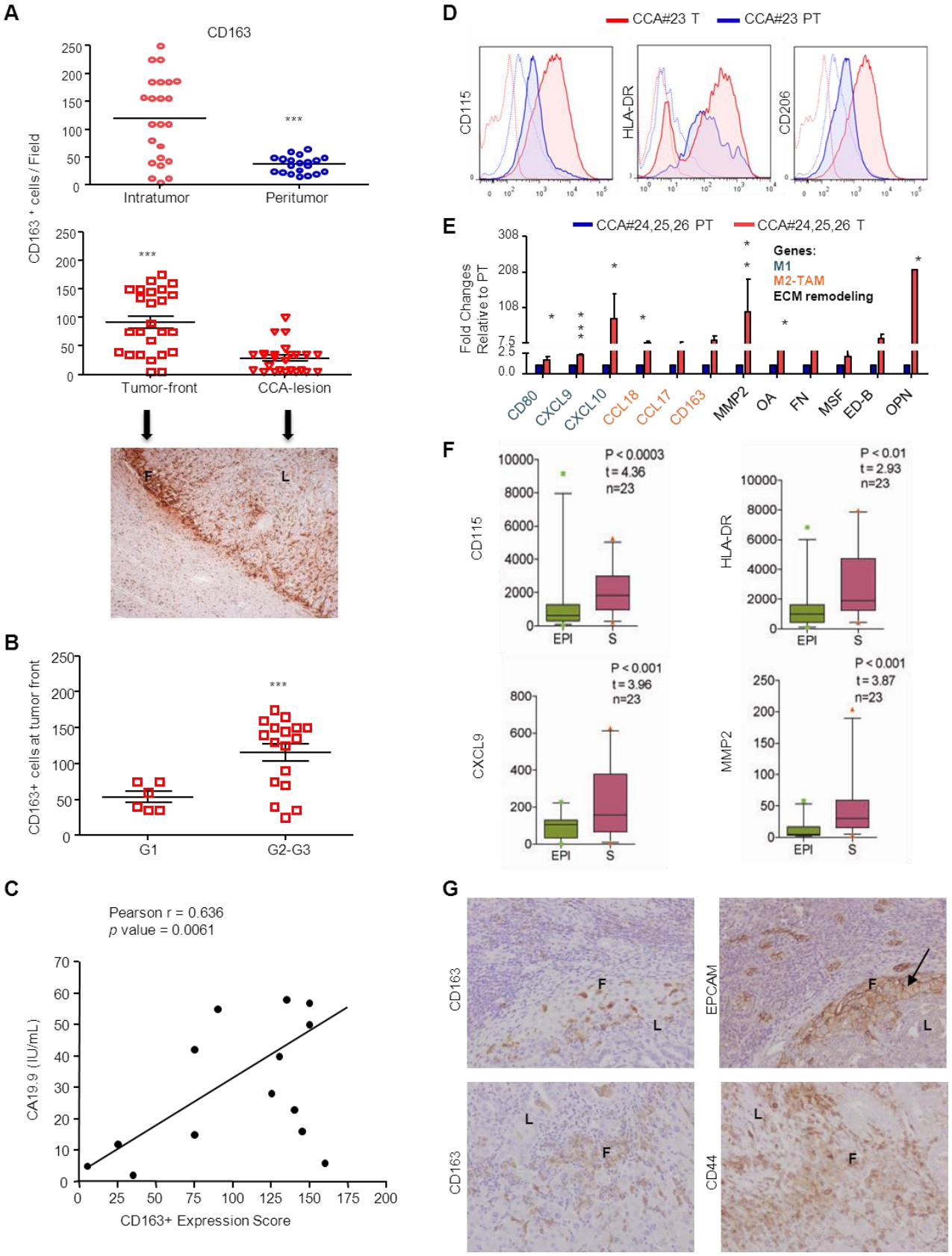
A
CD163
CD163 + cells / Field
Intratumor
Peritumor
Tumor-front
CCA-lesion
F
L
B
CD163+ cells at tumor front
G1
G2-G3
C
Pearson r = 0.636
p value = 0.0061
CA19.9 (IU/mL)
CD163+ Expression Score
D
CCA#23 T
CCA#23 PT
CD115
HLA-DR
CD206
E
CCA#24,25,26 PT
CCA#24,25,26 T
Fold Changes Relative to PT
Genes:
M1
M2-TAM
ECM remodeling
CD80
CXCL9
CXCL10
CCL18
CCL17
CD163
MMP2
OA
FN
MSF
ED-B
OPN
F
CD115
P < 0.0003
t = 4.36
n=23
HLA-DR
P < 0.01
t = 2.93
n=23
CXCL9
P < 0.001
t = 3.96
n=23
MMP2
P < 0.001
t = 3.87
n=23
EPI
S
G
CD163
EPCAM
CD163
CD44

Figure 13. Evaluation of TAM-infiltration in human CCA samples.

A) Quantification of CD163+ cells in both CCA intratumoral (T) and peritumoral (PT) regions. Mean ± SEM (n=23, *p value* versus PT). Distribution of CD163+ cells in CCA lesion (L) and tumor front (F) shown by a representative image and corresponding quantification. Mean ± SEM (n=23, *p value* versus F).

B) Correlation of %CD163+ cells tumor grade (G) (n=25, TableS2, One sided Student t-test applied to log ratios in order to compare G1 to G2-G3), as well C) CA19.9 serum levels in CCA patients (n=17, TableS2, Pearson correlation between two parameters was calculated using R and the cortest function, yelding correlation coefficients and *p value*).

D) Expression of CD115, HLA-DR and CD206 in CCA-infiltrated MØs by FACS included both CCA T and PT regions. Representative histograms of CCA#23 patient.

E) Relative expression of M1/M2 and matrix remodeling-related genes. GAPDH as internal control. All mRNA levels displayed as fold changes normalized to 1 (mean expression of PT-MØs). Histograms represent the average of three different CCA patients (#24, #25, #26 patients). Mean ± SEM (n=3, *p value* versus PT).

F) Gene expression evaluated in a set of CCA patients (n=23) where paired intratumoral epithelial (EPI) and stromal compartments (S) obtained by laser micro-dissection.

Student t test, * $p \leq 0.05$, ** $p \leq 0.01$, *** $p \leq 0.001$.

G) Representative images for IHC analysis of CD163 and CSC-related markers (CD44, EPCAM) in CCA sections (20X) (CCA lesion (L) and tumor front (F)).

Figure 14

A

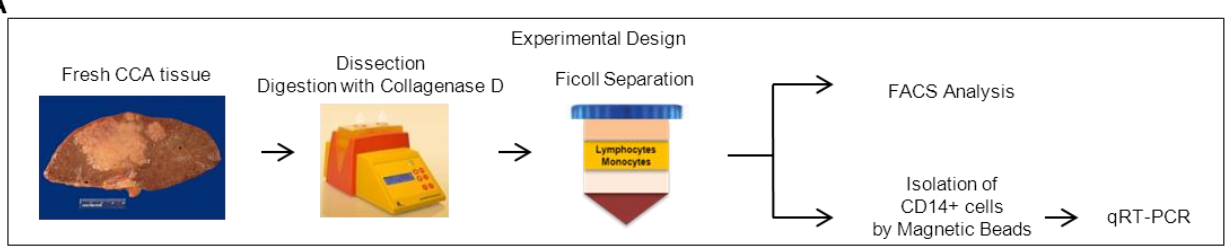

B

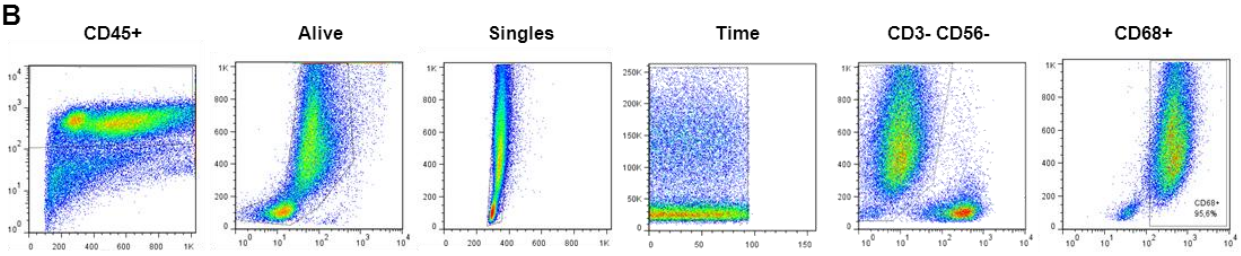

C

Clinical and pathological parameters of CCA patients used for molecular characterization (FACS and RT-PCR)

Patient	Grade	TNM classification			Tumor size (cm)	Perineural invasion	Angio-invasion
#CCA23	G2	T2b	NX	MX	8.5+1.5	no	yes
#CCA24	G3	T4	N0	MX	9.5	no	no
#CCA25	G2	T1	N0	MX	4.6	no	no
#CCA26	G3	T3a	N0	MX	9.5+3.7	no	no

D

MFI of CD115, HLA-DR and CD206 in CCA-infiltrated MØs by FACS, included both T and PT regions of three CCA patients (#23, #24, #25 patients).

Marker	Condition	MFI ± SEM	*p value*
CD115	T	172.8 ± 20	*0.0031*
	PT	40.0 ± 17	
CD206	T	100.8 ± 31	*0.0372*
	PT	9.9 ± 04	
HLA-DR	T	353.6 ± 24	*0.0348*
	PT	288.6 ± 19	
CD68	T	194.7 ± 28	*0.0264*
	PT	85.7 ± 14	

The data are mean ± SEM (n=3, *p value* versus PT by Student t test)

E

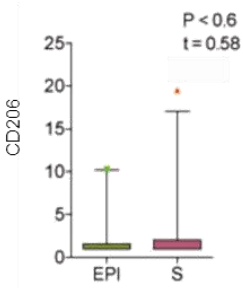

F

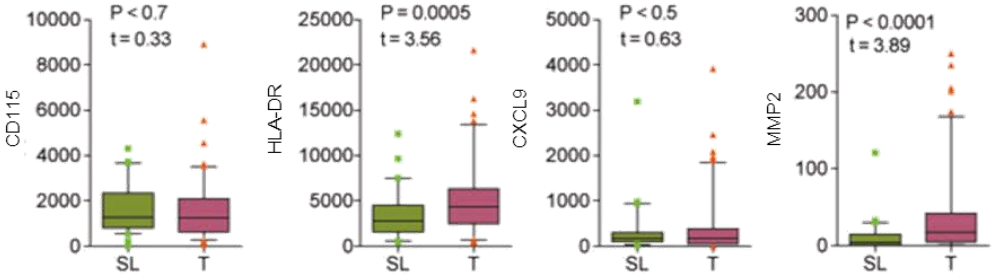

Figure 14. Phenotype of CCA-infiltrated macrophages in human samples

A) Experimental design to isolate mononuclear subset from freshly resected CCA tissue.

B) FACS setting to identify macrophage components associated with CCA specimens.

C) Clinical and pathological parameters of CCA patients used for molecular characterization (FACS and RT-PCR).

D) Mean Fluorescence Intensity (MFI) of CD115, HLA-DR and CD206 in CCA-infiltrated MØs by FACS, included both tumor (T) and peritumor (PT) regions of three CCA patients (#23, #24, #25 patient). Data are mean ± SEM (n=3, *p value* versus MON-injected mice by Student t test).

E) CD206 gene expression was evaluated in a set of CCA patients (n=23) where paired intratumoral epithelial (EPI) and stromal compartments (S) were obtained by laser micro-dissection. Pearson correlation between gene pairs was calculated using R and the "cortest" function, yielding correlation coefficients and *p value* versus EPI.

F) Validation of the key significant markers (CD115, HLA-DR, CXCL9, MMP2) in tumor lesions (T) and surrounding liver (SL) using transcriptome data from 104 CCA patients. Pearson correlation between gene pairs was calculated using R and the "cortest" function, yielding correlation coefficients and *p value* versus SL.

Figure 15

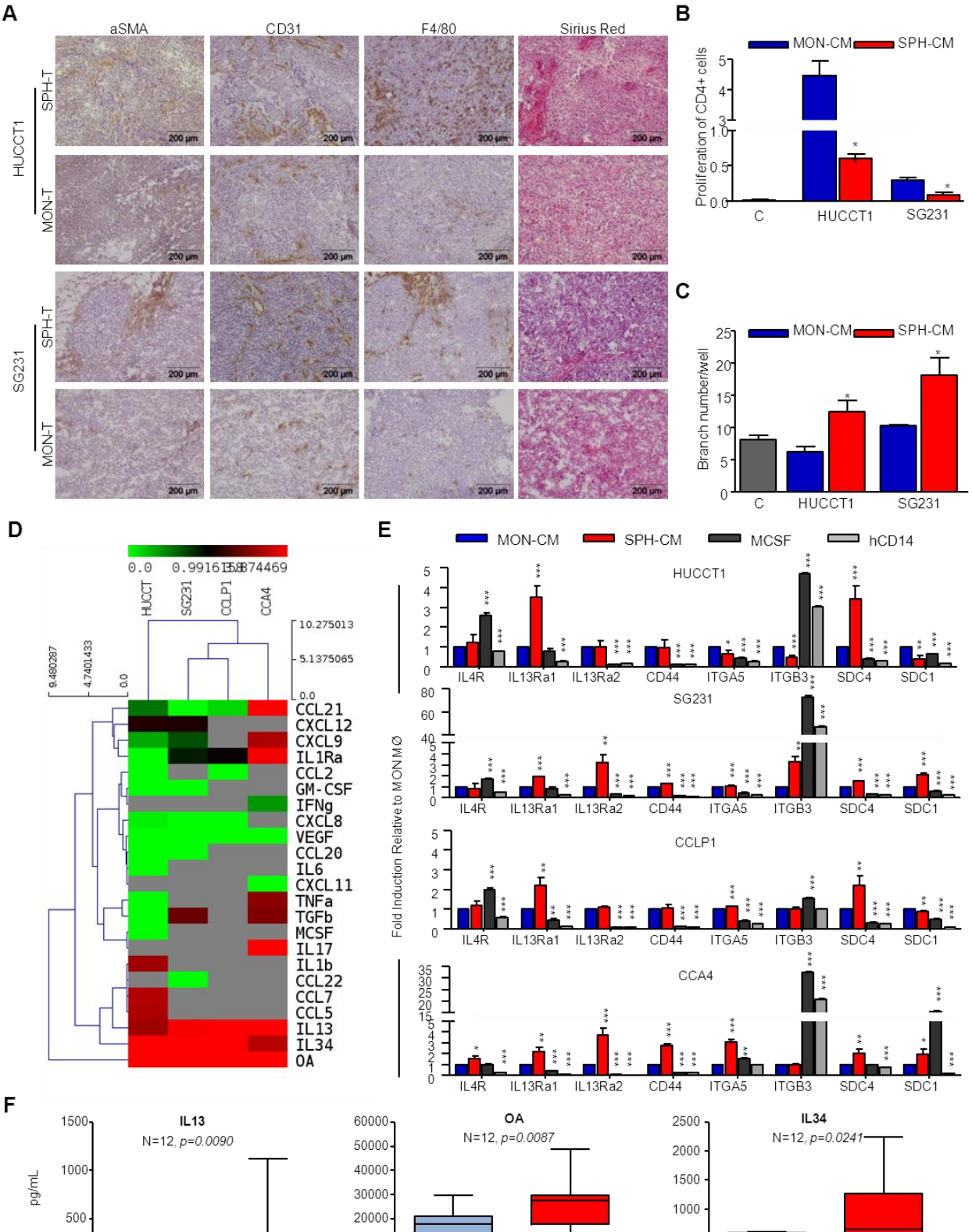
A
aSMA
CD31
F4/80
Sirius Red
HUCCT1
SPH-T
MON-T
SG231
SPH-T
MON-T
200 µm
B
MON-CM
SPH-CM
Proliferation of CD4+ cells
C
HUCCT1
SG231
C
MON-CM
SPH-CM
Branch number/well
C
HUCCT1
SG231
D
HUCCT
SG231
CCLP1
CCA4
CCL21
CXCL12
CXCL9
IL1Ra
CCL2
GM-CSF
IFNg
CXCL8
VEGF
CCL20
IL6
CXCL11
TNFa
TGFb
MCSF
IL17
IL1b
CCL22
CCL7
CCL5
IL13
IL34
OA
E
MON-CM
SPH-CM
MCSF
hCD14
HUCCT1
SG231
CCLP1
CCA4
Fold Induction Relative to MON MØ
IL4R
IL13Ra1
IL13Ra2
CD44
ITGA5
ITGB3
SDC4
SDC1
F
IL13
N=12, p=0.0090
OA
N=12, p=0.0087
IL34
N=12, p=0.0241
pg/mL
CTR
CCA

Figure 15. SPH-specific production of bioactive molecules.

A) Representative images show immunohistochemistry of aSMA, CD31, F4/80 and Sirius Red staining for collagen on SPH and MON tumor sections. Scale bar: 200 μm.

B) Effect of SPH- and MON-CM on CD4 + cells proliferation. CD4+ without stimulation used as control. Data presented as % of proliferating CD4+ cells. Mean ± SEM (n=3, *p value* versus MON-CM by Student t test, * p≤0.05, ** p≤0.01, *** p≤0.001).

C) Effect of SPH- and MON-CM on HUVEC tube formation. HUCCT1 and SG231 MON- and SPH-CM were added to the medium of HUVEC to assay their effect on the tube formation ability of HUVEC. Data presented as Number of branches/well . Mean ± SEM (n=3, *p value* versus MON-CM by Student t test, * p≤0.05, ** p≤0.01, *** p≤0.001).

D) Heat map representation of soluble mediators released by SPH and MON (ELISA). Concentration as pg/mL. Molecules clustered with names shown on right of heat map. Each raw corresponds to a single compound, and each column represents an independent condition. Heat-map color scale corresponds to relative molecule expression (on the top, minimum and maximum of all values). Results are average of three independent experiments.

E) Relative expression of transcript-encoding receptors for IL4 (IL4-R), IL13 (IL13Ra1, IL13Ra2), OA (CD44, ITGA5, ITGB3, SDC4) and IL34 (SDC1) in SPH and MON MØ. CD14+ cells as well M-CSF derived MØ, as controls. GAPDH as internal control. All mRNA levels are presented as fold changes normalized to 1 (mean expression of MON MØ).

F) IL13, OA and IL34 levels in CCA patients (n=12) and controls (CTR) (n=12) serum levels. Data are mean ± SEM (*p value* versus MON MØ by Student t test, * p≤0.05, ** p≤0.01, *** p≤0.001).

Figure 16

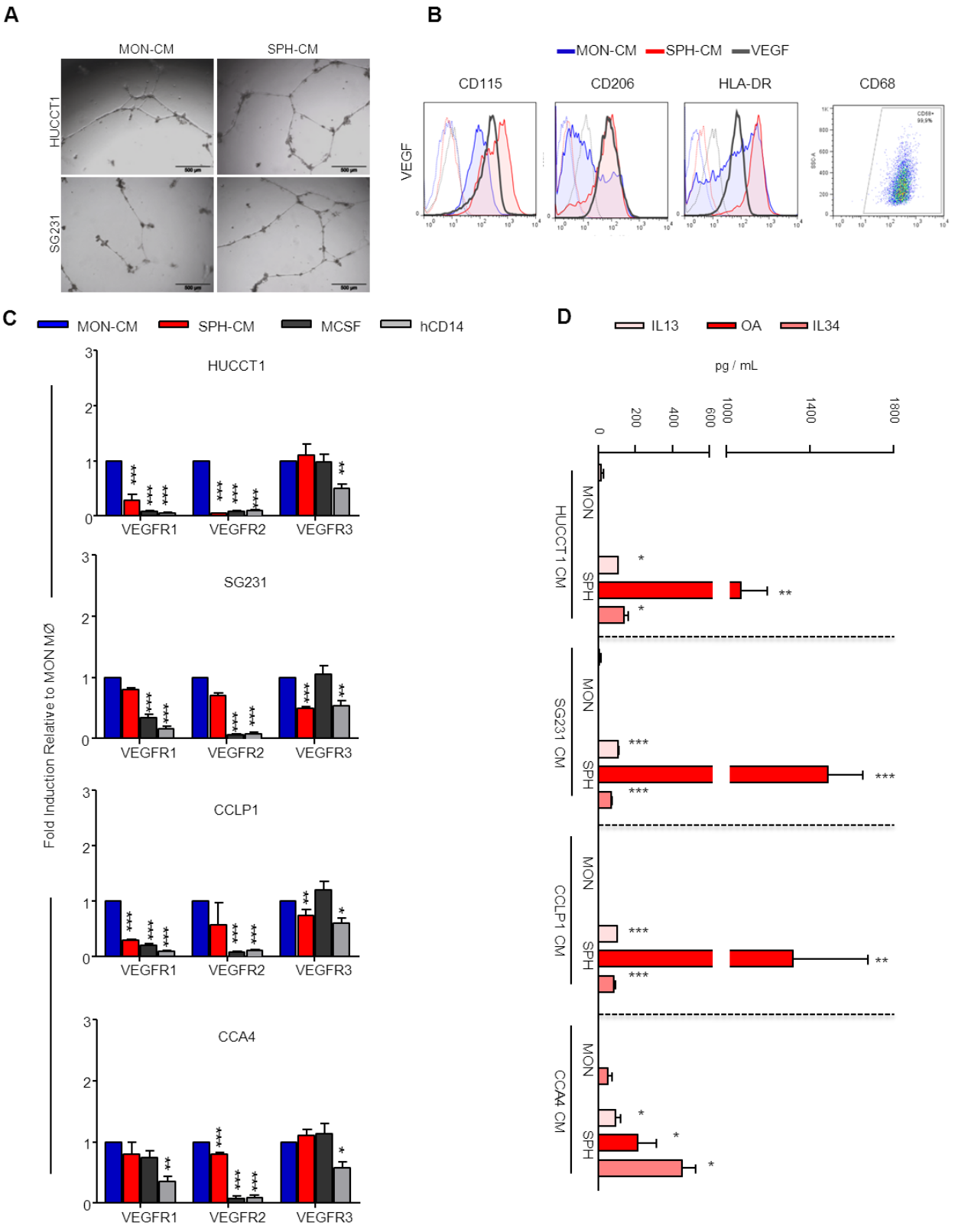
A
MON-CM
SPH-CM
HUCCT1
SG231
B
MON-CM
SPH-CM
VEGF
CD115
CD206
HLA-DR
CD68
VEGF
C
MON-CM
SPH-CM
MCSF
hCD14
HUCCT1
SG231
CCLP1
CCA4
VEGFR1
VEGFR2
VEGFR3
Fold Induction Relative to MON MØ
D
IL13
OA
IL34
pg / mL
0
200
400
600
1000
1400
1800
MON
SPH
HUCCT1 CM
SG231 CM
CCLP1 CM
CCA4 CM

Figure 16. Biological implication of CCA-SPH released factors

A) Representative pictures of tubules formed by HUVEC growth in MON and SPH-CM of both HUCCT1 and SG231 cells. Scale bar: 500 µm.

B) Effect of VEGF on macrophage differentiation**.** FACS histograms and percentage of positive cells for the CD115, CD206, HLA-DR and CD68 after addition of VEGF in fresh medium (in grey), as well as the addition of SPH-CM (in red) and MON-CM (in blue). The histograms and dot plots represent three independent experiments using macrophages from three different healthy donors.

C) Relative expression of transcript-encoding receptors for VEGF (VEGFR1, VEGFR2, VEGFR3) in macrophages differentiated in presence of SPH-CM (SPH MØ) as well as MON-CM (MON MØ). Freshly isolated human CD14+ cells used as control. GAPDH was used as an internal control. All mRNA levels are presented as fold changes normalized to 1 (mean expression of MON MØ). Data are mean ± SEM (*p value* versus MON MØ by Student t test, * p≤0.05, ** p≤0.01, *** p≤0.001). C) IL13, OA and IL34 levels in SPH and MON conditioned medium (n=3). Data are mean ± SEM (*p value* versus MON MØ by Student t test, * p≤0.05, ** p≤0.01, *** p≤0.001).

D) ELISA test of IL13, OA and IL34 concentration of SPH-CM and MON-CM in all tested CCA cells.

Figure 17

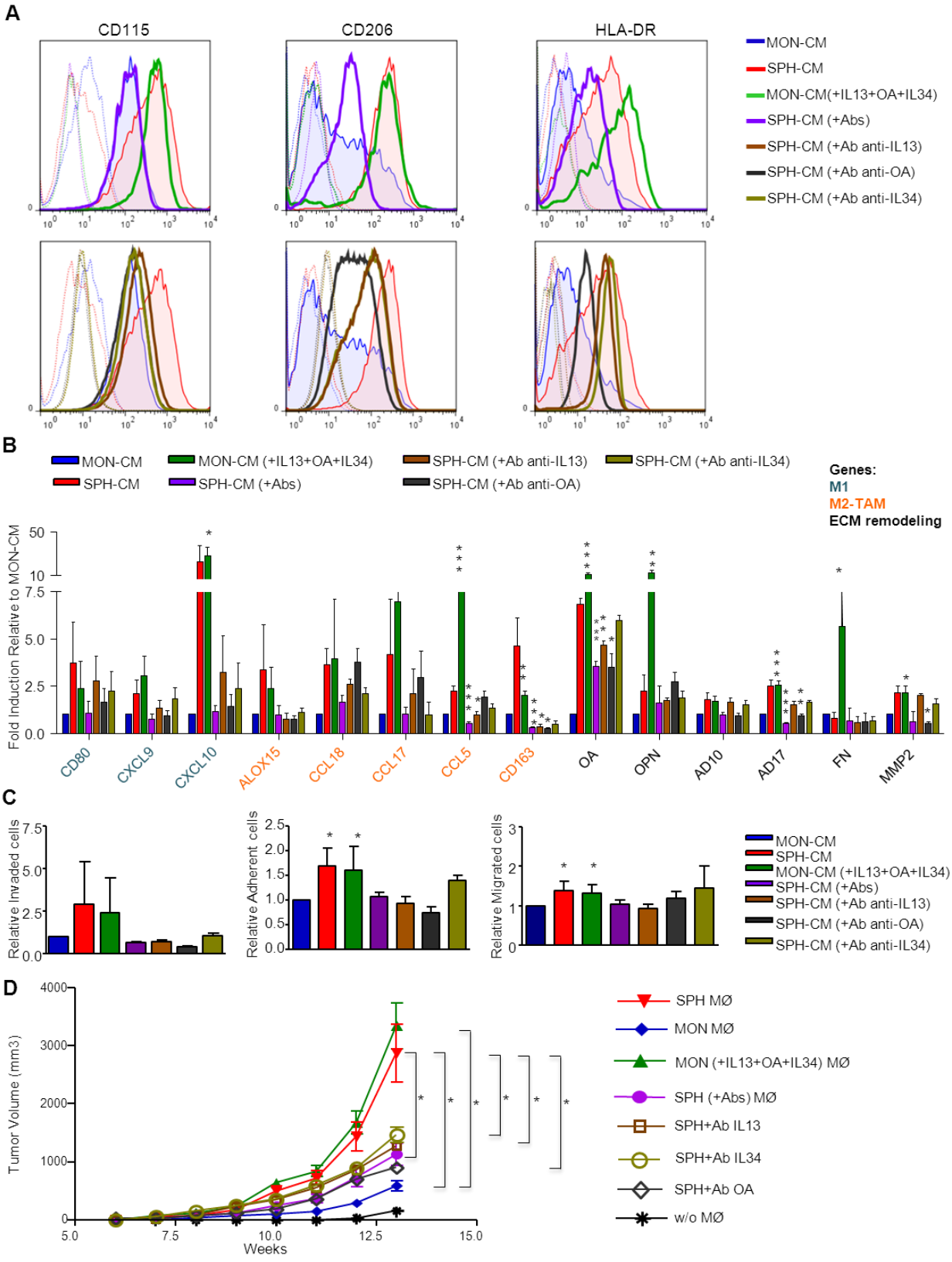
A
CD115
CD206
HLA-DR
MON-CM
SPH-CM
MON-CM(+IL13+OA+IL34)
SPH-CM (+Abs)
SPH-CM (+Ab anti-IL13)
SPH-CM (+Ab anti-OA)
SPH-CM (+Ab anti-IL34)
B
MON-CM
SPH-CM
MON-CM (+IL13+OA+IL34)
SPH-CM (+Abs)
SPH-CM (+Ab anti-IL13)
SPH-CM (+Ab anti-OA)
SPH-CM (+Ab anti-IL34)
Genes:
M1
M2-TAM
ECM remodeling
Fold Induction Relative to MON-CM
CD80
CXCL9
CXCL10
ALOX15
CCL18
CCL17
CCL5
CD163
OA
OPN
AD10
AD17
FN
MMP2
C
Relative Invaded cells
Relative Adherent cells
Relative Migrated cells
MON-CM
SPH-CM
MON-CM (+IL13+OA+IL34)
SPH-CM (+Abs)
SPH-CM (+Ab anti-IL13)
SPH-CM (+Ab anti-OA)
SPH-CM (+Ab anti-IL34)
D
Tumor Volume (mm3)
Weeks
SPH MØ
MON MØ
MON (+IL13+OA+IL34) MØ
SPH (+Abs) MØ
SPH+Ab IL13
SPH+Ab IL34
SPH+Ab OA
w/o MØ

Figure 17. IL13, OA, IL34 combination mimics SPH-like effects on MØ-differentiation and monocyte recruitment.

A) FACS-profile of CD115, HLA-DR and CD206 expression in MØs obtained by CD14+ cultured in presence of IL13 (80pg/mL), OA (0,9ng/mL) and IL34 (80pg/mL), added to the MON-CM (in green). Inhibitory impact of human antibodies anti IL13 (800ng/mL, 10.000X), OA (2700ng/mL, 3000X), IL34 (800ng/mL, 10.000X) alone (in brown, dark grey and dark green, respectively) or in combination was shown (in violet). Effects of both SPH- (in red) and MON- (in blue) CM also shown. Histograms represent three independent experiments using MØ from three different healthy donors.

B) Relative expression of M1/M2 and matrix remodeling-related genes. GAPDH as internal control. All mRNA levels displayed as fold changes normalized to 1 (mean expression of MON MØ) (n=3). Mean ± SEM (*p value* versus MON- or SPH-CM by Student t test, * p≤0.05, ** p≤0.01, *** p≤0.001).

C) Invasion and adhesion assay with FN-supports. Cells counted normalized to MON MØs(n=5). Migration assay of monocytes. Monocytes counted and normalized to monocyte migrated in presence of MON-CM (n=5). Mean ± SEM (*p value* versus MON- or SPH-CM by Student t test, * p≤0.05, ** p≤0.01, *** p≤0.001).

D) MØ-role in supporting *in vivo* tumorigenicity. 1,000 MONs (SG231) co-injected with 300 *in vitro*-educated MØs into NSG mice. Tumor growth evaluated. Mean±SEM (n=5, *p value* versus MON or SPH MØ at week 13 by Student t test, * p≤0.05, ** p≤0.01, *** p≤0.001).

Figure 18

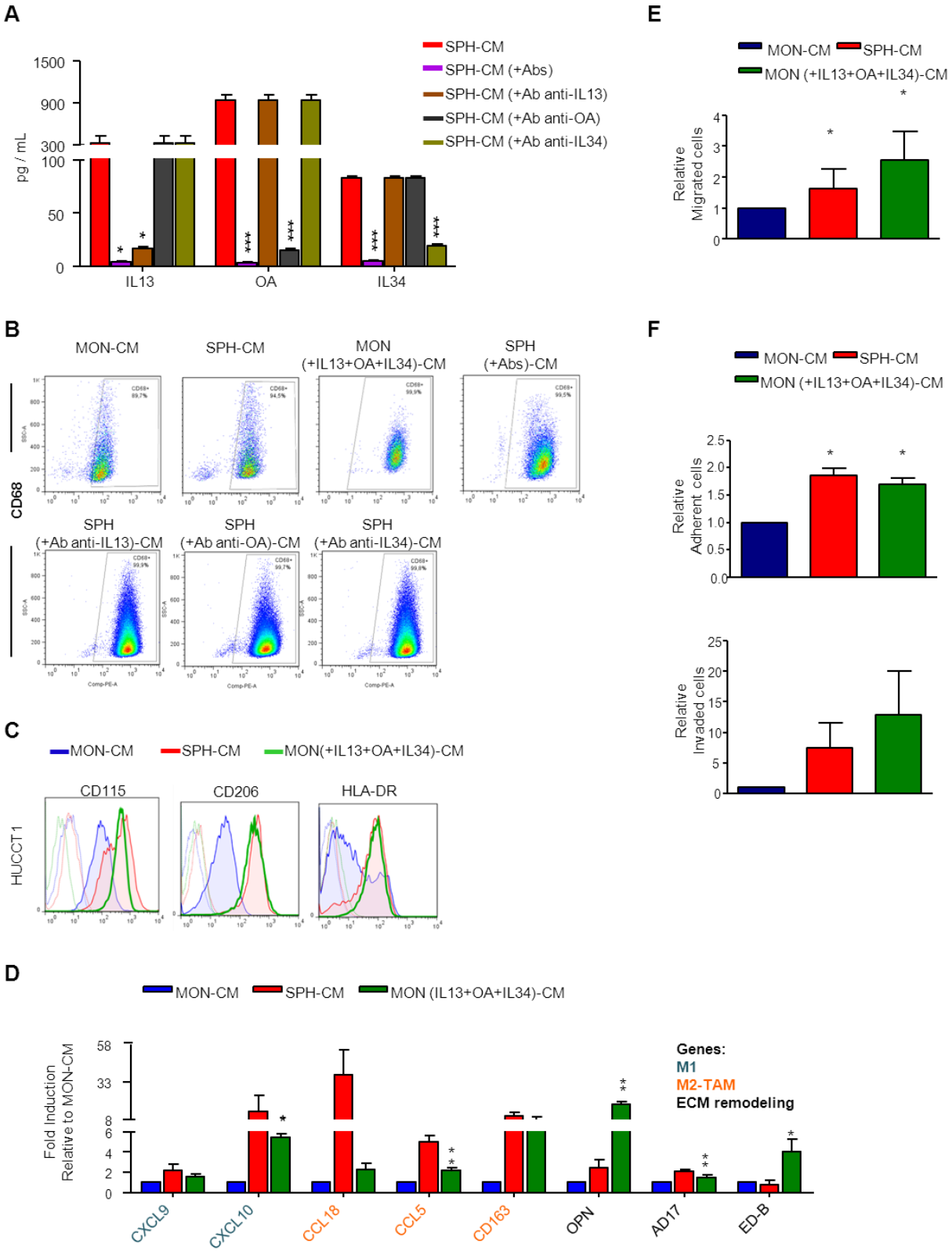
A
SPH-CM
SPH-CM (+Abs)
SPH-CM (+Ab anti-IL13)
SPH-CM (+Ab anti-OA)
SPH-CM (+Ab anti-IL34)
pg / mL
1500
900
300
100
50
0
IL13
OA
IL34
B
MON-CM
SPH-CM
MON (+IL13+OA+IL34)-CM
SPH (+Abs)-CM
CD68
SPH (+Ab anti-IL13)-CM
SPH (+Ab anti-OA)-CM
SPH (+Ab anti-IL34)-CM
C
MON-CM
SPH-CM
MON(+IL13+OA+IL34)-CM
CD115
CD206
HLA-DR
HUCCT1
D
MON-CM
SPH-CM
MON (IL13+OA+IL34)-CM
Fold Induction Relative to MON-CM
58
33
8
6
4
2
0
CXCL9
CXCL10
CCL18
CCL5
CD163
OPN
AD17
ED-B
Genes:
M1
M2-TAM
ECM remodeling
E
MON-CM
SPH-CM
MON (+IL13+OA+IL34)-CM
Relative Migrated cells
F
MON-CM
SPH-CM
MON (+IL13+OA+IL34)-CM
Relative Adherent cells
Relative Invaded cells

Figure 18. Macrophage differentiation induced by the combination of IL13, OA and IL34

A) ELISA test of IL13, OA and IL34 concentration to evaluate the inhibitory effect of single antibody or combination (antibodies anti IL13 (800ng/mL, 10.000X), OA (2700ng/mL, 3000X), IL34 (800ng/mL, 10.000X)) added to SG231 SPH-CM (in violet, brown, dark grey and dark green, respectively). The effect of SPH-CM (in red) was also shown.

B) Representative CD68 dot plots of macrophages derived by culture of CD14+ cells in the presence of IL13 (80pg/mL), OA (0,9ng/mL) and IL34 (80pg/mL), added to the SG231 MON-CM. Additionally, the inhibitory impact of human antibodies anti IL13 (800ng/mL, 10.000X), OA (2700ng/mL, 3000X), IL34 (800ng/mL, 10.000X) added alone or in combination to SG231 SPH-CM were shown. The effects of both SPH- and MON-CM are also shown. The dot plots represent three independent experiments using macrophages from three different healthy donors.

C) FACS profile of CD115, CD206A and HLA-DR positive cells after addition of a combination of IL13 (80pg/mL), OA (0,9ng/mL) and IL34 (80pg/mL) to HUCCT1 MON-CM (in green). The effects of both SPH- (in red) and MON-(in blue) CM are also shown. The histograms represent three independent experiments using macrophages from three different healthy donors.

D) Relative expression of transcript-encoding markers for M1 and M2 features as well for genes involved in ECM remodeling, adhesion, invasion in macrophages differentiated in presence of: HUCCT1 SPH-CM (in red), MON-CM (in blue), MON (+IL13 (80pg/mL)+OA (0,9ng/mL)+IL34 (80pg/mL))-CM (in green). GAPDH was used as an internal control. All mRNA levels are presented as fold changes normalized to 1 (mean expression of macrophages differentiated with MON-CM). Data are mean ± SEM (n=3, *p value* versus MON MØ by Student t test, * $p \leq 0.05$, ** $p \leq 0.01$, *** $p \leq 0.001$).

E) CD14+ cells migrated towards the combination of IL13 (80pg/mL), OA (0,9ng/mL) and IL34 (80pg/mL) added to HUCCT1 MON-CM (in green) (6 h). The

effects of both SPH- (in red) and MON-(in blue) CM are also shown. The CD14+ cells that migrated were counted and normalized to the number of CD14+ cells that migrated in the presence of MON-CM. Data are mean ± SEM (n=3, *p value* versus MON-CM by Student t test, * p≤0.05).

F) Invasion and adhesion assay of macrophages differentiated in presence of a combination of IL13 (80pg/mL), OA (0,9ng/mL) and IL34 (80pg/mL) to HUCCT1 MON-CM (in green). The effects of both SPH- (in red) and MON-(in blue) CM are also shown. The cells were counted and normalized to the number of MON-derived macrophages (MON MØ). Data are mean ± SEM (n=3, *p value* versus MON MØ by Student t test, * p≤0.05).

4.6 Tables

Table 2. Expression of CD115, CD206 and HLA-DR by MØ cultured in presence of CCA SPH- and MON-CM as well as in presence of M-CSF, IL4, LPS/INFγ and VEGF.

Marker	Cell Line-CM	Conditions	MFI ± SEM	*p value*
CD115	HUCCT1	SPH	532.7 ± 13	*0.0001*
		MON	159.3 ± 20	
	SG231	SPH	575.7 ± 23	*0.0003*
		MON	132.9 ± 30	
	CCLP1	SPH	1390.9 ± 27	*0.0000*
		MON	175.9 ± 32	
	CCA4	SPH	1275.3 ± 53	*0.0000*
		MON	240.9 ± 34	
		M-CSF	929.1 ± 41	
		VEGF	252.4 ± 14	
CD206	HUCCT1	SPH	372.4 ± 28	*0.0040*
		MON	178.2 ± 31	
	SG231	SPH	244.9 ± 26	*0.0019*
		MON	58.9 ± 17	
	CCLP1	SPH	172.5 ± 21	*0.2992*
		MON	152.8 ± 18	
	CCA4	SPH	341.3 ± 33	*0.0031*
		MON	124.9 ± 27	
		IL4	299.2 ± 26	
		LPS/INFγ	49,2 ± 19	
		VEGF	93.9 ± 12	
HLA-DR	HUCCT1	SPH	77.9 ± 05	*0.0038*
		MON	40.0 ± 06	
	SG231	SPH	112.1 ± 23	*0.0180*
		MON	12.7 ± 05	
	CCLP1	SPH	113.4 ± 10	*0.0032*
		MON	52.0 ± 07	
	CCA4	SPH	221.2 ± 26	*0.0131*
		MON	97.2 ± 31	
		IL4	14,8 ± 19	
		LPS/INFγ	170,8 ± 32	
		VEGF	94.5 ± 7	

The data are mean ± SEM (n=3, *p value* versus MON-CM by Student t test)

Table 3. Clinical and pathological parameters of CCA patients used for CD163 immunohistochemical staining.

Patient	Grade	TNM classification			Tumor size (cm)	Perineural invasion	Angio-invasion	CD163		CA19.9 (IU/mL)
								Intralesion	Tumor Front	
#CCA9	G1	T1	N0		3.8	no	no	75	75	42
#CCA14		T1	N0		2.8	no	no	35	35	2
#CCA21		T1	N0		3.5	no	no	35	75	15
#CCA27		T1	N0		2.5	no	no	30	40	nd
#CCA28		T1	N0		3.3	no	no	25	60	nd
#CCA29		T1	N0		3.6	no	no	45	35	nd
#CCA1	G2	T2b	NX	M1	33(multilobed)	nd	no	35	75	nd
#CCA2		nd	nd	nd	5	nd	no	7.5	5	5
#CCA3		T2b	N0	MX	6.3	yes	yes	7.5	35	nd
#CCA7		T1	N0	nd	3.1	yes	no	5	150	nd
#CCA8		T2	N0	nd	11	nd	yes	5	130	40
#CCA10		T2	N0	M1	5.7	nd	no	35	150	50
#CCA11		T2	N0	nd	7.5	nd	yes	5	125	28
#CCA13		T3	NX	nd	7	nd	no	5	40	nd
#CCA15		T1	N0	nd	11 (multilobed)	nd	no	5	160	6
#CCA17		T2b	NX	M1	33 (multilobed)	nd	no	35	70	nd
#CCA18		Nd	nd	nd	5	nd	no	7.5	5	5
#CCA19		T2a	N0	MX	6.3	yes	yes	15	25	12
#CCA22		T1	N1	MX	4	no	no	37	175	75
#CCA4	G3	T1	N1	nd	3.5	nd	no	7.5	140	23
#CCA5		nd	nd	nd	6.5	yes	yes	75	135	58
#CCA6		T3	N0	MX	6.9	nd	no	100	150	57
#CCA12		nd	nd	nd	6.3	nd	yes	35	165	95
#CCA16		T2b	N0	nd	14 (multinodular)	nd	yes	5	90	55
#CCA20		T1	N0	nd	2.8	no	no	35	145	16

Table 4. List of all 37 soluble mediators tested in sphere (SPH) and monolayer (MON) conditioned medium (CM) in all CCA cell lines.

Mediators	Production	HUCCT1-CM		SG231-CM		CCLP1-CM		CCA4-CM	
		MON	SPH	MON	SPH	MON	SPH	MON	SPH
VEGF	MON and SPH	1213±334	1165±44	1150±623	567±489	513±395	20±28	293±11	150±8
TNFa	MON or/and SPH	126±178	7±10	nd	nd	nd	4±5	nd	31±3
MCSF		216±239	nd	nd	nd	nd	nd	nd	nd
CCL21		35±49	50±71	53±75	48±68	43±60	47±67	43±60	151±23
TGFb		146±207	nd	26±36	119±169	nd	nd	nd	27±6
GM-CSF		1058± 913	214±157	14±20	nd	nd	nd	nd	nd
CCL22		nd	nd	33±6	3±4	nd	nd	nd	nd
CCL20		286±405	278±393	98±139	44±62	nd	nd	nd	nd
CXCL8		968±288	1008±355	328±234	89±98	102±145	nd	102±145	nd
CCL2		217±246	137±193	nd	nd	63±55	nd	63±55	nd
IL1b		nd	35±50	nd	nd	nd	nd	nd	nd
IL6		484±209	460±202	nd	nd	nd	nd	nd	nd
CXCL11		nd	nd	nd	nd	nd	nd	18±7	nd
IL17		nd	nd	nd	nd	nd	nd	nd	830±33
CXCL1		562±795	551±779	10±14	8±11	9±13	9±13	nd	nd
CCL5		1±1	26±36	nd	nd	nd	nd	nd	nd
CXCL9		nd	6±9	1±2	2±3	nd	nd	nd	40±13
CXCL12		nd	13±19	nd	13±18	nd	nd	nd	nd
IL2	No	nd	nd	nd	nd	nd	nd	nd	nd
IL10		nd	nd	nd	nd	nd	nd	nd	nd
IL12 p40		nd	nd	nd	nd	nd	nd	nd	nd
IFNg		nd	nd	nd	nd	nd	nd	nd	nd
CCL18		nd	nd	nd	nd	nd	nd	nd	nd
CCL17		nd	nd	nd	nd	nd	nd	nd	nd
CCL1		nd	nd	nd	nd	nd	nd	nd	nd
CCL7		nd	nd	nd	nd	nd	nd	nd	nd
CXCL10		nd	nd	nd	nd	nd	nd	nd	nd
IL7		nd	nd	nd	nd	nd	nd	nd	nd
CCL3		nd	nd	nd	nd	nd	nd	nd	nd
CCL8		nd	nd	nd	nd	nd	nd	nd	nd
CCL4		nd	nd	nd	nd	nd	nd	nd	nd
GDNF		nd	nd	nd	nd	nd	nd	nd	nd
IL12p70		nd	nd	nd	nd	nd	nd	nd	nd
IL13	SPH	15±10	107±1	nd	110±2	nd	103±7	nd	97±46
OA		nd	1069±223	nd	1483±295	nd	1318±620	nd	216±166
IL34		nd	142±34	nd	73±4	nd	87±13	53±37	453±126

Table 5. Clinical and pathological parameters of 12 CCA patients used for IL13, OA, and IL34 serum quantification.

Clinical Variables		No. (*n*=12)	%
Age (years)	<70	3	25.0
	>70	9	75.0
Gender	Male	7	58.3
	Female	5	41.7
TNM	I-II	0	00.0
	III-IV	9	75.0
	nd	3	25.0
Tumor stage	IIIA-B	2	16.7
	IVA-B	9	75.0
	nd	1	08.3
Relapse	yes	0	00.0
	no	12	100.0
Distant Metastasis	with	4	33.3
	without	3	25.0
	nd	5	41.7
Invasion	with	9	75.0
	without	0	00.0
	nd	3	25.0
Tumor resection	yes	4	33.3
	no	8	66.7
Chemotherapy	yes	7	58.3
	no	5	41.7
CA19.9 (IU/mL)	40-100	1	08.3
	100-1000	6	50.0
	> 1000	4	33.3
	nd	1	08.3
CA125 (UI/mL)	< 37	5	41.7
	> 37	6	50.0
	nd	1	08.3
1-year survival		4/10	40.0

Table 6. Correlation of SPH stem-like genes and OA, IL34 and IL13 in clinical CCA (n=104 patient tumors) using a microarray database [6]. Pearson correlation between gene pairs was calculated using R and the "cortest" function, yielding correlation coefficients and p-values.

Correlation of SPH stem-like genes and OA, IL34 and IL13 in clinical CCA (n=104 patient tumors)		
SPH Genes	**OA**	
	R	*p value*
BMI1	0.3504	*0.0003*
CD44	0.3844	*0.0001*
CTNNB1	0.4419	*0.0000*
KITLG	0.3975	*0.0000*
KLF4	0.3603	*0.0001*
LEF1	0.6321	*0.0000*
THY1	0.5118	*0.0000*
SPH Genes	**IL34**	
	R	*p value*
MAML1	0.3423	*0.0004*
THY1	0.2966	*0.0022*
SPH Genes	**IL13**	
	R	*p value*
LIN28A	0.4906	*0.0000*
POU5F1	0.2685	*0.0059*
SOX2	0.3121	*0.0013*

Table 7. Correlation of SPH stem-like genes and SPH MØ in clinical CCA (n=104 patient tumors) using a microarray database [6].

Correlation of SPH stem-like and SPH MØ genes in clinical CCA (n=104 patient tumors)		
SPH genes	CCL5	
	R	*p value*
LEF1	0.2709	*0.0054*
MAML1	0.2553	*0.0089*
SPH genes	CCL18	
	R	*p value*
CTNNB1	0.2563	*0.0086*
SPH genes	CD115	
	R	*p value*
LEF1	0.2942	*0.0024*
THY1	0.2517	*0.0100*
SPH genes	CD163	
	R	*p value*
ABCG2	0.2583	*0.0081*
CTNNB1	0.2941	*0.0024*
HNF4A	0.3300	*0.0006*
STAT3	0.3017	*0.0018*
SPH genes	CD206	
	R	*p value*
BMI1	0.3368	*0.0005*
KLF4	0.3241	*0.0008*
MYC	0.3056	*0.0016*
NOS2	0.2479	*0.0112*
SPH genes	CD68	
	R	*p value*
CD44	0.2392	*0.0145*
LGR5	0.2315	*0.0181*
SPH genes	HLA-DRA	
	R	*p value*
BMI1	0.3944	*0.0000*
CTNNB1	0.4342	*0.0000*
LEF1	0.5412	*0.0000*
THY1	0.3587	*0.0002*
SPH genes	MMP2	
	R	*p value*
CD44	0.3561	*0.0002*
CTNNB1	0.5208	*0.0000*
KLF4	0.2790	*0.0041*
LEF1	0.7343	*0.0000*
THY1	0.8105	*0.0000*
YAP1	0.2786	*0.0042*
SPH genes	OPN	
	R	*p value*
BCL2L1	0.3511	*0.0002*
EPCAM	0.2446	*0.0123*
FGFR2	0.3939	*0.0000*
ITGB1	0.5934	*0.0000*

Pearson correlation between gene pairs was calculated using R and the "cortest" function, yielding correlation coefficients and p-values.

Table 8. Expression of CD115, CD206 and HLA-DR by MØ cultured in presence of CCA SPH- and MON-CM as well as in presence of MON-CM added with 3 sphere-specific released molecules and SPH-CM added with antibodies for the 3 sphere-specific released molecules.

Marker	Cell Line-CM	Conditions	MFI ± SEM	
CD115	HUCCT1	SPH	532.7 ± 13	
		MON	159.3 ± 20	***
		MON+IL13+OA+IL34	463.3 ± 22	**
		MON+IL13	47.9 ± 13	***
		MON+IL34	113.2 ± 21	*
		MON+OA	76.4 ± 16	
	SG231	SPH	575.7 ± 23	
		MON	132.9 ± 30	***
		MON+IL13+OA+IL34	547.2 ± 35	***
		SPH+Abs	130.7 ± 27	***
		SPH+Ab anti-IL13	241.0 ± 32	***
		SPH+Ab anti-OA	160.1 ± 29	***
		SPH+Ab anti IL34	172.0 ± 33	
CD206	HUCCT1	SPH	372.4 ± 28	
		MON	178.2 ± 31	**
		MON+IL13+OA+IL34	358.3 ± 33	**
		MON+IL13	1333.9 ± 130	**
		MON+IL34	1825.2 ± 104	**
		MON+OA	1071.0 ± 86	
	SG231	SPH	244.9 ± 26	
		MON	58.9 ± 17	**
		MON+IL13+OA+IL34	264.7 ± 31	**
		SPH+Abs	25.3 ± 12	**
		SPH+Ab anti-IL13	94.0 ± 22	***
		SPH+Ab anti-OA	45.6 ± 13	**
		SPH+Ab anti-IL34	90.2 ± 19	
HLA-DR	HUCCT1	SPH	77.9 ± 5	
		MON	40.0 ± 6	*
		MON+IL13+OA+IL34	86.4 ± 17	ns
		MON+IL13	90.4 ± 21	ns
		MON+IL34	56.4 ± 14	**
		MON+OA	149.8 ± 28	
	SG231	SPH	112.7 ± 23	
		MON	12.7 ± 5	**
		MON+IL13+OA+IL34	200.6 ± 24	*
		SPH+Abs	14.7 ± 7	*
		SPH+Ab anti-IL13	40.2 ± 15	**
		SPH+Ab anti-OA	14.8 ± 7	*
		SPH+Ab anti-IL34	55.7 ± 18	

The data are mean ± SEM (n=3, *p value* versus MON- or SPH-CM by Student t test,
* p≤0.05, ** p≤0.01, *** p≤0.001, ns=not significant)

5. DISCUSSION

Current CCA treatment strategies are largely ineffective, making this tremendous aggressive disease an unmet medical need [4, 5, 7]. Therefore, understanding the pathogenesis of CCA is essential for identifying potential curative targets. The recently proposed concept of stemness-driven carcinogenesis highlights the existence of a therapeutically challenging cellular subset responsible for tumor initiation, dissemination and drug-resistance, termed CSCs [24].

Our study mainly focused on exploration of stem-compartment in human intrahepatic CCA by using a 3D culture system as a well-known functional tool to select and enrich for tumor-stem like cells. CSCs represent a still poorly explored research line in CCA field, likely because of the absence of CCA-CSC specific markers, that strongly limits the use of classical antigenic approach to isolate CSCs. Moreover, a recent work showed that CCA-CSCs are extremely heterogeneous in terms of marker expression, emphasizing the importance to use an alternative tool to isolate CSC subpopulation [77]. Specifically, 3D sphere assay has never been used to enrich CCA stem-like cells and in our study we demonstrated its strenght, even compare to antigenic approach (by using THY1 as general CCA-CSC marker). Accordingly with our hypothesis, only oncogenic transformed cholangiocytes were capable to initiate 3D sphere formation compare to the normal counterpart, suggesting a potential existence of stem-like subset possibly responsible for tumor initiation and progression in CCA. Notably, heterogeneity in sphere forming capability is evident across our panel of CCA cell lines, as indication of a possible correlation with diverse patterns of molecular expression and different grades of tumorigenic potential *in vivo*. Thus, by using *in vitro* spherogenicity and *in vivo* tumorigenicity as criteria of stemness properties, for the first time we provided extensive molecular and functional evidence for CCA stem-like compartment identified by 3D cultures. First, although with a certain degree of heterogeneity between cell lines, all CCA-SPH displayed an higher drug resistance compare to CCA-MON, stressing the

relevance of drug resistance as a common well known CSC feature. Moreover, the extensive molecular characterization of CCA-SPH performed by pathway-focused PCR arrays showed cell line-specific over-expression of key genes associated to CSC-like features, embryonic stem cell signaling and liver oncogenic pathways. Despite the cell line-specific gene upregulation, we were able to identify a set of 30 common deregulated genes in all CCA-SPH (23 CSC-genes, 6 liver cancer related markers and 1 ESC factor), suggesting that CSCs might maintain a common stemness-related gene expression signature, with a clinically potential translational value.

Secondly, here we proposed that tumor stem-like cells might model their immunopathological-niche according to their necessities. Indeed, we focused on CSC-secretome responsible for infiltrating-monocyte recruitment and MØ-priming. Pertinently, aim of this study was the exploration of CSC impact on TAM traits in CCA. Indeed, we showed that TAMs, as highly plastic population [180, 182], are able to acquire a peculiar phenotype dependent on bioactive CSC-secretome. Since it's became clear that CSC-TAM crosstalk is bidirectional, further studies are required to deepen SPH MØ impact on tumorigenic potential and drug-resistance of SPH cells.

A variety of modulators released by stromal and tumor cells recruit circulating monocytes to tumor sites, cause their differentiation into MØs and severely affect their functions [226, 240-242]. In this respect, we demonstrated that SPH-CM act as a potent monocyte-attractor. Moreover, our results showed profound molecular and functional differences among MØ activated by CCA-SPH in comparison to MON MØs suggesting that different TAM-compartments within same tumor may reflect diverse responses to divergent local signals. Indeed, tumor stem-like associated-TAMs displayed mixed M1-M2 molecular traits, including the expression of M1-M2 surface markers (CD206 and HLA-DR) as well as M1-M2 typical associated genes (e.g., CXCL10, CCL18, CD163). Overexpression of CCL5 could be consistent with TAM ability to recruit new

peripheral blood circulating monocyte at tumor site, in order to sustain tumor growth and progression. Moreover, SPH MØ retained higher invasion and adhesion capability, also in accordance with increased expression of genes involved in ECM remodeling (e.g., OA, OPN, FN, MMP-2). Hence, a mixed state of MØ-subsets reinforced the concept of TAM plasticity. It's important to note that CSC ability to modulate a macrophage dominated inflammatory response is similar to the reactive phenotype displayed by cholangiocytes of dysplastic bile ducts in a mouse model of congenital hepatic fibrosis [243], a disease with high risk of CCA development.

Our *in vitro* finding were extensively validated in our 'patient-like' mouse model and human CCA specimen, underlining the strength of our results. Regarding the limitations of our 'patient-like' animal model, we knowledge that orthotopic allograft models for human CCA represent the impeccable tool to recapitulate key clinical, cellular and molecular features of this aggressive tumor [244]. Moreover, mice harboring a human immune system (humanized mice with human CD34+ transplantation) could recreate a human-type TME for tumors growing as xenografts [225, 245, 246], likely preserving a CSC-niche that is more similar to that present in cancer patients, thus facilitating our understanding of the role of CSCs in tumorigenesis. Unfortunately, while diverse animal models of CCA (including numerous new genetic models) do exist, an effective patient-like CCA animal model remains to be established [244]. Thus, this lack represents a limitation in the understanding the CCA pathogenesis. Nevertheless, in this study we alternatively presented a first human CCA–like setting (humanized mice with transplantation of hPBMCs) as preclinical platform to investigate mechanisms bridging CCA-disease to CCA-infiltrating MØs for synergistic therapies. Notably, despite several limitations, our humanized xenograft (s.c. patient CCA-SPH and i.v. hPBMC) highlights SPH biological relevance in priming associated-MØs.

Of relevance, our findings indicated that CCA-SPH specific released molecules, such as IL13, OA and IL34, are responsible for modeling the macrophage component associated to CSCs.

Interestingly, IL34 has recently been identified as a second ligand for hematopoietic colony stimulating factor-1 receptor (CSF-1R) together with the cytokine CSF1, also known as M-CSF [247]. CSF1-R activation establishes signaling cascades leading to differentiation and functionality of monocytes, tissue-MØs and antigen-presenting dendritic cells [236, 240]. Thus, MØ-differentiation may be possibly driven by IL34 or alternative mechanisms (e.g., VEGF) proposing new clues for CCA-immunotherapy strategies [241].

Consistently, IL13 has been described as a typical Th_2 type cytokine that, together with IL4, generated alternatively activated M2-MØs [236, 240]. This clearly suggested that SPH induced-MØs resemble M2-polarized cells.

Lastly, OA (also known as glycoprotein non-metastatic melanoma protein b [gpnmb]), a type 1 transmembrane glycoprotein, is produced by embryonic nervous system, developing nephrons, osteoblasts and osteoclasts. Remarkably, OA is overexpressed in patients with glioblastoma multiform and significantly correlated with poor outcome [248]. Moreover, in breast cancer cells, OA high expression levels are required for their enhanced invasiveness and osteolytic bone metastases formation .

Notably, levels of these 3 CCA-SPH specific associated factors were significantly found elevated in CCA patients compared to healthy control subjects, suggesting their potential crucial role in colangiocarcinogenesis. Future analysis with greater sample size are surely needed, in order to validate the association of CSC-secreted factors with CCA-disease (e.g., with clinical pathological features of CCA patients, tumor stage or grade).

Together our observations pointed to a stem-like secretome (IL13, OA, IL34 production) and resulting-MØ phenotype in human CCA. Although additional studies are warranted to formally dissect molecular mechanisms underlying

differentiation of recruited monocytes towards SPH MØ-subset, we provide a rationale for IL13, OA and IL34 targeting. Indeed, extra analyses are essential in demonstrating the base knowledge for effective prevention and/or treatment of malignant SPH MØ-subset, thus leading to exploration of combination therapies in CCA patients.

In summary, the current study provides a partial map of the multilayered relationship between TAMs and CSCs in CCA. Although at initial level, this work offers numerous new insights within somewhat intricate network of CSC-TAM in CCA, with potentially future clinical implications. Indeed, since immune plasticity represents an important hallmark of tumor and CSCs are able to manipulate stromal cells to their needs, a better definition of key deregulated immune subtype responsible to cooperate in supporting tumor initiation may facilitate the development of new therapeutic approaches. Considering that human CCA represents a clinical emergency, it is essential to move to predictive models to understand the adaptive process of macrophage component (imprinting, polarization and maintenance) engaged by tumor stem-like compartment. Hence, a better understanding of CSC-macrophage interplay, partially provided here, may be a very clinically helpful adjunct in the context of CCA multi-targeting strategies. Indeed, reprogramming CSC–TAM crosstalk could also be an interesting approach to yield a therapeutic effect. To this end, in the contest of nanotechnology medicine, *in vivo* administration of IL13, OA and IL34 antibodies combined with chemotherapies, potentially represent a versatile biomedical tool to improve CCA outcome.
More research is warranted in this area to harness the great potential that this emerging knowledge offers.

6. REFERENCES

1 El-Serag HB. Hepatocellular carcinoma. The New England journal of medicine 2011; 365: 1118-1127.

2 Oikawa T. Cancer Stem cells and their cellular origins in primary liver and biliary tract cancers. Hepatology 2016; 64: 645-651.

3 Kumar M, Zhao X, Wang XW. Molecular carcinogenesis of hepatocellular carcinoma and intrahepatic cholangiocarcinoma: one step closer to personalized medicine? Cell & bioscience 2011; 1: 5.

4 Shaib Y, El-Serag HB. The epidemiology of cholangiocarcinoma. Seminars in liver disease 2004; 24: 115-125.

5 Banales JM, Cardinale V, Carpino G, Marzioni M, Andersen JB, Invernizzi P *et al*. Expert consensus document: Cholangiocarcinoma: current knowledge and future perspectives consensus statement from the European Network for the Study of Cholangiocarcinoma (ENS-CCA). Nature reviews Gastroenterology & hepatology 2016; 13: 261-280.

6 Andersen JB, Spee B, Blechacz BR, Avital I, Komuta M, Barbour A *et al*. Genomic and genetic characterization of cholangiocarcinoma identifies therapeutic targets for tyrosine kinase inhibitors. Gastroenterology 2012; 142: 1021-1031 e1015.

7 Blechacz B, Gores GJ. Cholangiocarcinoma: advances in pathogenesis, diagnosis, and treatment. Hepatology 2008; 48: 308-321.

8 Rizvi S, Gores GJ. Pathogenesis, diagnosis, and management of cholangiocarcinoma. Gastroenterology 2013; 145: 1215-1229.

9 Blechacz B, Komuta M, Roskams T, Gores GJ. Clinical diagnosis and staging of cholangiocarcinoma. Nature reviews Gastroenterology & hepatology 2011; 8: 512-522.

10 Zabron A, Edwards RJ, Khan SA. The challenge of cholangiocarcinoma: dissecting the molecular mechanisms of an insidious cancer. Disease models & mechanisms 2013; 6: 281-292.

11 Khan SA, Thomas HC, Davidson BR, Taylor-Robinson SD. Cholangiocarcinoma. Lancet 2005; 366: 1303-1314.

12 Sakaguchi T, Suzuki S, Morita Y, Oishi K, Suzuki A, Fukumoto K *et al*. Impact of the preoperative des-gamma-carboxy prothrombin level on prognosis after hepatectomy for hepatocellular carcinoma meeting the Milan criteria. Surgery today 2010; 40: 638-645.

13 Shirabe K, Kanematsu T, Matsumata T, Adachi E, Akazawa K, Sugimachi K. Factors linked to early recurrence of small hepatocellular carcinoma after hepatectomy: univariate and multivariate analyses. Hepatology 1991; 14: 802-805.

14 Yamashita Y, Adachi E, Toh Y, Ohgaki K, Ikeda O, Oki E *et al*. Risk factors for early recurrence after curative hepatectomy for colorectal liver metastases. Surgery today 2011; 41: 526-532.

15 Leyva-Illades D, McMillin M, Quinn M, Demorrow S. Cholangiocarcinoma pathogenesis: Role of the tumor microenvironment. Translational gastrointestinal cancer 2012; 1: 71-80.

16 Aljiffry M, Walsh MJ, Molinari M. Advances in diagnosis, treatment and palliation of cholangiocarcinoma: 1990-2009. World journal of gastroenterology : WJG 2009; 15: 4240-4262.

17 Moeini A, Sia D, Bardeesy N, Mazzaferro V, Llovet JM. Molecular Pathogenesis and Targeted Therapies for Intrahepatic Cholangiocarcinoma. Clinical cancer research : an official journal of the American Association for Cancer Research 2016; 22: 291-300.

18 Sia D, Tovar V, Moeini A, Llovet JM. Intrahepatic cholangiocarcinoma: pathogenesis and rationale for molecular therapies. Oncogene 2013; 32: 4861-4870.

19 Kongpetch S, Jusakul A, Ong CK, Lim WK, Rozen SG, Tan P *et al*. Pathogenesis of cholangiocarcinoma: From genetics to signalling pathways. Best Pract Res Clin Gastroenterol 2015; 29: 233-244.

20 Cardinale V, Carpino G, Reid L, Gaudio E, Alvaro D. Multiple cells of origin in cholangiocarcinoma underlie biological, epidemiological and clinical heterogeneity. World journal of gastrointestinal oncology 2012; 4: 94-102.

21 Raggi C, Invernizzi P, Andersen JB. Impact of microenvironment and stem-like plasticity in cholangiocarcinoma: molecular networks and biological concepts. Journal of hepatology 2015; 62: 198-207.

22 Chong DQ, Zhu AX. The landscape of targeted therapies for cholangiocarcinoma: current status and emerging targets. Oncotarget 2016.

23 Simbolo M, Fassan M, Ruzzenente A, Mafficini A, Wood LD, Corbo V *et al*. Multigene mutational profiling of cholangiocarcinomas identifies actionable molecular subgroups. Oncotarget 2014; 5: 2839-2852.

24 Pattabiraman DR, Weinberg RA. Tackling the cancer stem cells - what challenges do they pose? Nat Rev Drug Discov 2014; 13: 497-512.

25 Berthiaume EP, Wands J. The molecular pathogenesis of cholangiocarcinoma. Seminars in liver disease 2004; 24: 127-137.

26 Komuta M, Spee B, Vander Borght S, De Vos R, Verslype C, Aerts R *et al*. Clinicopathological study on cholangiolocellular carcinoma suggesting hepatic progenitor cell origin. Hepatology 2008; 47: 1544-1556.

27 Zhou H, Wang H, Zhou D, Wang Q, Zou S, Tu Q *et al*. Hepatitis B virus-associated intrahepatic cholangiocarcinoma and hepatocellular carcinoma may hold common disease process for carcinogenesis. Eur J Cancer 2010; 46: 1056-1061.

28 Lee JS, Heo J, Libbrecht L, Chu IS, Kaposi-Novak P, Calvisi DF *et al*. A novel prognostic subtype of human hepatocellular carcinoma derived from hepatic progenitor cells. Nature medicine 2006; 12: 410-416.

29 Yamashita T, Ji J, Budhu A, Forgues M, Yang W, Wang HY *et al*. EpCAM-positive hepatocellular carcinoma cells are tumor-initiating cells with stem/progenitor cell features. Gastroenterology 2009; 136: 1012-1024.

30 Nomoto K, Tsuneyama K, Cheng C, Takahashi H, Hori R, Murai Y *et al*. Intrahepatic cholangiocarcinoma arising in cirrhotic liver frequently expressed p63-positive basal/stem-cell phenotype. Pathology, research and practice 2006; 202: 71-76.

31 Roskams T. Liver stem cells and their implication in hepatocellular and cholangiocarcinoma. Oncogene 2006; 25: 3818-3822.

32 Roskams T. Different types of liver progenitor cells and their niches. Journal of hepatology 2006; 45: 1-4.

33 Kitade M, Factor VM, Andersen JB, Tomokuni A, Kaji K, Akita H *et al*. Specific fate decisions in adult hepatic progenitor cells driven by MET and EGFR signaling. Genes & development 2013; 27: 1706-1717.

34 Woo HG, Lee JH, Yoon JH, Kim CY, Lee HS, Jang JJ *et al*. Identification of a cholangiocarcinoma-like gene expression trait in hepatocellular carcinoma. Cancer research 2010; 70: 3034-3041.

35 Zhang F, Chen XP, Zhang W, Dong HH, Xiang S, Zhang WG *et al*. Combined hepatocellular cholangiocarcinoma originating from hepatic progenitor cells: immunohistochemical and double-fluorescence immunostaining evidence. Histopathology 2008; 52: 224-232.

36 Andersen JB, Thorgeirsson SS. Genetic profiling of intrahepatic cholangiocarcinoma. Current opinion in gastroenterology 2012; 28: 266-272.

37 Carpino G, Cardinale V, Onori P, Franchitto A, Berloco PB, Rossi M *et al*. Biliary tree stem/progenitor cells in glands of extrahepatic and intraheptic bile ducts: an anatomical in situ study yielding evidence of maturational lineages. J Anat 2012; 220: 186-199.

38 Razumilava N, Gores GJ. Notch-driven carcinogenesis: the merging of hepatocellular cancer and cholangiocarcinoma into a common molecular liver cancer subtype. Journal of hepatology 2013; 58: 1244-1245.

39 Zucman-Rossi J, Nault JC, Zender L. Primary liver carcinomas can originate from different cell types: a new level of complexity in hepatocarcinogenesis. Gastroenterology 2013; 145: 53-55.

40 Holczbauer A, Factor VM, Andersen JB, Marquardt JU, Kleiner DE, Raggi C *et al*. Modeling pathogenesis of primary liver cancer in lineage-specific mouse cell types. Gastroenterology 2013; 145: 221-231.

41 Fan B, Malato Y, Calvisi DF, Naqvi S, Razumilava N, Ribback S *et al*. Cholangiocarcinomas can originate from hepatocytes in mice. The Journal of clinical investigation 2012; 122: 2911-2915.

42 Sekiya S, Suzuki A. Intrahepatic cholangiocarcinoma can arise from Notch-mediated conversion of hepatocytes. The Journal of clinical investigation 2012; 122: 3914-3918.

43 Fidler IJ, Hart IR. Biological diversity in metastatic neoplasms: origins and implications. Science 1982; 217: 998-1003.

44 Heppner GH, Miller BE. Tumor heterogeneity: biological implications and therapeutic consequences. Cancer metastasis reviews 1983; 2: 5-23.

45 Kreso A, Dick JE. Evolution of the cancer stem cell model. Cell stem cell 2014; 14: 275-291.

46 Morrison SJ, Kimble J. Asymmetric and symmetric stem-cell divisions in development and cancer. Nature 2006; 441: 1068-1074.

47 Clarke MF, Dick JE, Dirks PB, Eaves CJ, Jamieson CH, Jones DL *et al*. Cancer stem cells--perspectives on current status and future directions: AACR Workshop on cancer stem cells. Cancer research 2006; 66: 9339-9344.

48 Beachy PA, Karhadkar SS, Berman DM. Tissue repair and stem cell renewal in carcinogenesis. Nature 2004; 432: 324-331.

49 Plaks V, Kong N, Werb Z. The cancer stem cell niche: how essential is the niche in regulating stemness of tumor cells? Cell stem cell 2015; 16: 225-238.

50 Yamashita T, Wang XW. Cancer stem cells in the development of liver cancer. The Journal of clinical investigation 2013; 123: 1911-1918.

51 Mani SA, Guo W, Liao MJ, Eaton EN, Ayyanan A, Zhou AY *et al*. The epithelial-mesenchymal transition generates cells with properties of stem cells. Cell 2008; 133: 704-715.

52 O'Brien CA, Pollett A, Gallinger S, Dick JE. A human colon cancer cell capable of initiating tumour growth in immunodeficient mice. Nature 2007; 445: 106-110.

53 Borovski T, De Sousa EMF, Vermeulen L, Medema JP. Cancer stem cell niche: the place to be. Cancer research 2011; 71: 634-639.

54 Ma S, Lee TK, Zheng BJ, Chan KW, Guan XY. CD133+ HCC cancer stem cells confer chemoresistance by preferential expression of the Akt/PKB survival pathway. Oncogene 2008; 27: 1749-1758.

55 Virchow R. An Address on the Value of Pathological Experiments. British medical journal 1881; 2: 198-203.

56 Sainz B, Jr., Carron E, Vallespinos M, Machado HL. Cancer Stem Cells and Macrophages: Implications in Tumor Biology and Therapeutic Strategies. Mediators of inflammation 2016; 2016: 9012369.

57 Rais Y, Zviran A, Geula S, Gafni O, Chomsky E, Viukov S *et al*. Deterministic direct reprogramming of somatic cells to pluripotency. Nature 2013; 502: 65-70.

58 Chaffer CL, Brueckmann I, Scheel C, Kaestli AJ, Wiggins PA, Rodrigues LO *et al*. Normal and neoplastic nonstem cells can spontaneously convert to a stem-like state. Proceedings of the National Academy of Sciences of the United States of America 2011; 108: 7950-7955.

59 Wang JC, Dick JE. Cancer stem cells: lessons from leukemia. Trends in cell biology 2005; 15: 494-501.

60 Cheng L, Ramesh AV, Flesken-Nikitin A, Choi J, Nikitin AY. Mouse models for cancer stem cell research. Toxicol Pathol 2010; 38: 62-71.

61 Marquardt JU, Raggi C, Andersen JB, Seo D, Avital I, Geller D *et al*. Human hepatic cancer stem cells are characterized by common stemness traits and diverse oncogenic pathways. Hepatology 2011; 54: 1031-1042.

62 Ma S, Chan KW, Hu L, Lee TK, Wo JY, Ng IO *et al*. Identification and characterization of tumorigenic liver cancer stem/progenitor cells. Gastroenterology 2007; 132: 2542-2556.

63 Raggi C, Factor VM, Seo D, Holczbauer A, Gillen MC, Marquardt JU *et al*. Epigenetic reprogramming modulates malignant properties of human liver cancer. Hepatology 2014.

64 Yamashita T, Forgues M, Wang W, Kim JW, Ye Q, Jia H *et al*. EpCAM and alpha-fetoprotein expression defines novel prognostic subtypes of hepatocellular carcinoma. Cancer research 2008; 68: 1451-1461.

65 Kokuryo T, Yokoyama Y, Nagino M. Recent advances in cancer stem cell research for cholangiocarcinoma. Journal of hepato-biliary-pancreatic sciences 2012; 19: 606-613.

66 Suetsugu A, Nagaki M, Aoki H, Motohashi T, Kunisada T, Moriwaki H. Characterization of CD133+ hepatocellular carcinoma cells as cancer stem/progenitor cells. Biochemical and biophysical research communications 2006; 351: 820-824.

67 Rountree CB, Ding W, He L, Stiles B. Expansion of CD133-expressing liver cancer stem cells in liver-specific phosphatase and tensin homolog deleted on chromosome 10-deleted mice. Stem Cells 2009; 27: 290-299.

68 Zhu Z, Hao X, Yan M, Yao M, Ge C, Gu J *et al*. Cancer stem/progenitor cells are highly enriched in CD133+CD44+ population in hepatocellular carcinoma. International journal of cancer 2010; 126: 2067-2078.

69 Yang W, Yan HX, Chen L, Liu Q, He YQ, Yu LX *et al*. Wnt/beta-catenin signaling contributes to activation of normal and tumorigenic liver progenitor cells. Cancer research 2008; 68: 4287-4295.

70 Yang ZF, Ho DW, Ng MN, Lau CK, Yu WC, Ngai P *et al*. Significance of CD90(+) cancer stem cells in human liver cancer. Cancer Cell 2008; 13: 153-166.

71 Yang ZF, Ngai P, Ho DW, Yu WC, Ng MNP, Lau CK *et al*. Identification of local and circulating cancer stem cells in human liver cancer. Hepatology 2008; 47: 919-928.

72 Haraguchi N, Ishii H, Mimori K, Tanaka F, Ohkuma M, Kim HM *et al*. CD13 is a therapeutic target in human liver cancer stem cells. The Journal of clinical investigation 2010; 120: 3326-3339.

73 Lee TK, Castilho A, Cheung VC, Tang KH, Ma S, Ng IO. CD24(+) liver tumor-initiating cells drive self-renewal and tumor initiation through STAT3-mediated NANOG regulation. Cell stem cell 2011; 9: 50-63.

74 Lee TK, Cheung VC, Lu P, Lau EY, Ma S, Tang KH *et al*. Blockade of CD47-mediated cathepsin S/protease-activated receptor 2 signaling provides a therapeutic target for hepatocellular carcinoma. Hepatology 2014; 60: 179-191.

75 Chiba T, Kita K, Zheng YW, Yokosuka O, Saisho H, Iwama A *et al*. Side population purified from hepatocellular carcinoma cells harbors cancer stem cell-like properties. Hepatology 2006; 44: 240-251.

76 Ma S, Chan KW, Lee TK, Tang KH, Wo JY, Zheng BJ *et al*. Aldehyde dehydrogenase discriminates the CD133 liver cancer stem cell populations. Molecular cancer research : MCR 2008; 6: 1146-1153.

77 Cardinale V, Renzi A, Carpino G, Torrice A, Bragazzi MC, Giuliante F *et al*. Profiles of cancer stem cell subpopulations in cholangiocarcinomas. The American journal of pathology 2015; 185: 1724-1739.

78 Chiba T, Zheng YW, Kita K, Yokosuka O, Saisho H, Onodera M *et al*. Enhanced self-renewal capability in hepatic stem/progenitor cells drives cancer initiation. Gastroenterology 2007; 133: 937-950.

79 Whittaker S, Marais R, Zhu AX. The role of signaling pathways in the development and treatment of hepatocellular carcinoma. Oncogene 2010; 29: 4989-5005.

80 Pez F, Lopez A, Kim M, Wands JR, Caron de Fromentel C, Merle P. Wnt signaling and hepatocarcinogenesis: molecular targets for the development of innovative anticancer drugs. Journal of hepatology 2013; 59: 1107-1117.

81 Ji J, Wang XW. Clinical implications of cancer stem cell biology in hepatocellular carcinoma. Seminars in oncology 2012; 39: 461-472.

82 Wang XQ, Zhang W, Lui EL, Zhu Y, Lu P, Yu X *et al*. Notch1-Snail1-E-cadherin pathway in metastatic hepatocellular carcinoma. International journal of cancer 2012; 131: E163-172.

83 Gao J, Dong Y, Zhang B, Xiong Y, Xu W, Cheng Y *et al*. Notch1 activation contributes to tumor cell growth and proliferation in human hepatocellular carcinoma HepG2 and SMMC7721 cells. International journal of oncology 2012; 41: 1773-1781.

84 Strazzabosco M, Fabris L. Notch signaling in hepatocellular carcinoma: guilty in association! Gastroenterology 2012; 143: 1430-1434.

85 Zender S, Nickeleit I, Wuestefeld T, Sorensen I, Dauch D, Bozko P *et al*. A critical role for notch signaling in the formation of cholangiocellular carcinomas. Cancer Cell 2013; 23: 784-795.

86 Chiba S. Notch signaling in stem cell systems. Stem Cells 2006; 24: 2437-2447.

87 Villanueva A, Alsinet C, Yanger K, Hoshida Y, Zong Y, Toffanin S *et al*. Notch signaling is activated in human hepatocellular carcinoma and induces tumor formation in mice. Gastroenterology 2012; 143: 1660-1669 e1667.

88 El Khatib M, Kalnytska A, Palagani V, Kossatz U, Manns MP, Malek NP *et al*. Inhibition of hedgehog signaling attenuates carcinogenesis in vitro and increases necrosis of cholangiocellular carcinoma. Hepatology 2013; 57: 1035-1045.

89 Chen X, Lingala S, Khoobyari S, Nolta J, Zern MA, Wu J. Epithelial mesenchymal transition and hedgehog signaling activation are associated with chemoresistance and invasion of hepatoma subpopulations. Journal of hepatology 2011; 55: 838-845.

90 Philips GM, Chan IS, Swiderska M, Schroder VT, Guy C, Karaca GF *et al*. Hedgehog signaling antagonist promotes regression of both liver fibrosis and hepatocellular carcinoma in a murine model of primary liver cancer. PloS one 2011; 6: e23943.

91 Majumdar A, Curley SA, Wu X, Brown P, Hwang JP, Shetty K *et al*. Hepatic stem cells and transforming growth factor beta in hepatocellular carcinoma. Nature reviews Gastroenterology & hepatology 2012; 9: 530-538.

92 Wu K, Ding J, Chen C, Sun W, Ning BF, Wen W *et al*. Hepatic transforming growth factor beta gives rise to tumor-initiating cells and promotes liver cancer development. Hepatology 2012; 56: 2255-2267.

93 Tang Y, Kitisin K, Jogunoori W, Li C, Deng CX, Mueller SC *et al*. Progenitor/stem cells give rise to liver cancer due to aberrant TGF-beta and IL-6 signaling. Proceedings of the National Academy of Sciences of the United States of America 2008; 105: 2445-2450.

94 Shackel NA, McCaughan GW, Warner FJ. Hepatocellular carcinoma development requires hepatic stem cells with altered transforming growth factor and interleukin-6 signaling. Hepatology 2008; 47: 2134-2136.

95 Lin L, Amin R, Gallicano GI, Glasgow E, Jogunoori W, Jessup JM *et al*. The STAT3 inhibitor NSC 74859 is effective in hepatocellular cancers with disrupted TGF-beta signaling. Oncogene 2009; 28: 961-972.

96 Chiba T, Seki A, Aoki R, Ichikawa H, Negishi M, Miyagi S *et al*. Bmi1 promotes hepatic stem cell expansion and tumorigenicity in both Ink4a/Arf-dependent and -independent manners in mice. Hepatology 2010; 52: 1111-1123.

97 Chiba T, Miyagi S, Saraya A, Aoki R, Seki A, Morita Y *et al*. The polycomb gene product BMI1 contributes to the maintenance of tumor-initiating side population cells in hepatocellular carcinoma. Cancer research 2008; 68: 7742-7749.

98 Yuri S, Fujimura S, Nimura K, Takeda N, Toyooka Y, Fujimura Y *et al*. Sall4 is essential for stabilization, but not for pluripotency, of embryonic stem cells by repressing aberrant trophectoderm gene expression. Stem Cells 2009; 27: 796-805.

99 Yong KJ, Chai L, Tenen DG. Oncofetal gene SALL4 in aggressive hepatocellular carcinoma. The New England journal of medicine 2013; 369: 1171-1172.

100 Zeng SS, Yamashita T, Kondo M, Nio K, Hayashi T, Hara Y *et al*. The transcription factor SALL4 regulates stemness of EpCAM-positive hepatocellular carcinoma. Journal of hepatology 2014; 60: 127-134.

101 Liu C, Liu L, Shan J, Shen J, Xu Y, Zhang Q *et al*. Histone deacetylase 3 participates in self-renewal of liver cancer stem cells through histone modification. Cancer letters 2013; 339: 60-69.

102 Raggi C, Invernizzi P. Methylation and liver cancer. Clinics and research in hepatology and gastroenterology 2013; 37: 564-571.

103 You H, Ding W, Rountree CB. Epigenetic regulation of cancer stem cell marker CD133 by transforming growth factor-beta. Hepatology 2010; 51: 1635-1644.

104 Chai S, Tong M, Ng KY, Kwan PS, Chan YP, Fung TM *et al*. Regulatory role of miR-142-3p on the functional hepatic cancer stem cell marker CD133. Oncotarget 2014; 5: 5725-5735.

105 Ma S, Tang KH, Chan YP, Lee TK, Kwan PS, Castilho A *et al*. miR-130b Promotes CD133(+) liver tumor-initiating cell growth and self-renewal via tumor protein 53-induced nuclear protein 1. Cell stem cell 2010; 7: 694-707.

106 Iliopoulos D, Hirsch HA, Struhl K. An epigenetic switch involving NF-kappaB, Lin28, Let-7 MicroRNA, and IL6 links inflammation to cell transformation. Cell 2009; 139: 693-706.

107 Wang YC, Chen YL, Yuan RH, Pan HW, Yang WC, Hsu HC *et al*. Lin-28B expression promotes transformation and invasion in human hepatocellular carcinoma. Carcinogenesis 2010; 31: 1516-1522.

108 Ji J, Yamashita T, Budhu A, Forgues M, Jia HL, Li C *et al*. Identification of microRNA-181 by genome-wide screening as a critical player in EpCAM-positive hepatic cancer stem cells. Hepatology 2009; 50: 472-480.

109 Hermann PC, Huber SL, Herrler T, Aicher A, Ellwart JW, Guba M *et al*. Distinct populations of cancer stem cells determine tumor growth and metastatic activity in human pancreatic cancer. Cell stem cell 2007; 1: 313-323.

110 Riener MO, Vogetseder A, Pestalozzi BC, Clavien PA, Probst-Hensch N, Kristiansen G *et al*. Cell adhesion molecules P-cadherin and CD24 are markers for carcinoma and dysplasia in the biliary tract. Human pathology 2010; 41: 1558-1565.

111 Agrawal S, Kuvshinoff BW, Khoury T, Yu J, Javle MM, LeVea C *et al*. CD24 expression is an independent prognostic marker in cholangiocarcinoma. Journal of gastrointestinal surgery : official journal of the Society for Surgery of the Alimentary Tract 2007; 11: 445-451.

112 Ma Y, Liang D, Liu J, Wen JG, Servoll E, Waaler G *et al*. SHBG Is an Important Factor in Stemness Induction of Cells by DHT In Vitro and Associated with Poor Clinical Features of Prostate Carcinomas. PloS one 2013; 8: e70558.

113 Ho DW, Yang ZF, Yi K, Lam CT, Ng MN, Yu WC *et al*. Gene expression profiling of liver cancer stem cells by RNA-sequencing. PloS one 2012; 7: e37159.

114 de Boer CJ, van Krieken JH, Janssen-van Rhijn CM, Litvinov SV. Expression of Ep-CAM in normal, regenerating, metaplastic, and neoplastic liver. The Journal of pathology 1999; 188: 201-206.

115 Wilson GS, Hu Z, Duan W, Tian A, Wang XM, McLeod D *et al*. Efficacy of using cancer stem cell markers in isolating and characterizing liver cancer stem cells. Stem cells and development 2013; 22: 2655-2664.

116 Li X, Lewis MT, Huang J, Gutierrez C, Osborne CK, Wu MF *et al*. Intrinsic resistance of tumorigenic breast cancer cells to chemotherapy. Journal of the National Cancer Institute 2008; 100: 672-679.

117 Baguley BC. Multiple drug resistance mechanisms in cancer. Molecular biotechnology 2010; 46: 308-316.

118 Zhou S, Schuetz JD, Bunting KD, Colapietro AM, Sampath J, Morris JJ *et al*. The ABC transporter Bcrp1/ABCG2 is expressed in a wide variety of stem cells and is a molecular determinant of the side-population phenotype. Nature medicine 2001; 7: 1028-1034.

119 Goodell MA, Brose K, Paradis G, Conner AS, Mulligan RC. Isolation and functional properties of murine hematopoietic stem cells that are replicating in vivo. The Journal of experimental medicine 1996; 183: 1797-1806.

120 Guo Z, Jiang JH, Zhang J, Yang HJ, Yang FQ, Qi YP *et al*. COX-2 Promotes Migration and Invasion by the Side Population of Cancer Stem Cell-Like Hepatocellular Carcinoma Cells. Medicine (Baltimore) 2015; 94: e1806.

121 Yang X, Wang J, Qu S, Zhang H, Ruan B, Gao Y *et al*. MicroRNA-200a suppresses metastatic potential of side population cells in human hepatocellular carcinoma by decreasing ZEB2. Oncotarget 2015; 6: 7918-7929.

122 Cao L, Fan X, Jing W, Liang Y, Chen R, Liu Y *et al*. Osteopontin promotes a cancer stem cell-like phenotype in hepatocellular carcinoma cells via an integrin-NF-kappaB-HIF-1alpha pathway. Oncotarget 2015; 6: 6627-6640.

123 Cao L, Zhou Y, Zhai B, Liao J, Xu W, Zhang R *et al*. Sphere-forming cell subpopulations with cancer stem cell properties in human hepatoma cell lines. BMC gastroenterology 2011; 11: 71.

124 Ginestier C, Hur MH, Charafe-Jauffret E, Monville F, Dutcher J, Brown M *et al*. ALDH1 is a marker of normal and malignant human mammary stem cells and a predictor of poor clinical outcome. Cell stem cell 2007; 1: 555-567.

125 Carpentino JE, Hynes MJ, Appelman HD, Zheng T, Steindler DA, Scott EW *et al*. Aldehyde dehydrogenase-expressing colon stem cells contribute to tumorigenesis in the transition from colitis to cancer. Cancer research 2009; 69: 8208-8215.

126 Li T, Su Y, Mei Y, Leng Q, Leng B, Liu Z *et al*. ALDH1A1 is a marker for malignant prostate stem cells and predictor of prostate cancer patients' outcome. Laboratory investigation; a journal of technical methods and pathology 2010; 90: 234-244.

127 Singh SK, Hawkins C, Clarke ID, Squire JA, Bayani J, Hide T *et al*. Identification of human brain tumour initiating cells. Nature 2004; 432: 396-401.

128 Ponti D, Costa A, Zaffaroni N, Pratesi G, Petrangolini G, Coradini D *et al*. Isolation and in vitro propagation of tumorigenic breast cancer cells with stem/progenitor cell properties. Cancer research 2005; 65: 5506-5511.

129 Reynolds BA, Weiss S. Generation of neurons and astrocytes from isolated cells of the adult mammalian central nervous system. Science 1992; 255: 1707-1710.

130 Lukacs RU, Lawson DA, Xin L, Zong Y, Garraway I, Goldstein AS *et al*. Epithelial stem cells of the prostate and their role in cancer progression. Cold Spring Harbor symposia on quantitative biology 2008; 73: 491-502.

131 Shaw FL, Harrison H, Spence K, Ablett MP, Simoes BM, Farnie G *et al*. A detailed mammosphere assay protocol for the quantification of breast

stem cell activity. Journal of mammary gland biology and neoplasia 2012; 17: 111-117.

132 Alison MR, Lim SM, Nicholson LJ. Cancer stem cells: problems for therapy? The Journal of pathology 2011; 223: 147-161.

133 Takahashi K, Yamanaka S. Induction of pluripotent stem cells from mouse embryonic and adult fibroblast cultures by defined factors. Cell 2006; 126: 663-676.

134 Schoenhals M, Kassambara A, De Vos J, Hose D, Moreaux J, Klein B. Embryonic stem cell markers expression in cancers. Biochemical and biophysical research communications 2009; 383: 157-162.

135 Jeter CR, Badeaux M, Choy G, Chandra D, Patrawala L, Liu C *et al*. Functional evidence that the self-renewal gene NANOG regulates human tumor development. Stem Cells 2009; 27: 993-1005.

136 Segal E, Friedman N, Koller D, Regev A. A module map showing conditional activity of expression modules in cancer. Nature genetics 2004; 36: 1090-1098.

137 Wong DJ, Liu H, Ridky TW, Cassarino D, Segal E, Chang HY. Module map of stem cell genes guides creation of epithelial cancer stem cells. Cell stem cell 2008; 2: 333-344.

138 Ben-Porath I, Thomson MW, Carey VJ, Ge R, Bell GW, Regev A *et al*. An embryonic stem cell-like gene expression signature in poorly differentiated aggressive human tumors. Nature genetics 2008; 40: 499-507.

139 Nusse R, van Ooyen A, Cox D, Fung YK, Varmus H. Mode of proviral activation of a putative mammary oncogene (int-1) on mouse chromosome 15. Nature 1984; 307: 131-136.

140 Mikhail S, He AR. Liver cancer stem cells. International journal of hepatology 2011; 2011: 486954.

141 Salomon DS, Kim N, Saeki T, Ciardiello F. Transforming growth factor-alpha: an oncodevelopmental growth factor. Cancer Cells 1990; 2: 389-397.

142 Villanueva A, Llovet JM. Second-line therapies in hepatocellular carcinoma: emergence of resistance to sorafenib. Clinical cancer research : an official journal of the American Association for Cancer Research 2012; 18: 1824-1826.

143 Morell CM, Strazzabosco M. Notch signaling and new therapeutic options in liver disease. Journal of hepatology 2014; 60: 885-890.

144 Zong Y, Stanger BZ. Molecular mechanisms of liver and bile duct development. Wiley interdisciplinary reviews Developmental biology 2012; 1: 643-655.

145 Gao J, Song Z, Chen Y, Xia L, Wang J, Fan R *et al*. Deregulated expression of Notch receptors in human hepatocellular carcinoma. Digestive and liver disease : official journal of the Italian Society of Gastroenterology and the Italian Association for the Study of the Liver 2008; 40: 114-121.

146 Thayer SP, di Magliano MP, Heiser PW, Nielsen CM, Roberts DJ, Lauwers GY *et al*. Hedgehog is an early and late mediator of pancreatic cancer tumorigenesis. Nature 2003; 425: 851-856.

147 Liao X, Siu MK, Au CW, Wong ES, Chan HY, Ip PP *et al*. Aberrant activation of hedgehog signaling pathway in ovarian cancers: effect on prognosis, cell invasion and differentiation. Carcinogenesis 2009; 30: 131-140.

148 Kango-Singh M, Singh A. Regulation of organ size: insights from the Drosophila Hippo signaling pathway. Developmental dynamics : an official publication of the American Association of Anatomists 2009; 238: 1627-1637.

149 Huang J, Wu S, Barrera J, Matthews K, Pan D. The Hippo signaling pathway coordinately regulates cell proliferation and apoptosis by inactivating Yorkie, the Drosophila Homolog of YAP. Cell 2005; 122: 421-434.

150 Lian I, Kim J, Okazawa H, Zhao J, Zhao B, Yu J *et al*. The role of YAP transcription coactivator in regulating stem cell self-renewal and differentiation. Genes & development 2010; 24: 1106-1118.

151 Lu L, Li Y, Kim SM, Bossuyt W, Liu P, Qiu Q *et al*. Hippo signaling is a potent in vivo growth and tumor suppressor pathway in the mammalian liver. Proceedings of the National Academy of Sciences of the United States of America 2010; 107: 1437-1442.

152 Kim GJ, Kim H, Park YN. Increased expression of Yes-associated protein 1 in hepatocellular carcinoma with stemness and combined hepatocellular-cholangiocarcinoma. PloS one 2013; 8: e75449.

153 Lee KP, Lee JH, Kim TS, Kim TH, Park HD, Byun JS *et al*. The Hippo-Salvador pathway restrains hepatic oval cell proliferation, liver size, and liver tumorigenesis. Proceedings of the National Academy of Sciences of the United States of America 2010; 107: 8248-8253.

154 Li J, Razumilava N, Gores GJ, Walters S, Mizuochi T, Mourya R *et al*. Biliary repair and carcinogenesis are mediated by IL-33-dependent cholangiocyte proliferation. The Journal of clinical investigation 2014.

155 Stauffer JK, Scarzello AJ, Andersen JB, De Kluyver RL, Back TC, Weiss JM *et al*. Coactivation of AKT and beta-catenin in mice rapidly induces formation of lipogenic liver tumors. Cancer research 2011; 71: 2718-2727.

156 Lau CK, Yang ZF, Fan ST. Role of stem cells in normal liver and cancer. Anti-cancer agents in medicinal chemistry 2011; 11: 522-528.

157 Sato Y, Harada K, Itatsu K, Ikeda H, Kakuda Y, Shimomura S *et al*. Epithelial-mesenchymal transition induced by transforming growth factor-{beta}1/Snail activation aggravates invasive growth of cholangiocarcinoma. The American journal of pathology 2010; 177: 141-152.

158 Andersen JB, Thorgeirsson SS. A perspective on molecular therapy in cholangiocarcinoma: present status and future directions. Future Medicine (Hepatic Oncology) 2014; 1: 143-157.

159 Zhou B, Damrauer JS, Bailey ST, Hadzic T, Jeong Y, Clark K *et al*. Erythropoietin promotes breast tumorigenesis through tumor-initiating cell self-renewal. The Journal of clinical investigation 2014; 124: 553-563.

160 Cook AM, Li L, Ho Y, Lin A, Stein A, Forman S *et al*. Role of altered growth factor receptor-mediated JAK2 signaling in growth and maintenance of human acute myeloid leukemia stem cells. Blood 2014; 123: 2826-2837.

161 Sherry MM, Reeves A, Wu JK, Cochran BH. STAT3 is required for proliferation and maintenance of multipotency in glioblastoma stem cells. Stem Cells 2009; 27: 2383-2392.

162 Liu RY, Zeng Y, Lei Z, Wang L, Yang H, Liu Z *et al*. JAK/STAT3 signaling is required for TGF-beta-induced epithelial-mesenchymal transition in lung cancer cells. International journal of oncology 2014; 44: 1643-1651.

163 Rokavec M, Oner MG, Li H, Jackstadt R, Jiang L, Lodygin D *et al*. IL-6R/STAT3/miR-34a feedback loop promotes EMT-mediated colorectal cancer invasion and metastasis. The Journal of clinical investigation 2014; 124: 1853-1867.

164 Junttila MR, de Sauvage FJ. Influence of tumour micro-environment heterogeneity on therapeutic response. Nature 2013; 501: 346-354.

165 Grivennikov SI, Greten FR, Karin M. Immunity, inflammation, and cancer. Cell 2010; 140: 883-899.

166 Korkaya H, Liu S, Wicha MS. Breast cancer stem cells, cytokine networks, and the tumor microenvironment. The Journal of clinical investigation 2011; 121: 3804-3809.

167 Moore KA, Lemischka IR. Stem cells and their niches. Science 2006; 311: 1880-1885.

168 Hernandez-Gea V, Toffanin S, Friedman SL, Llovet JM. Role of the microenvironment in the pathogenesis and treatment of hepatocellular carcinoma. Gastroenterology 2013; 144: 512-527.

169 Lin G, Liu Y, Li S, Mao Y, Wang J, Shuang Z *et al*. Elevated neutrophil-to-lymphocyte ratio is an independent poor prognostic factor in patients with intrahepatic cholangiocarcinoma. Oncotarget 2016.

170 Sabbatino F, Villani V, Yearley JH, Deshpande V, Cai L, Konstantinidis IT *et al*. PD-L1 and HLA Class I Antigen Expression and Clinical Course of the

Disease in Intrahepatic Cholangiocarcinoma. Clinical cancer research : an official journal of the American Association for Cancer Research 2016; 22: 470-478.

171 Mao ZY, Zhu GQ, Xiong M, Ren L, Bai L. Prognostic value of neutrophil distribution in cholangiocarcinoma. World journal of gastroenterology : WJG 2015; 21: 4961-4968.

172 Sasaki M, Tsuneyama K, Ishikawa A, Nakanuma Y. Intrahepatic cholangiocarcinoma in cirrhosis presents granulocyte and granulocyte-macrophage colony-stimulating factor. Human pathology 2003; 34: 1337-1344.

173 Noy R, Pollard JW. Tumor-associated macrophages: from mechanisms to therapy. Immunity 2014; 41: 49-61.

174 Mantovani A. The yin-yang of tumor-associated neutrophils. Cancer Cell 2009; 16: 173-174.

175 Mantovani A, Allavena P, Sica A. Tumour-associated macrophages as a prototypic type II polarised phagocyte population: role in tumour progression. Eur J Cancer 2004; 40: 1660-1667.

176 Mantovani A, Allavena P, Sica A, Balkwill F. Cancer-related inflammation. Nature 2008; 454: 436-444.

177 Mantovani A, Biswas SK, Galdiero MR, Sica A, Locati M. Macrophage plasticity and polarization in tissue repair and remodelling. The Journal of pathology 2013; 229: 176-185.

178 Coussens LM, Zitvogel L, Palucka AK. Neutralizing tumor-promoting chronic inflammation: a magic bullet? Science 2013; 339: 286-291.

179 Wilson E, Leszczynska K, Poulter NS, Edelmann F, Salisbury VA, Noy PJ *et al*. RhoJ interacts with the GIT-PIX complex and regulates focal adhesion disassembly. Journal of cell science 2014; 127: 3039-3051.

180 Mantovani A, Sozzani S, Locati M, Allavena P, Sica A. Macrophage polarization: tumor-associated macrophages as a paradigm for polarized M2 mononuclear phagocytes. Trends in immunology 2002; 23: 549-555.

181 Solinas G, Schiarea S, Liguori M, Fabbri M, Pesce S, Zammataro L *et al*. Tumor-conditioned macrophages secrete migration-stimulating factor: a new marker for M2-polarization, influencing tumor cell motility. J Immunol 2010; 185: 642-652.

182 Mantovani A, Sica A. Macrophages, innate immunity and cancer: balance, tolerance, and diversity. Current opinion in immunology 2010; 22: 231-237.

183 Korkaya H, Wicha MS. Inflammation and autophagy conspire to promote tumor growth. Cell Cycle 2011; 10: 2623-2624.

184 Porta C, Rimoldi M, Raes G, Brys L, Ghezzi P, Di Liberto D *et al*. Tolerance and M2 (alternative) macrophage polarization are related processes orchestrated by p50 nuclear factor kappaB. Proceedings of the National Academy of Sciences of the United States of America 2009; 106: 14978-14983.

185 Porta C, Larghi P, Rimoldi M, Totaro MG, Allavena P, Mantovani A *et al*. Cellular and molecular pathways linking inflammation and cancer. Immunobiology 2009; 214: 761-777.

186 Murray PJ, Allen JE, Biswas SK, Fisher EA, Gilroy DW, Goerdt S *et al*. Macrophage activation and polarization: nomenclature and experimental guidelines. Immunity 2014; 41: 14-20.

187 Locati M, Mantovani A, Sica A. Macrophage activation and polarization as an adaptive component of innate immunity. Advances in immunology 2013; 120: 163-184.

188 Allavena P, Sica A, Solinas G, Porta C, Mantovani A. The inflammatory micro-environment in tumor progression: the role of tumor-associated macrophages. Critical reviews in oncology/hematology 2008; 66: 1-9.

189 Liu S, Ginestier C, Ou SJ, Clouthier SG, Patel SH, Monville F *et al*. Breast cancer stem cells are regulated by mesenchymal stem cells through cytokine networks. Cancer research 2011; 71: 614-624.

190 Mosser DM, Edwards JP. Exploring the full spectrum of macrophage activation. Nature reviews Immunology 2008; 8: 958-969.

191 Qian BZ, Pollard JW. Macrophage diversity enhances tumor progression and metastasis. Cell 2010; 141: 39-51.

192 Gordon S, Martinez FO. Alternative activation of macrophages: mechanism and functions. Immunity 2010; 32: 593-604.

193 Biswas SK, Mantovani A. Macrophage plasticity and interaction with lymphocyte subsets: cancer as a paradigm. Nature immunology 2010; 11: 889-896.

194 Margol AS, Robison NJ, Gnanachandran J, Hung LT, Kennedy RJ, Vali M *et al*. Tumor-associated macrophages in SHH subgroup of medulloblastomas. Clinical cancer research : an official journal of the American Association for Cancer Research 2015; 21: 1457-1465.

195 Movahedi K, Laoui D, Gysemans C, Baeten M, Stange G, Van den Bossche J *et al*. Different tumor microenvironments contain functionally distinct subsets of macrophages derived from Ly6C(high) monocytes. Cancer research 2010; 70: 5728-5739.

196 Lewis CE, Pollard JW. Distinct role of macrophages in different tumor microenvironments. Cancer research 2006; 66: 605-612.

197 Sica A, Larghi P, Mancino A, Rubino L, Porta C, Totaro MG *et al*. Macrophage polarization in tumour progression. Seminars in cancer biology 2008; 18: 349-355.

198 Biswas SK, Allavena P, Mantovani A. Tumor-associated macrophages: functional diversity, clinical significance, and open questions. Seminars in immunopathology 2013; 35: 585-600.

199 Richards DM, Hettinger J, Feuerer M. Monocytes and macrophages in cancer: development and functions. Cancer microenvironment : official journal of the International Cancer Microenvironment Society 2013; 6: 179-191.

200 Riether C, Schurch CM, Ochsenbein AF. Regulation of hematopoietic and leukemic stem cells by the immune system. Cell death and differentiation 2015; 22: 187-198.

201 Hasita H, Komohara Y, Okabe H, Masuda T, Ohnishi K, Lei XF *et al*. Significance of alternatively activated macrophages in patients with intrahepatic cholangiocarcinoma. Cancer science 2010; 101: 1913-1919.

202 Subimerb C, Pinlaor S, Khuntikeo N, Leelayuwat C, Morris A, McGrath MS *et al*. Tissue invasive macrophage density is correlated with prognosis in cholangiocarcinoma. Mol Med Rep 2010; 3: 597-605.

203 Oishi K, Sakaguchi T, Baba S, Suzuki S, Konno H. Macrophage density and macrophage colony-stimulating factor expression predict the postoperative prognosis in patients with intrahepatic cholangiocarcinoma. Surgery today 2015; 45: 715-722.

204 Atanasov G, Hau HM, Dietel C, Benzing C, Krenzien F, Brandl A *et al*. Prognostic significance of macrophage invasion in hilar cholangiocarcinoma. BMC Cancer 2015; 15: 790.

205 Ohira S, Sasaki M, Harada K, Sato Y, Zen Y, Isse K *et al*. Possible regulation of migration of intrahepatic cholangiocarcinoma cells by interaction of CXCR4 expressed in carcinoma cells with tumor necrosis factor-alpha and stromal-derived factor-1 released in stroma. The American journal of pathology 2006; 168: 1155-1168.

206 Ohira S, Itatsu K, Sasaki M, Harada K, Sato Y, Zen Y *et al*. Local balance of transforming growth factor-beta1 secreted from cholangiocarcinoma cells and stromal-derived factor-1 secreted from stromal fibroblasts is a factor involved in invasion of cholangiocarcinoma. Pathology international 2006; 56: 381-389.

207 Thanee M, Loilome W, Techasen A, Namwat N, Boonmars T, Pairojkul C *et al*. Quantitative changes in tumor-associated M2 macrophages characterize cholangiocarcinoma and their association with metastasis. Asian Pacific journal of cancer prevention : APJCP 2015; 16: 3043-3050.

208 Techasen A, Loilome W, Namwat N, Dokduang H, Jongthawin J, Yongvanit P. Cytokines released from activated human macrophages induce epithelial mesenchymal transition markers of cholangiocarcinoma cells. Asian Pacific journal of cancer prevention : APJCP 2012; 13 Suppl: 115-118.

209 Techasen A, Namwat N, Loilome W, Bungkanjana P, Khuntikeo N, Puapairoj A *et al*. Tumor necrosis factor-alpha (TNF-alpha) stimulates the epithelial-mesenchymal transition regulator Snail in cholangiocarcinoma. Med Oncol 2012; 29: 3083-3091.

210 Franchitto A, Onori P, Renzi A, Carpino G, Mancinelli R, Alvaro D *et al*. Expression of vascular endothelial growth factors and their receptors by hepatic progenitor cells in human liver diseases. Hepatobiliary surgery and nutrition 2013; 2: 68-77.

211 Pollard JW. Trophic macrophages in development and disease. Nature reviews Immunology 2009; 9: 259-270.

212 Sica A, Mantovani A. Macrophage plasticity and polarization: in vivo veritas. The Journal of clinical investigation 2012; 122: 787-795.

213 He KF, Zhang L, Huang CF, Ma SR, Wang YF, Wang WM *et al*. CD163+ tumor-associated macrophages correlated with poor prognosis and cancer stem cells in oral squamous cell carcinoma. BioMed research international 2014; 2014: 838632.

214 Fan QM, Jing YY, Yu GF, Kou XR, Ye F, Gao L *et al*. Tumor-associated macrophages promote cancer stem cell-like properties via transforming growth factor-beta1-induced epithelial-mesenchymal transition in hepatocellular carcinoma. Cancer letters 2014; 352: 160-168.

215 Yamashina T, Baghdadi M, Yoneda A, Kinoshita I, Suzu S, Dosaka-Akita H *et al*. Cancer stem-like cells derived from chemoresistant tumors have a unique capacity to prime tumorigenic myeloid cells. Cancer research 2014; 74: 2698-2709.

216 Jinushi M, Chiba S, Yoshiyama H, Masutomi K, Kinoshita I, Dosaka-Akita H *et al*. Tumor-associated macrophages regulate tumorigenicity and

anticancer drug responses of cancer stem/initiating cells. Proceedings of the National Academy of Sciences of the United States of America 2011; 108: 12425-12430.

217 Yang J, Liao D, Chen C, Liu Y, Chuang TH, Xiang R *et al*. Tumor-associated macrophages regulate murine breast cancer stem cells through a novel paracrine EGFR/Stat3/Sox-2 signaling pathway. Stem Cells 2013; 31: 248-258.

218 Lu H, Clauser KR, Tam WL, Frose J, Ye X, Eaton EN *et al*. A breast cancer stem cell niche supported by juxtacrine signalling from monocytes and macrophages. Nature cell biology 2014; 16: 1105-1117.

219 Mitchem JB, Brennan DJ, Knolhoff BL, Belt BA, Zhu Y, Sanford DE *et al*. Targeting tumor-infiltrating macrophages decreases tumor-initiating cells, relieves immunosuppression, and improves chemotherapeutic responses. Cancer research 2013; 73: 1128-1141.

220 Hao NB, Lu MH, Fan YH, Cao YL, Zhang ZR, Yang SM. Macrophages in tumor microenvironments and the progression of tumors. Clinical & developmental immunology 2012; 2012: 948098.

221 Zhou W, Ke SQ, Huang Z, Flavahan W, Fang X, Paul J *et al*. Periostin secreted by glioblastoma stem cells recruits M2 tumour-associated macrophages and promotes malignant growth. Nature cell biology 2015; 17: 170-182.

222 Wan S, Zhao E, Kryczek I, Vatan L, Sadovskaya A, Ludema G *et al*. Tumor-associated macrophages produce interleukin 6 and signal via STAT3 to promote expansion of human hepatocellular carcinoma stem cells. Gastroenterology 2014; 147: 1393-1404.

223 Jinushi M, Baghdadi M, Chiba S, Yoshiyama H. Regulation of cancer stem cell activities by tumor-associated macrophages. American journal of cancer research 2012; 2: 529-539.

224 Hanahan D, Coussens LM. Accessories to the crime: functions of cells recruited to the tumor microenvironment. Cancer Cell 2012; 21: 309-322.

225 Su S, Liu Q, Chen J, Chen F, He C, Huang D *et al*. A positive feedback loop between mesenchymal-like cancer cells and macrophages is essential to breast cancer metastasis. Cancer Cell 2014; 25: 605-620.

226 Biswas SK, Sica A, Lewis CE. Plasticity of macrophage function during tumor progression: regulation by distinct molecular mechanisms. J Immunol 2008; 180: 2011-2017.

227 Miyagiwa M, Ichida T, Tokiwa T, Sato J, Sasaki H. A new human cholangiocellular carcinoma cell line (HuCC-T1) producing carbohydrate antigen 19/9 in serum-free medium. In vitro cellular & developmental biology : journal of the Tissue Culture Association 1989; 25: 503-510.

228 Han C, Wu T. Cyclooxygenase-2-derived prostaglandin E2 promotes human cholangiocarcinoma cell growth and invasion through EP1 receptor-mediated activation of the epidermal growth factor receptor and Akt. The Journal of biological chemistry 2005; 280: 24053-24063.

229 Shimizu Y, Demetris AJ, Gollin SM, Storto PD, Bedford HM, Altarac S *et al*. Two new human cholangiocarcinoma cell lines and their cytogenetics and responses to growth factors, hormones, cytokines or immunologic effector cells. International journal of cancer 1992; 52: 252-260.

230 Saeed AI, Sharov V, White J, Li J, Liang W, Bhagabati N *et al*. TM4: a free, open-source system for microarray data management and analysis. BioTechniques 2003; 34: 374-378.

231 Dang W, Qin Z, Fan S, Wen Q, Lu Y, Wang J *et al*. miR-1207-5p suppresses lung cancer growth and metastasis by targeting CSF1. Oncotarget 2016; 7: 32421-32432.

232 Chen J, Yao Y, Gong C, Yu F, Su S, Liu B *et al*. CCL18 from tumor-associated macrophages promotes breast cancer metastasis via PITPNM3. Cancer Cell 2011; 19: 541-555.

233 Sirica AE, Zhang Z, Lai GH, Asano T, Shen XN, Ward DJ *et al*. A novel "patient-like" model of cholangiocarcinoma progression based on bile

duct inoculation of tumorigenic rat cholangiocyte cell lines. Hepatology 2008; 47: 1178-1190.

234 Quintana E, Shackleton M, Sabel MS, Fullen DR, Johnson TM, Morrison SJ. Efficient tumour formation by single human melanoma cells. Nature 2008; 456: 593-598.

235 Raggi C, Mousa HS, Correnti M, Sica A, Invernizzi P. Cancer stem cells and tumor-associated macrophages: a roadmap for multitargeting strategies. Oncogene 2015.

236 Sica A, Schioppa T, Mantovani A, Allavena P. Tumour-associated macrophages are a distinct M2 polarised population promoting tumour progression: potential targets of anti-cancer therapy. Eur J Cancer 2006; 42: 717-727.

237 Steidl C, Lee T, Shah SP, Farinha P, Han G, Nayar T *et al*. Tumor-associated macrophages and survival in classic Hodgkin's lymphoma. The New England journal of medicine 2010; 362: 875-885.

238 Bingle L, Brown NJ, Lewis CE. The role of tumour-associated macrophages in tumour progression: implications for new anticancer therapies. The Journal of pathology 2002; 196: 254-265.

239 Schmidt T, Brodesser A, Schnitzler N, Gruger T, Brandenburg K, Zinserling J *et al*. CD66b Overexpression and Loss of C5a Receptors as Surface Markers for Staphylococcus aureus-Induced Neutrophil Dysfunction. PloS one 2015; 10: e0132703.

240 Mantovani A, Allavena P. The interaction of anticancer therapies with tumor-associated macrophages. The Journal of experimental medicine 2015; 212: 435-445.

241 Franklin RA, Liao W, Sarkar A, Kim MV, Bivona MR, Liu K *et al*. The cellular and molecular origin of tumor-associated macrophages. Science 2014; 344: 921-925.

242 Van Overmeire E, Laoui D, Keirsse J, Van Ginderachter JA, Sarukhan A. Mechanisms driving macrophage diversity and specialization in distinct

tumor microenvironments and parallelisms with other tissues. Frontiers in immunology 2014; 5: 127.

243 Locatelli L, Cadamuro M, Spirli C, Fiorotto R, Lecchi S, Morell CM *et al*. Macrophage recruitment by fibrocystin-defective biliary epithelial cells promotes portal fibrosis in congenital hepatic fibrosis. Hepatology 2016; 63: 965-982.

244 De Minicis S, Kisseleva T, Francis H, Baroni GS, Benedetti A, Brenner D *et al*. Liver carcinogenesis: rodent models of hepatocarcinoma and cholangiocarcinoma. Digestive and liver disease : official journal of the Italian Society of Gastroenterology and the Italian Association for the Study of the Liver 2013; 45: 450-459.

245 Hiramatsu H, Nishikomori R, Heike T, Ito M, Kobayashi K, Katamura K *et al*. Complete reconstitution of human lymphocytes from cord blood CD34+ cells using the NOD/SCID/gammacnull mice model. Blood 2003; 102: 873-880.

246 Takagi S, Saito Y, Hijikata A, Tanaka S, Watanabe T, Hasegawa T *et al*. Membrane-bound human SCF/KL promotes in vivo human hematopoietic engraftment and myeloid differentiation. Blood 2012; 119: 2768-2777.

247 Felix J, Elegheert J, Gutsche I, Shkumatov AV, Wen Y, Bracke N *et al*. Human IL-34 and CSF-1 establish structurally similar extracellular assemblies with their common hematopoietic receptor. Structure 2013; 21: 528-539.

248 Kuan CT, Wakiya K, Dowell JM, Herndon JE, 2nd, Reardon DA, Graner MW *et al*. Glycoprotein nonmetastatic melanoma protein B, a potential molecular therapeutic target in patients with glioblastoma multiforme. Clinical cancer research : an official journal of the American Association for Cancer Research 2006; 12: 1970-1982.

7. APPENDIX

Under the editorial permission, several parts of 'Introduction' section have been used from the following reviews:

- Raggi C, Mousa H, Correnti M, Sica A, Invernizzi P. Cancer Stem Cells and Tumor-Associated Macrophages: a Roadmap for Multitargeting Strategies. *Oncogene 2015*
- Correnti M and Raggi C. Stem-like plasticity and heterogeneity of circulating tumor cells: current status and prospect challenges in liver cancer. *Oncotarget 2016*

In addition, 'Methods', 'Results' and 'Discussion' sections from:

- Raggi C*, Correnti M*, Sica A, Andersen JB, Cardinale V, Alvaro D, Chiorino G, Forti E, Glaser S, Alpini G, Destro A, Sozio F, Di Tommaso L, Roncalli M, Banales JM, Coulouam C, Bujanda L, Torzilli G, Invernizzi P. Cholangiocarcinoma Stem-like Subset Shapes Tumor-initiating Niche by Educating Associated Macrophages. *Journal of Hepatology 2016 *first authors*

CORRENTI Margherita RIC

From: Oncogene <Oncogene@us.nature.com>
Sent: mercoledì 26 ottobre 2016 11.16
To: CORRENTI Margherita RIC
Subject: RE: copyright transfer agreement

Dear Ms Correnti

As per clause 2 of our licence agreement you do not need permission to reuse the information in your paper as the authors retain copyright. I've pasted the information below.

Kind regards
Sally

2. Ownership of copyright remains with the Author(s), and provided that, when reproducing the Contribution or extracts from it or the Supplementary Information (defined below), the Author(s) acknowledge first and reference publication in the Journal, the Author(s) retain only the following nonexclusive rights:
(a) to reproduce the Contribution in whole or in part in any printed volume (book or thesis) of which they are the Author(s);
(b) they and any academic institution where they work may reproduce the Contribution for the purpose of course teaching;
(c) to post a copy of the Contribution as accepted for publication after peer review (in a locked word processing file, or a PDF version thereof) on the Author(s)' own web sites, or institutional repositories, or the Author(s)' funding body(s)' archive, six months after publication of the printed or online edition of the Journal, provided that they also link to the Contribution on NPG's web site; and
(d) to reuse figures or tables created by the Author(s) and contained in the Contribution in oral presentations and other works created by them.

Sally Hawkins
Editorial Assistant

Springer Nature
The Campus, 4 Crinan Street, London N1 9XW, UK
www.springernature.com

From: CORRENTI Margherita RIC [mailto:Margherita.Correnti@humanitasresearch.it]
Sent: 24 October 2016 16:51
To: Oncogene
Subject: copyright transfer agreement

Dear Oncogene
Nature Publishing Group

We have submitted in 2015 the review: "Cancer stem cells and tumor-associated macrophages: a roadmap for multitargeting strategies" by Chiara Raggi, Hani S. Mousa, Margherita Correnti, Antonio Sica, Pietro Invernizzi.
The review was accepted and published.
I'm a co-author of the review and I'm a PhD Student. Now I'm writing my PhD thesis and I need to use the published review (wording).
You can kindly issue me a permission to use it?

Thank you for your consideration.

Sincerely,

Margherita CORRENTI, PhD Student
Center for Autoimmune Liver Diseases
Humanitas Clinical and Research Center
Via Manzoni 113
20089 ROZZANO (MI)
ITALY
Tel: +39 0282245169

CORRENTI Margherita RIC

From: Editorial Office <editorialoffice@oncotarget.com>
Sent: domenica 20 novembre 2016 8.18
To: CORRENTI Margherita RIC
Subject: Re: copyright transfer agreement

Permission is not required, as long as the source is cited, in accordance with the license we use for all of our papers: http://creativecommons.org/licenses/by/3.0/

On Wed, Nov 16, 2016 at 11:02 AM, CORRENTI Margherita RIC <Margherita.Correnti@humanitasresearch.it> wrote:

Dear Prof. Mikhail V. Blagosklonny,

Co-Editor-in-Chief

Oncotarget

We have recently submitted the the review: "Stem-like Plasticity and Heterogeneity of Circulating Tumor Cells: Current Status and Prospect Challenges in Liver Cancer " by Margherita Correnti and Chiara Raggi.

The manuscript was accepted and published.

I'm the first author of this review and I'm a PhD Student. Now I'm writing my PhD thesis and I need to use some parts of the published manuscript (wording and tables).

You can kindly issue me a permission to use it?

Thank you for your consideration.

Sincerely,

Margherita Correnti

Margherita CORRENTI, PhD Student

Center for Autoimmune Liver Diseases

Humanitas Clinical and Research Center

Via Manzoni 113

20089 ROZZANO (MI)

ITALY

Tel: +39 0282245169

e-mail: Margherita.Correnti@humanitasresearch.it

--

CORRENTI Margherita RIC

From: Boer Iwema, Sybrand (ELS-AMS) <S.BoerIwema@elsevier.com>
Sent: martedì 25 ottobre 2016 17.31
To: CORRENTI Margherita RIC
Cc: Rajiv Jalan; joel.walicki@easloffice.eu
Subject: RE: copyright transfer agreement

Dear Dr. Correnti,

Please allow me to introduce myself as the publisher of the Journal of Hepatology. Thank you for your message about your PhD thesis, which was forwarded to me. As author of the paper you certainly retain the rights to use the paper and the images in your thesis. This is considered personal use as listed here: https://www.elsevier.com/about/company-information/policies/copyright. You don't need to get further formal approval.

If you have any questions, please don't hesitate to let me know.

Kind regards,

Sybrand

Sybrand Boer Iwema
Executive Publisher
Elsevier
Radarweg 29
1043 NX Amsterdam
The Netherlands
s.boeriwema@elsevier.com
+31 (0)20 485 2781 (office)
+31 (0)6 2241 7893 (mobile)

From: Rajiv Jalan [mailto:r.jalan@ucl.ac.uk]
Sent: 24 October 2016 18:34
To: joel.walicki@easloffice.eu; Boer Iwema, Sybrand (ELS-AMS)
Subject: Fwd: copyright transfer agreement

Please see below. Is this ok?
In my view, this should not be a problem.
Cheers
Rajiv

Rajiv Jalan
Professor of Hepatology
Editor in Chief: Journal of Hepatology
Head, Liver Failure Group
ILDH, Division of Medicine
UCL Medical School
Royal Free Campus
Rowland Hill Street
London NW32PF

Phone: +442074332795

Begin forwarded message:

From: CORRENTI Margherita RIC <Margherita.Correnti@humanitasresearch.it>
Date: 24 October 2016 at 16:43:53 BST
To: "r.jalan@ucl.ac.uk" <r.jalan@ucl.ac.uk>
Cc: "jhepatology@easloffice.eu" <jhepatology@easloffice.eu>, "permissions@elsevier.com" <permissions@elsevier.com>
Subject: copyright transfer agreement

Dear Dr Rajiv Jalan
Editor-In-Chief, Journal of Hepatology

We have recently submitted the the manuscript "JHEPAT-D-16-01153": "Cholangiocarcinoma Stem-like Subset Shapes the Tumor-Initiating Niche by Educating Associated Macrophages" by Chiara Raggi, Margherita Correnti, Antonio Sica, Jesper B Andersen, Vincenzo Cardinale, Domenico Alvaro, Giovanna Chiorino, Elisa Forti, Shannon Glaser, Gianfranco Alpini, Annarita Destro, Francesca Sozio, Luca Di Tommaso, Massimo Roncalli, Jesus M Banales, Cédric Coulouarn, Luis Bujanda, Guido Torzilli, Pietro Invernizzi.
The manuscript was accepted and published.
I'm the co-first author of this manuscript and I'm a PhD Student. Now I'm writing my PhD thesis and I need to use the published manuscript (wording and data).
You can kindly issue me a permission to use it?

Thank you for your consideration.

Sincerely,
Margherita Correnti

Margherita CORRENTI, PhD Student
Center for Autoimmune Liver Diseases
Humanitas Clinical and Research Center
Via Manzoni 113
20089 ROZZANO (MI)
ITALY
Tel: +39 0282245169